University of Cape Town

Department of Electrical and Electronic Engineering

# Design of a low pressure system to determine the acoustic nonlinearity parameter B/A for small volumes of sample liquids



Prepared By: Bjorn Prenzlow
University of Cape Town
South Africa

Prepared for: Associate Prof. J Tapson
Department of Electrical Engineering
University of Cape Town

Date: 2003-09-29

# Acknowledgements

The author wishes to thank the following people for their contribution towards this project:

- My Supervisor. Prof. J Tapson, and Dr. J. Davies for their support and advice during this project.
- Mr. S. Marais, for his advice concerning the design of the mechanical structure.
- Mr. V. Balden, for his work on the finite element analysis of the thermal system.
- My family and friends for their encouragement and support during the completion of this project.
- The N.R.F (National Research Foundation) for the financial support towards this project.

# Terms of Reference

This project was commissioned by Prof. J Tapson, Dr. B Mortimer and Dr. J. Davies from the Department of Electrical Engineering at the University of Cape Town, in order to complete an MSc. Degree in Electrical Engineering.

The project requirements were:

- To design a system to measure B/A using low pressure sinusoidal waves ($P_{max} << 20$ kPa).
- To do research on small diameter piezo tubes in order to use them for the measurement of sound speed in the liquid.
- To attempt to understand the thermal effect upon the liquid sample so as to determine its significance.
- To obtain accurate results for B/A on a small sample of liquid in comparison to results obtained in literature.

# Synopsis

Since the description of the acoustic nonlinearity parameter, B/A, in the 1960's, several papers relating to its measurements and uses have been published. The nonlinearity parameter describes the relationship between the pressure and density of a liquid, and can be manipulated to obtain the change in sound speed in a liquid in relation to pressure. It has been used to describe the thermodynamic and mechanical properties of liquid, to obtain molecular information, to determine biological tissue composition and even to detect mines.

This thesis aimed to design a measurement system to obtain B/A readings for different liquids using the isentropic phase method. The resulting system uses a sinusoidal wave source that operates on less than 20kPa to pressurize a sample liquid of less than 0.2 ml. The advantage of the system is that it can obtain measurements using relatively few parameters of the liquid, requiring only density and sound speed, and that it can obtain a result in a relatively short amount of time (less than 15 minutes after system has reached thermal equilibrium).

This study also included work on understanding the problems and advantages of implementing a small volume piezo-ceramic tube to obtain accurate sound speed measurements, and a study of thermal effects due to the change in pressure in the air surrounding the sample. The results obtained for B/A compare very well to literature results obtained by other B/A measurement systems.

# Table of Contents

# List of Figures and Tables

*Chapter 1*

# Introduction

The study of finite amplitude waves, in the 1950s, brought attention to a non-linearity in the shape of received sound waves, especially over extended distances. This nonlinearity was described and a parameter called B/A was defined to approximate its effect for different liquids.

Several techniques have been devised to measure the B/A of different liquids. These methods required either large pressure fluctuations (>200kPa) to obtain results, or required knowledge of several unrelated parameters to measure it indirectly, as is described in chapter 3. Also these systems tended to require relatively large volumes of sample liquids, and a long duration to obtain an accurate result.

This work aims to refine a previous technique for measurement the B/A of a sample in such a way as to produce accurate results without needing excessive volumes or physical parameters of the sample liquids.

The author attempted to create a system that could obtain reasonably accurate results using only small pressure waves (<20kPa) and requiring only a very small volume of sample liquid (< 150 $mm^3$). The decrease in pressure change and sample volume increases the difficulty of obtaining accurate results; however it creates the ability to test rare or pressure sensitive samples. Due to the use of a smaller volume of sample liquid, the system was more sensitive to thermal fluctuations. Therefore, a sinusoidal pressure source was used to obtain more predictable results. Also, the small sample size implied the use of smaller sensors, especially for measurement of the speed of sound. This has practical implications for the accuracy of the sensors. These effects were modelled to ensure accurate results.

*Chapter 2*

# Formulation of Finite Amplitude Waves and B/A

In early applications of ultrasound the assumption was always made that the intensity of the sound in a medium was low enough that it did not have a significant effect on the parameters of the medium in which it was travelling [24]. This is known as the infinitesimal wave theory, and proves useful in most simple ultrasonic applications. However, as more uses for ultrasound were discovered, and as the techniques that were used became more refined, this assumption was questioned, and the parameters of finite amplitude waves were calculated.



## *Describing Finite Amplitude Waves*

In the 1960's Robert Beyer published a paper describing finite amplitude waves, where he introduced the non-linearity parameter of liquids and gases [4]. This parameter was derived from the relationship between density and pressure of fluids. For ideal gases this is described by the equation $p = p_0\left(\frac{\rho}{\rho_0}\right)^{\gamma}$ for adiabatic conditions, where $p$ and $p_0$ are current and initial pressures, $\rho$ and $\rho_0$ are current and initial densities, and $\gamma$ is the ratio of molar specific heats of the gas. The relationship between density and pressure of liquids is rather more complex [3]. Prior to Beyer's work, the relationship was simply assumed to be linear. The linear parameter is called bulk modulus, and is defined as $B = \frac{\Delta p}{\left(\Delta\rho/\rho\right)}$ [17]. This attempt, though useful in most other applications, proved to be an oversimplification, thus a Taylor polynomial is introduced to approximate the relationship.

$$p = p_0 + \left(\frac{\partial p}{\partial \rho}\right)_{0,s}(\rho - \rho_0) + \left(\frac{\partial^2 p}{\partial \rho^2}\right)_{0,s}\frac{(\rho - \rho_0)^2}{2} + \left(\frac{\partial^3 p}{\partial \rho^3}\right)_{0,s}\frac{(\rho - \rho_0)^3}{6} + \cdots \tag{2.1}$$

Since the majority of the information about the relationship is normally contained in the first few terms of a Taylor polynomial, only the first 3 terms will be considered. Equation 2.1 is rewritten so that the function is a polynomial of fractional changes in density.

$$p - p_0 = \left[\rho_0\left(\frac{\partial p}{\partial \rho}\right)_{0,s}\right]\left(\frac{\rho - \rho_0}{\rho_0}\right) + \frac{1}{2}\left[\rho_0^2\left(\frac{\partial^2 p}{\partial \rho^2}\right)_{0,s}\right]\left(\frac{\rho - \rho_0}{\rho_0}\right)^2 + \frac{1}{6}\left[\rho_0^3\left(\frac{\partial^3 p}{\partial \rho^3}\right)_{0,s}\right]\left(\frac{\rho - \rho_0}{\rho_0}\right)^3 \tag{2.2}$$

Equation 2.2 was simplified by substituting variables for the thermodynamic coefficients

$$p - p_0 = A\left(\frac{\rho - \rho_0}{\rho_0}\right) + \frac{1}{2}B\left(\frac{\rho - \rho_0}{\rho_0}\right)^2 + \frac{1}{6}C\left(\frac{\rho - \rho_0}{\rho_0}\right)^3 \tag{2.3}$$

$$\text{Where } A = \rho_0\left(\frac{\partial p}{\partial \rho}\right)_{0,s},\ B = \rho_0^2\left(\frac{\partial^2 p}{\partial \rho^2}\right)_{0,s} \text{ and } C = \rho_0^3\left(\frac{\partial^3 p}{\partial \rho^2}\right)_{0,s} \quad (2.4);\ (2.5);\ (2.6)$$

By using the infinitesimal sound speed equation, $c_0 = \sqrt{\frac{\partial p}{\partial \rho}}$, equation 2.4 describing $A$ can be rewritten so as to remove the derivative [4], so that $A = \rho_0 c_0^2$. Looking at this thermodynamic coefficient, one can note that $A$ is the bulk modulus of the liquid. Also $B$ represents the rate of change in $A$ and thus essentially the amount the nonlinearity in the system. $C$ is usually very small and thus mostly ignored [8].

Further manipulation, using the infinitesimal sound speed equation, allows equation 2.3 to be rewritten with reference to sound speed. This is where this relationship becomes interesting with reference to ultrasound.

$$c^2 = \left(\frac{\partial P}{\partial \rho}\right)_S = \frac{1}{\rho_0}\left[\frac{\partial P}{\partial (\psi)}\right]_S \text{, where } \psi = \frac{\rho - \rho_0}{\rho_0} \tag{2.7}$$

$$\text{Thus } c^2 = \frac{1}{\rho_0}\left(A + B\psi + \frac{C}{2}\psi^2 + \cdots\right) = c_0^2\left(1 + \frac{B}{A}\psi + \frac{C}{2A}\psi^2 + \cdots\right) \tag{2.8}$$

As seen in the above equation (2.8) the amount that the sound speed fluctuates from a constant value is dependent on the ratio of the thermodynamic coefficients. Previous experiments have shown that for most cases the B/A term is substantially dominant over the C/A term [2].

## *Calculating B/A*

From the division of the thermodynamic coefficients (equations 2.4 and 2.5), that were described in the previous section, the formula was derived that is used in direct implementations for calculation of B/A.

$$B/A = \frac{\rho_0}{c_0^2}\left(\frac{\partial^2 P}{\partial \rho^2}\right)_{S,\rho=\rho_0} = \frac{\rho_0}{c_0^2}\left(\frac{\partial}{\partial \rho}\left[\frac{\partial P}{\partial \rho}\right]\right)_{S,\rho=\rho_0} = \frac{\rho_0}{c_0^2}\left(\frac{\partial c^2}{\partial \rho}\right)_{S,\rho=\rho_0}$$
$$= \left(\frac{\rho_0}{c_0}\left[\frac{\partial c}{\partial \rho}\right]\right)_{S,\rho=\rho_0} = 2\rho_0 c_0\left(\frac{\partial c}{\partial P}\right)_{S,\rho=\rho_0} \tag{2.9}$$

Thus by measuring the change in sound speed of the sample media, for specific changes in pressure, under isentropic conditions, the B/A of a sample can be calculated. However due to the difficulties in creating isentropic conditions, the first attempts at reading B/A split this equation (2.9) into its two thermodynamic components (the addition of the isobaric and isothermal readings) [4].

$$B/A = 2\rho_0 c_0\left(\frac{\partial c}{\partial P}\right)_T + 2\left(\frac{T\beta\rho_0}{c_p}\right)\left(\frac{\partial c}{\partial T}\right)_p \tag{2.10}$$

Where $\beta$ is the volume coefficient of thermal expansion and $c_p$ is the specific heat at constant pressure.

The nonlinearity parameter is a tool in describing the thermodynamic [8] and mechanical [11] properties of liquid and has been used to obtain molecular information [18], determine biological tissue composition [1] and even to detect mines [25]. As more liquids are being measured, more applications for the parameter are becoming apparent.

*Chapter 3:*

# Historical Techniques for Calculating B/A

Since the 1960's when the non-linearity parameter was first described, several direct and indirect techniques have been developed for its measurement. The direct techniques focus on the formulas (2.9),(2.10) as described in the previous chapter, where the indirect techniques use the distortion of shockwaves due to the effect of B/A to measure the value of B/A. This chapter aims to briefly describe previous techniques that have been developed, showing their usefulness, accuracy and the effects on the samples.

As discussed in the previous chapter, B/A can be determined by measuring the effect on sound speed that changes of pressure produce, under constant entropy. From this knowledge, two techniques have been developed: The Thermodynamic technique (by Coppens et al. [8], initially proposed by Rudnick [31]) and the Isentropic Phase technique.

## *Thermodynamic Technique*

Based directly on the equations in the previous chapter, the calculation of B/A can be split into the summation of two thermodynamic terms:

$$B/A = 2\rho_0 c_0 \left(\frac{\partial c}{\partial P}\right)_T + 2\left(\frac{T\varphi c_0}{C_p}\right)\left(\frac{\partial c}{\partial T}\right)_P \qquad (2.10)$$

Where the first term of the equation represents an isothermal change in pressure and the second an isobaric change in temperature. Since the second term normally has a less that 5% effect on B/A, it is often neglected [26].

Firstly a sample's sound speed is measured at different temperatures while it is kept at atmospheric pressure. From this data, $\left(\frac{\partial c}{\partial T}\right)_P$ at a specific pressure and over a temperature range can be obtained. Then the sample's sound speed is measured at different hydrostatic pressures, while being kept at a constant temperature. Substituting these values into equation 2.10, B/A can be obtained for a specific temperature.

This is rather easily implemented and obtains accurate results (around 3% error) [36]. However, the main disadvantages of this system are the extreme pressure (0-14MPa) and temperature (0-80°C) differentials required to obtain accurate readings [16], since these variations could do damage to sensitive samples [7]. The time frame for taking these readings is much longer than most other techniques since many separate steady state readings must be taken. Also, some components in the isobaric part of the equation are difficult to obtain accurately for small volume samples.



### *Isentropic Phase Method*

The reason that equation 2.9 was split into its thermodynamic components for the above technique is because of the difficulties associated with creating an isentropic system, i.e. a system to which no heat is added or removed. Consider a sample which is quickly pressurized and depressurized ($T < 5s$), with relatively low pressures (200kPa). Under such conditions very little heat will be transferred in or out of the sample and thus such a system can be assumed to be isothermal for that period [9], since constant entropy is valid for no transfer of heat. The faster this occurs the more accurate the assumption.

Taking the readings under these conditions ensures that the isobaric component of equation 2.10, used in the previous method, can be avoided, thus improving inaccuracies to around 1% [36]. It should however, still be noted though that thermal regulation is required to prevent external heat being transferred in or out of the sample. Another noticeable difference between the techniques is the requirement for an automated sampling system to ensure that sufficient samples are taken

within the 5s time period, whereas in the thermodynamic method, only one sample needs to be taken at each set point [9].

## *Other Methods*

As can be seen from previous equation the speed of sound increases with fractional changes in density, at a rate dependent on B/A. Thus as a planar wave travels though a sample media, the crest of the wave will travel faster than the trough [30] [33] [34]. This distortion becomes more apparent the higher the frequency of the source and the further waveform is from the source. The indirect methods use this distortion of sound waves in order to calculate B/A.

Two techniques for calculating B/A from this phenomenon, have been developed: the Finite Amplitude Absorption and the Optical Diffraction technique. Since these techniques were not in the scope of this project only a very brief explanation of them will be given.

The Finite Amplitude Absorption technique involves placing a receiver a known distance away from a relatively powerful acoustic source. The receiver measures the size of the transmitted waveform and its harmonics, and the value of B/A is calculated from the amplitude relationship between the fundamental and second harmonic. The transmitted sound waves that have been used vary from amplitude 80kPa to 620kPa at 3MHz [6]. This technique does not require isentropic conditions nor need constant temperature [6]. However, due to the difficulties in analytically calculating some parameters required for this technique to obtain B/A, it can sometimes be quite inaccurate (around 5% error) [36]. Experimental data shows that this method tends to produce inflated results.

The other implementation that uses the same phenomenon is the Optical Diffraction technique. A laser is pointed normal to ultrasonic waves. As a wave travels though the liquid and moves under the laser, the light is diffracted due to the phase grating effect of the liquid [19]. The measurement of light intensity of a diffraction order, in comparison to wave profile, can be used to determine B/A [20]. This technique obtains a more accurate result than the Finite Amplitude method, with an error around 4% [23], however it is limited to transparent media.

Although both indirect systems are very useful and function under fluctuating temperatures, they do not obtain the same accuracy as the direct techniques, and thus many systems designed for taking accurate B/A readings use one of the direct techniques.

*Chapter 4*

# Measuring B/A using Small Sinusoidal Pressure Waves

This is an attempt to measure B/A using a direct method, based on the isentropic phase technique. In order to implement an isentropic system, no heat exchange can take place in the sample while the readings are occurring. This is obviously impractical. The isentropic phase technique assumes that if the pressure fluctuations are fast enough, there is insufficient time for significant heat to be transferred into the sample. Thus, isentropic conditions can be assumed.

Previous implementations of this technique have used pressure bursts from a regulated pressure source through a pressure restrictor. As the pressure on the sample rises, measurements of pressure and sound speed are taken. These are later analyzed to obtain a value for B/A. The restrictor is designed to give a sufficiently slow rise in pressure so that sufficient data points can be taken, and yet have the sample at full pressure within a short time (say two seconds), after which the pressure can be removed, in order to keep the system quasi-isentropic.

This technique gives excellent results. However, since only positive pressures are applied to the system, only positive heat is created and removed by the pressure pulse. Thus, although for a single iteration this heat is negligible, continuous operation might cause compounded heat and thus create an error in measurement. To avoid this sufficient time must be allowed between readings to ensure that each reading is taken at steady state.

A possible solution to this dilemma is to substitute the pulsed pressure source with a sinusoidal source. Then, heat generated by the positive pressures would be cancelled by the heat absorbed in the negative pressures. so the system should remain in a steady state. Also, since pressure is fluctuating continuously, readings can taken and a real-time B/A can be calculated. The same thermodynamic considerations still hold though, in order for the sample to be assumed to be isentropic the pressure waves still need to occur at a relatively fast rate. Another advantage of

attempting to create sinusoidal waves that can be easily changed in magnitude and period of the pressure, is that the temperature effects due to the fluctuation of pressure in the system can be experimentally studied.

This study is intended to use small pressure changes (<20kPa) to take the readings of B/A of small samples (<0.15 ml) of liquid, with the aim that the system could be used on delicate samples that cannot survive large pressure fluctuations and are not available in large quantities. The use of small samples will make the system more susceptible to changes in surrounding temperature, since it will take less time to heat up the smaller amount of liquid. This will have to be overcome by either running the pressure system at a high enough speed, or attempting to cancel out the effect of the cyclic temperature fluctuations.

*Chapter 5*

# Techniques for measuring Speed of Sound

By far the most stringent requirement to obtain accurate measurements for B/A, is to measure the speed of sound inside the sample liquid. To put this measurement into perspective, consider a sample of water at 30°C. It has, from previous measurements, a B/A of about 5.2. That translates to a fractional change of sound speed, for every 1kPa change in pressure, of $1.5 \times 10^{-6}$.

## *"Time of Flight" Techniques*

Traditionally, speed of sound is measured using the "Time of Flight" technique. This technique has a rich history and is implemented in many, if not most, distance measurement and velocity calculation techniques. An ultrasonic transmitter is placed a known distance from a receiver. The liquid sample is placed in the cavity between transmitter and the receiver. A pulse of ultrasound is emitted by the transmitter and the time is measured for the signal to arrive at the receiver. Although distance between the transmitter and the receiver can be measured very accurately, the difficulty of this technique is to obtain a very accurate time measurement.



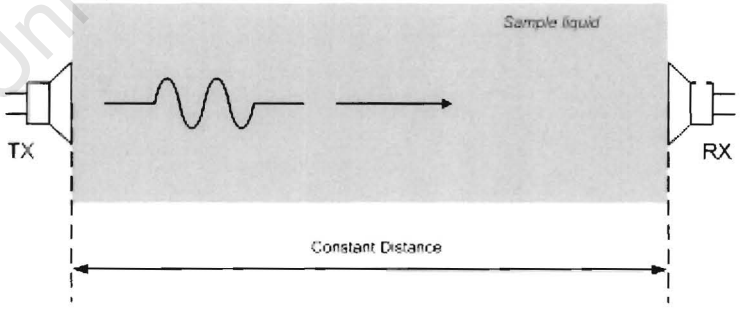


*Fig 5.1: Illustration of a "Time of Flight" system, showing a single ultrasonic pulse travelling through the liquid. The time taken between the pulse being transmitted and the pulse arriving at the receiver allows for the sound speed of the liquid to be determined.*

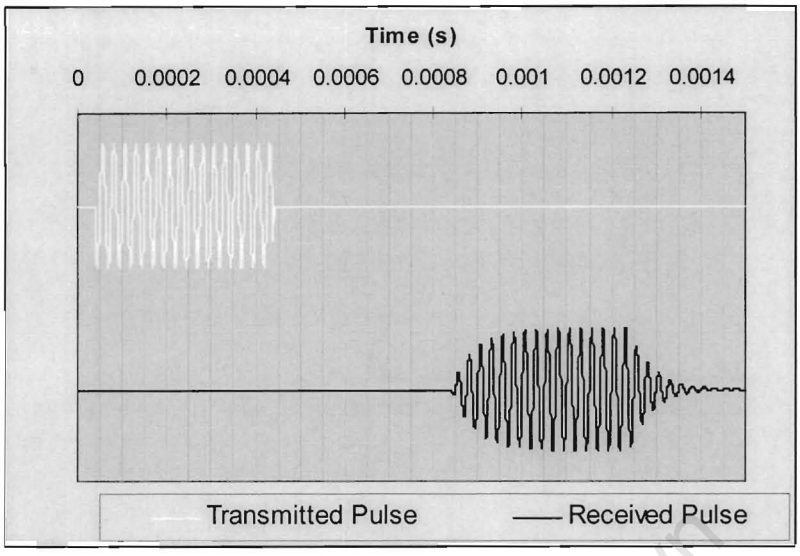


*Fig 5.2: Simulated transmit and received signal from a "Time of Flight" system. The upper waveform represents the signal used to drive the transmitter and the lower waveform represents the receivers signal. Note the nonlinearity in the received pulse.*



The accuracy of this time measurement is mostly affected by the distortion of the pulse as it travels through the liquid medium. The liquid acts as an acoustic filter, as can be seen in the figure above. Notice that the first few waves are reduced in size and that the pulse rings down as it completes. This makes it difficult to measure the exact point when the pulse started or ended. Thus, an error is introduced into the measurement system. This error is often represents itself as a timing offset since the system's parameters are often quite consistent. Several techniques have been developed to work around this problem:

1. *Sing-Around System*

   The transmit signal is triggered by the arrival of the receive signal. The time of flight can be calculated as the period between triggers. This system still has some of the previously mentioned errors, and also suffers from an additional error from timing delays between the signal arriving and the new one being triggered (accuracy around 0.01%) [14].

2. *Pulse Superposition*

   The pulses are triggered at a constant frequency, which is adjusted so that the received pulse and echoes, from previous pulses, line up with newly transmitted pulse. Thus a

constant integer number of pulses are in the sample at any time. By using the number of pulses in the sample and the triggering frequency, the speed of sound can be calculated (accuracy round 0.006%) [27]. This system has proved to be more accurate since the pulses and echoes can be lined up to ensure that the effect of the distortion mentioned above is cancelled out. Generally this is a manual operation suited only for static systems.

3. *Pulse-Echo Overlap method*

   This uses the same principle as the Pulse Superposition method, except that only one pulse is in the sample liquid at a time. This removes the ambiguity regarding the number of waves are in the sample. However, it will be more difficult to get accurate readings since there will be fewer echoes to superimpose.

The techniques described above have one major disadvantage in comparison with the simple time-of-flight technique, being that in order for them to be accurate they need to be controlled manually. This is acceptable for the Thermodynamic technique, however for the isentropic phase technique, the speed at which the samples need to be taken, requires an automated system [9].



## Pulsed Phase Methods

For this method, both pulsed phase systems and continuous wave locking techniques have previously been implemented. The pulse phase systems work on the basis that the phase information of the returned pulses will give an improved resolution on the sound speed measurement over simple amplitude thresholding. Two streams of thought have been implemented for this purpose.

1. *Pulse Phase measurement*

   For this technique the received pulse is multiplied with the carrier waveform that is used to create the transmit pulses. This multiplication gives 2 components; one is a DC value proportional to the cosine of the phase between the waveforms, and the other a sinusoidal component at twice the original frequency. This high frequency component is filtered away. Thus the phase angle can now be approximated between the transmitted and received

waveforms. The equation for calculating B/A was then manipulated to use this phase information. [15]

$$\frac{B}{A} = -\frac{2\rho_0 c_0^3}{l\omega_0}\left(\frac{\Delta\phi}{\Delta p}\right)_S \tag{5.1}$$

Where $\phi$ is the phase angle and $\omega$ is the transmitted frequency.

Thus as the pressure in the system changes, the returning pulse arrives back at a slightly faster or slower rate. Thus the phase angle will change and this will be used to calculate B/A. Although this technique has been successfully implemented [15], it is prone to some errors (B/A error around 3%). Most of the error can be attributed to the phase detector. It can only be assumed to be linear with phase angles around zero, so if the locked angle is larger or if the phase changes a large amount with pressure (large B/A), the relationship between phase angle and pressure will be distorted. Also, the phase reading is dependent on the magnitude of the reference and received waves. Thus if the size of the return pulse changes, the phase reading will be affected. An obvious case in point is the distortion of the return pulse by the acoustic filter affect.



2. *Pulse Phase Locking*

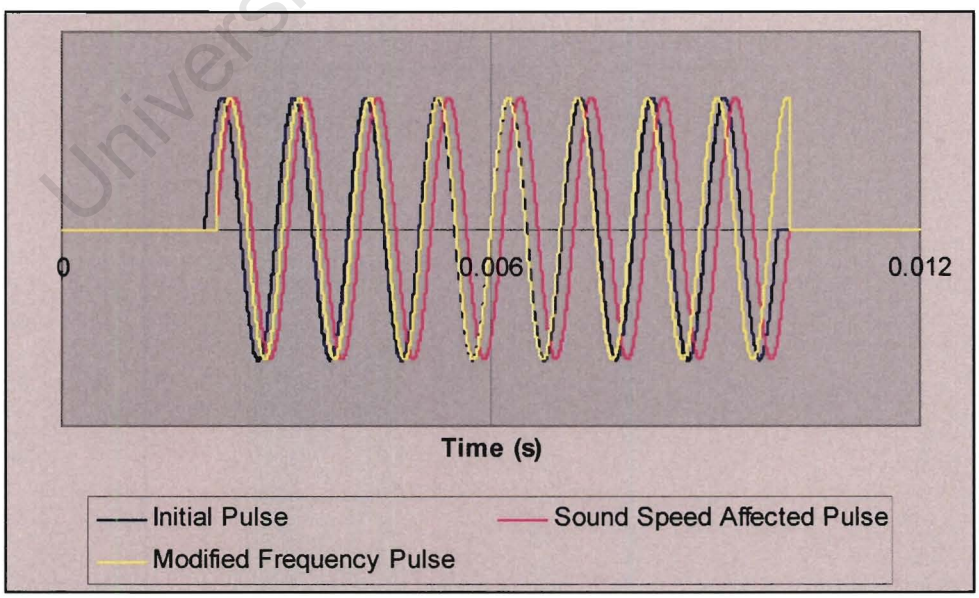


*Fig 5.3: Demonstration of Pulse Phase locking technique for decrease in sound speed and t0 at 0.006s. If the initial and sound speed affected pulses are compared, one can see that*

*the have a phase difference. Thus at the sampled point (T=0.006) there is an error. The Carrier frequency is then adjusted so that the initial and Modified Frequency pulses line up at the sampling time.*

A specific time, $t_0$, after a pulse (at a specific carrier frequency) is transmitted, a voltage sample is taken from the receiver. This time is manually set for each experiment so as to coincide with being roughly halfway in the received pulse and to be at a phase angle of about zero degrees. The first sample acts as a reference for all samples to follow. When the sound speed changes, the pulse will arrive at a different time index compared to the original waveform and the sampled voltage will be at a different point at the received sine wave. The frequency of the carrier waveform is then adjusted so as to return to the reference voltage. From figure 5.3, this means the "Modified Frequency Pulse" is adjusted in such a way as to make it line up with the "Initial Pulse" at the reference time ($t_0$ = 0.006s). The equation to calculate B/A is manipulated to use the fractional change in the carrier frequency.

$$\frac{B}{A} = \frac{2c_0^2\rho}{f_0}\left[\frac{\Delta f}{\Delta p}\right]_{Sq} \tag{5.2}$$

Where $\Delta f$ is the amount that the frequency needed to be adjusted and $f_0$ is the initial frequency of the pulse.

This technique has better results (compared to the phase measurement system) (B/A accurate to around 1%) [12], since the control loop removes the inaccuracies of the phase detector. However it is sensitive to changes in magnitude of the received pulse associated with the frequency dependence of liquid attenuation, and it is also sensitive to moving the carrier frequency away from the resonant frequency of the transducers [9].

## Continuous Wave Technique

Continuous wave locking techniques were proposed by Sehgal et al.[32] as an alternative to the pulsed techniques previously used. A transmitter and receiver are placed a constant distance apart.

Then phase locked loop is used to set up standing waves, in the sample media, between the transmitter and the receiver.

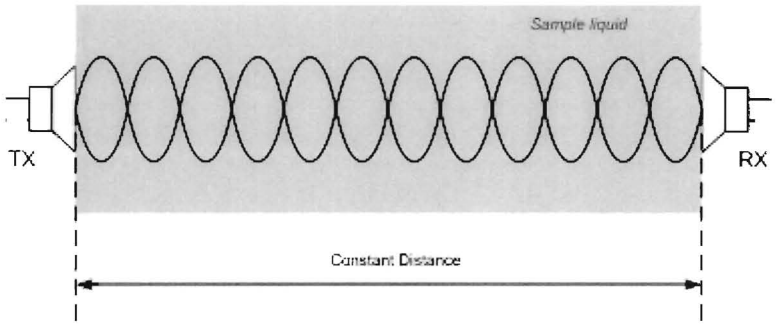


*Fig 5.4: Illustration of a continuous wave system, showing standing waves that have been set up inside the liquid. The frequency of the standing wave will change with sound speed.*

The frequency of the controlled wave is proportional to the speed of sound in the media and inversely proportional to the distance which the sound needs to travel. Also, since there are multiple waveforms in the system, the frequency, inside the Sample liquid, is an integer multiple higher than the fundamental. Therefore: $f = \frac{nc}{d}$, where $f$ is the frequency, $n$ is the number of waveforms, $c$ is the speed of sound in the media and $d$ is the distance between the receiver and the transmitter. Since the distance is constant due to the design, the frequency proves to be an accurate measurement for the speed of sound.

However there is still an ambiguity since the number of waves that are within the media is not known. Also, if the speed of sound is calculated from the above equation, the distance between transmitter and receiver must be measured to a high resolution, to ensure the necessary accuracy in sound measurements.

From the above equation, and by observation, the controlled frequency in the media is a scaled measurement of the speed of sound. Thus fractional changes in the frequency will equal fractional changes in the speed of sound:

$$\frac{\Delta f}{f_0} = \frac{\Delta c}{c_0} \tag{5.3}$$

Where $f_0$ and $c_0$ are the initial frequency and sound speed.

From this knowledge, Everbach [12] rewrote the equation for B/A so that fractional changes in frequency relative to changes in pressure can be used instead of changes in sound speed. Thus:

$$\frac{B}{A} = \frac{2c_0^2\rho}{f_0}\left[\frac{\Delta f}{\Delta p}\right]_{Sq} \tag{5.4}$$

The continuous wave locking techniques have several advantages. Firstly the locked frequency proves to be a more accurate measurement than the time of flight techniques previously used. Also the readings taken are done in real time. Another improvement is that the systems thermodynamics are at steady state since the transducer is permanently driven and locked onto a specific impedance point. The difficulty in obtaining accurate results with this technique is to avoid the nonlinearities that occur in the frequency measurement due to phenomena like frequency pulling [9] and changes in the acoustical system. These effects are due to parameters of the piezo driver that is used and will be described in the next chapter.

An alternative transducer implementation of this technique, proposed by Davies[9], is the use of a piezo-electric tube instead of the transmitter and receiver pair. When a standing wave is set up in the tube, the electrical characteristics of the tube change substantially, therefore the standing waves can be tracked. This is the technique that has been implemented in this study.

*Chapter 6*

# Measuring the Sample Medium Parameters

Essentially the fundamental part of this project is the accurate measurement of pressure and sound speed in the medium under isentropic conditions. This chapter aims at providing insight to how these measurements were achieved and also shows the limitations of the implementations.

Care was taken when the sensors were implemented to ensure that they are accurate, fast enough and also small enough to fit within the confines of a thermal jacket. The sensors were chosen in such a way that they remain at thermal steady state while in operation.

The measurements that needed to be taken from the liquid were the frequency of a standing wave of sound in the liquid, the pressure of the liquid and the temperature inside the measurement cavity. The techniques used to take these measurements are described below with reference to the need, implementation and accuracy of the sensor.



## *Speed of Sound of Liquid Sample*

The following section describes the sensor used to measure the sound speed of the liquid sample. The design of the sensor can be split into two parts, the conditioning of the actual sensor to ensure that it produces accurate results, and the electronics used to convert the change in impedance properties of the sensor into a useful format. This is achieved using a Phase Locked Loop (PLL).

### The Piezo-Ceramic Tube

Piezo electric ceramics are materials that have been designed in such a manner that if a voltage is applied across a specific polarized axis, the material in that axis will expand or contract depending on the sign of the voltage. The inverse is also true, if the material is under strain in the polarized direction, a voltage is induced. These materials are created by heating specific types of ceramics to

high temperatures and allowing them to cool while being exposed to an intense magnetic field. The polarized direction of the piezo is in the orientation of that magnetic field.

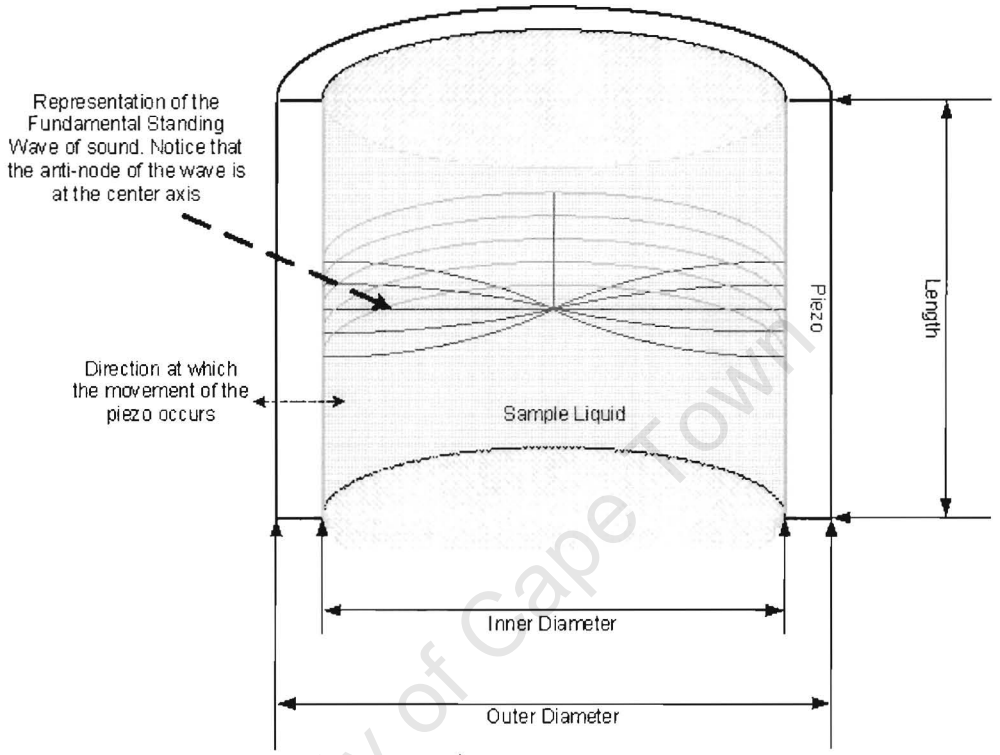


*Fig 6.1: Illustration of a liquid filled piezo tube, with the front half of the tube hidden. The wall of the tube sets up a standing wave in the liquid since when a standing wave is set up, the exact sound speed can be determined. Although the fundamental wave is represented, any multiple of it can be used.*

A single tube shaped piezo was used instead of two separate parallel transducers, since it proved much easier to implement. The bottom of the tube was simply closed so that the sample could be loaded into the cup that the tube and base form. As the top of the tube is open, the sample is exposed to the pressure of the air from above. This is much easier to implement than having two transducers that need to be parallel to each other. The cavity wherein the sample will be, in a 2 transducer method, also needs to be primed and a port would have to be added to ensure that the sample liquid can be pressurized. Also the two transducers would have to be rather well matched.

The piezo transducer implemented was a tube made from PZ27 compound and was polarized inwards. Thus as a voltage was applied to the piezo tube, it would contract or expand with reference to the tube's centre axis.

A piezo tube has 3 main natural resonances:

- *Thickness mode*: This is the mode that is created due to the thickness of the tube. It has the largest effect and around it will be the liquid modes that will be later used.
- *Circumferential mode:* This mode occurs through the diameter of the tube. It is at a much lower frequency that the thickness mode.
- *Length mode:* As the thickness of the piezo material reduces the length of the piezo will increase proportionally via Poisson's ratio. Thus there is a length mode. Due to the common dimensions of the tube this mode also normally occurs at a significantly lower frequency that the thickness mode.



| Thickness Mode | Circumferential Mode | Length Mode |
|---|---|---|
| $f_r = \frac{2N_t}{OD - ID}$ *where OD and ID are outer and inner diameters respectively* | $f_r = \frac{2N_c}{OD + ID}$ | $f_r = \frac{N_{31}}{L}$ *where L is the length of the tube* |

*Table 6.1: Formula describing the frequencies of the fundamental modes of a piezo tube [22].*

When a liquid is placed inside the tube, the movement of the piezo is coupled into the liquid. If the piezo is made to oscillate at a frequency dependent on the diameter of the tube and the parameters of the liquid, it can set up a standing wave inside the cylinder, as illustrated in figure 6.1. While a standing wave is set up, less energy is required to move the piezo tube since returning waves aid in setting up new waves. Thus the electrical characteristics of the liquid filled piezo tube will fluctuate around frequencies where standing waves are set up.

For this implementation, the piezo was fixed to a brass base using a silicon sealer. Since the silicon is a relatively loose joint, it has a negligible affect on the piezo tube. Then a sample liquid is then loaded to full the cylinder. To observe the liquid modes, and to see what effect the thickness mode has on them, an impedance spectrum was taken with the cylinder both empty and full.

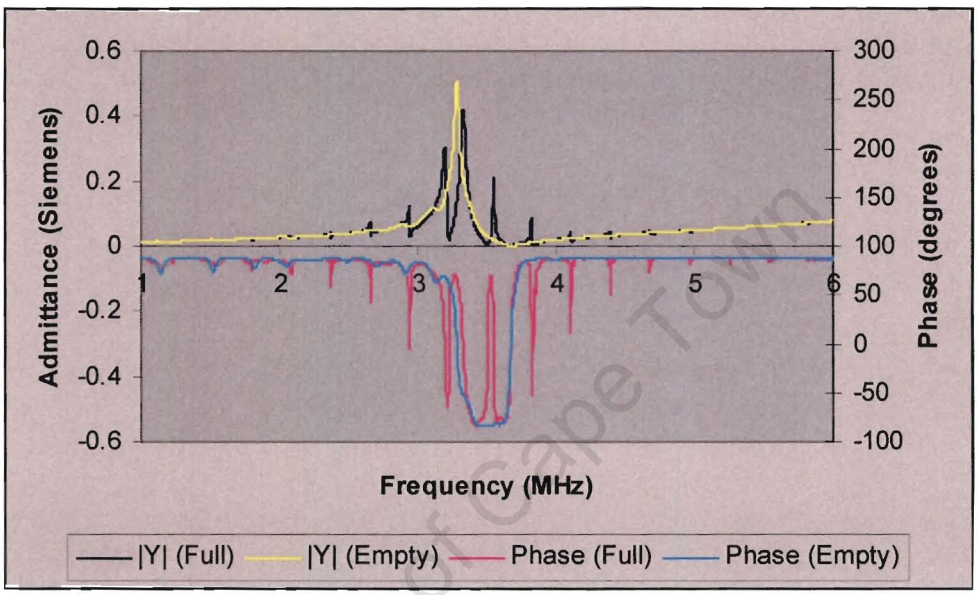


*Fig 6.2: Impedance spectra of an empty and water filled piezo tube to illustrate the effect that the liquid has on the piezo. The additional modes that can be seen on the full plots are due to standing waves being set up in the tube. This tube has an inner diameter 5.2 mm and outer diameter of 6.35 mm.*



Firstly in the middle of the empty spectrum is the thickness mode of the tube. It should occur at 3.4 MHz ± 10% for a tube of PZ27 with a wall thickness of 0.575mm from the formulas mentioned above. Comparing empty and full spectra, one can see the water modes. Each one represents a standing wave of sound in the liquid, as each multiple of the initial standing wave is a standing wave itself. Also note that the water modes that are around the thickness mode are much larger than the modes that are near to the extremities. This is because the thickness mode acts to amplify the water modes. Unfortunately the thickness mode also has an effect on the positioning of the water modes that will be discussed later.

The size and the positioning of the liquid modes are dependent on several parameters of the liquid and the tubes itself. The main effects are listed below:

## 1. *Sound Speed*

The most obvious effect is that the speed of sound dictates the frequencies at which the modes occur. With a low speed of sound, the time taken to travel through the cylinder will be longer, thus the standing wave will have a large period and thus the frequency intervals between the liquid's modes will be rather short. Liquids with a high speed of sound, like water, have modes that are rather spread out. Also, since the exact location of the mode is dependent on speed of sound, the movement of a single mode is what will be used to measure fractional changes in speed of sound.

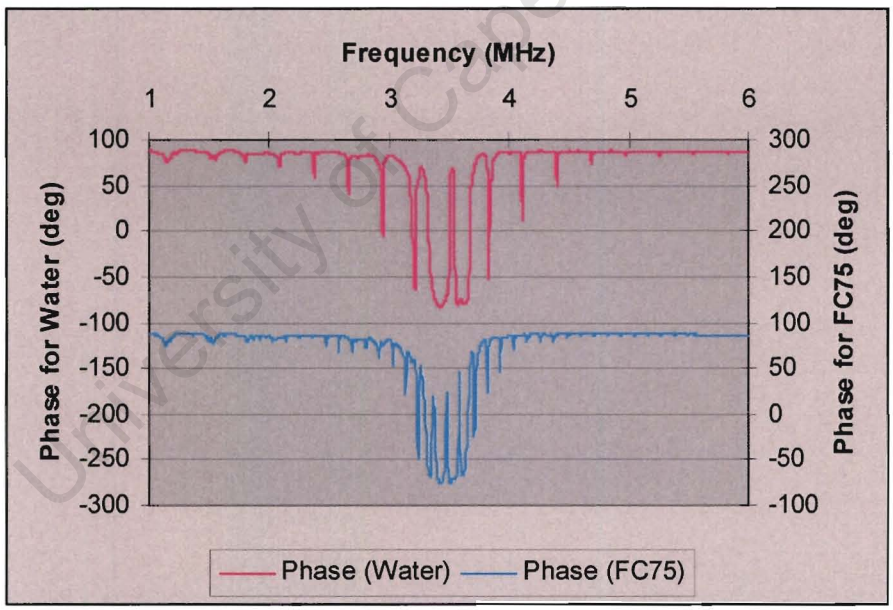


*Fig: 6.3: Phase spectra of the tube filled with water and with FC75. FC75 has a lower sound speed than water and thus the liquid modes are closer together.*

Thus the equation for the frequencies at which the modes occur is $f_n = \frac{nc}{d}$ (equ.6.1)[9], where $n$ is the mode number, $c$ is the speed of sound of a specific sample liquid and $d$ is the diameter of the tube. Since the tube has a specific diameter and the fluctuations in that diameter are

extremely small compared to the diameter, it can be assumed that any changes in frequency are dependent on the changes in speed of sound only. Thus for the sample of water each mode should be about 285 kHz apart, which can be observed in the spectrum. It should be noted that this equation only holds true for modes that are not on top of the thickness mode.

## 2. *Frequency pulling*

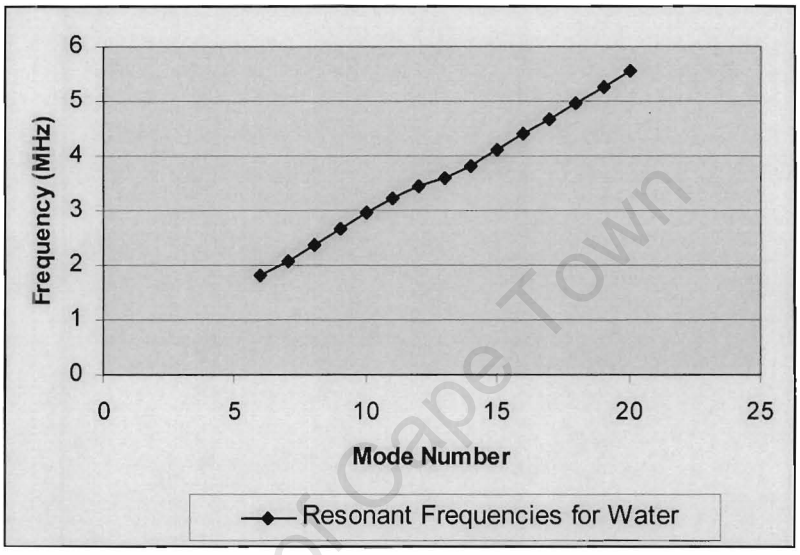


*Fig 6.4: Plot of Resonant Frequency vs. Mode Number to show frequency pulling. The nonlinearity around Mode Number 12 is due to frequency pulling happening around the thickness mode of the tube (3.5 MHz).*



Frequency pulling is an effect influencing the liquid modes that are on top or very close to the thickness resonance of the cylinder. The frequency intervals between modes deviate from the linear relationship (defined in equation 6.1) when they lie over the thickness resonance, while the modes before and after the thickness resonance are still at the same frequency interval [9]. What is also important to note is that the movement of these modes due to changes in sound speed will also be distorted for the modes that are in the frequency pulling range. This will introduce errors in B/A readings taken from the affected modes. Measurements that are to either side of the affected area will produce very accurate results [9].

### 3. *Acoustic Coupling*

The size of the liquid modes is largely proportional to how well the mechanical energy is coupled from the piezo into the liquid. In a system with good coupling between liquid and piezo, the standing wave will have a larger effect on the piezo tube's spectrum and thus the system will have more dominant liquid modes. Some liquids attach themselves better to solids, like soaps, and thus have better coupling properties, while others, like plain water, have smaller modes.

Obviously, if the modes are too small it makes them difficult to track, and in some cases even hard to see at all. Davies [9] came up with a solution to this problem. He would wet the tube with a soapy liquid and then wash it off again. After the soapy water is removed, the new sample could be loaded. Although there is no soapy water left in the cylinder, the walls of the cylinder still seem to be affected and a vast improvement the coupling between the liquid and the piezo could be seen. The phenomenon has been called the wetting effect. If the tube was left to dry for a couple of days, the effect diminishes again.

### 4. *Level of liquid*

Due to the small size of the cylinder that was used, small changes in level had a proportionally large change in the size of liquid modes. Thus the effect of changes in level was examined more carefully. This was done by using a larger cylinder and progressively filling it with water. An impedance spectra was taken at each of the different levels.

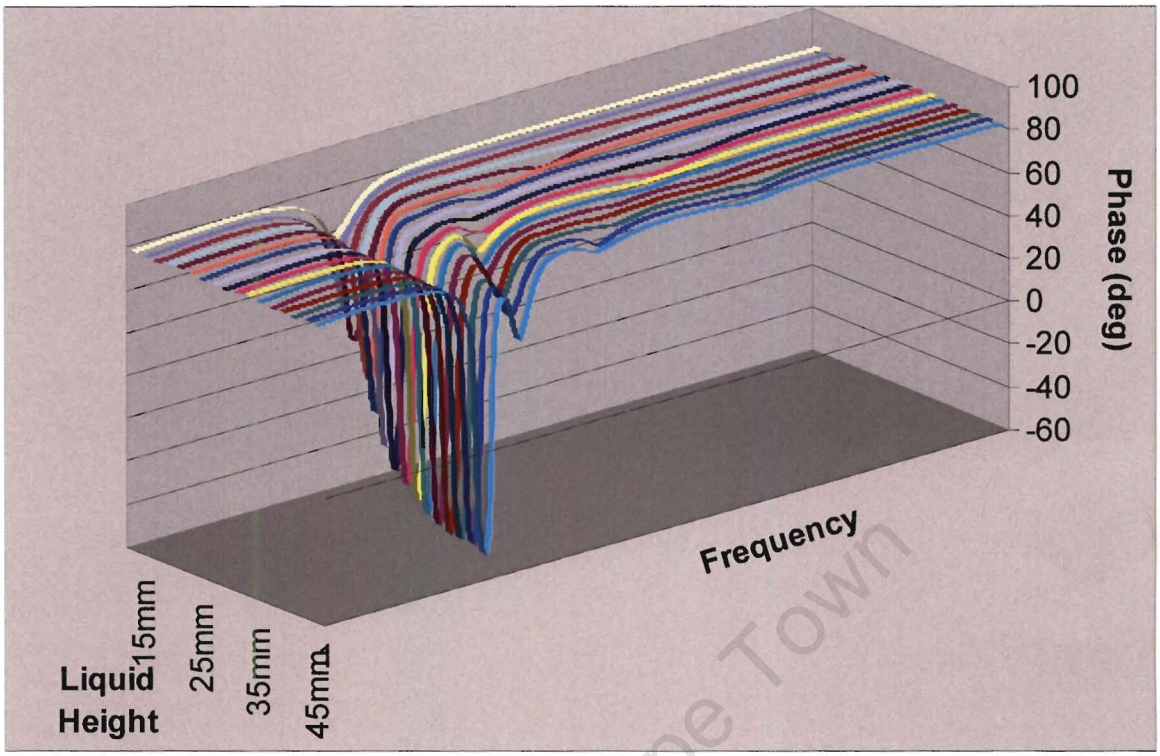


*Fig 6.5: A set of phase spectra of a single water mode as the level was increased in the cylinder, showing the effect of liquid level to mode size. Also observe the smaller length modes moving in closer to the liquid mode with increase in mode size.*



As can be seen from figure 6.5, the size of the mode becomes larger as the level of the water rises. Thus as more surface area of the piezo tube is exposed to the water, the sound coupled into the water increases and the mode will increase in size. Another interesting phenomenon can be seen when examining the smaller modes arriving from the right of the graph with higher levels.

As the level increases the small modes get closer together. The effect can be attributed to length modes that are set up by lengthening and shortening of the piezo according to Poisson's ratio as mentioned before. As the level of the liquid is increased, the frequency gap of the standing waves set up along the piezo tube's length decreases. The equation is $f_{gap} = \frac{c}{2L}$ (equation 6.2). However it is difficult to confirm this equation since the frequency pulling is occurring between liquid mode and the length mode. Due to the size of these

smaller modes, their effect is negligible. Also as long as the level is constant, the movement of these modes with changes in sound speed will be consistent with the movements of the liquid modes.

Since the level of the liquid obviously has major effects on the tube, and the tube that was implemented had a diameter of only 5.2mm (near the size of water's meniscus) the stability of the mode sizes proved to be unreliable. To overcome this, a brass ring tube was siliconed on the top surface of the tube to allow the liquid to be loaded an extra 2mm above the top of the piezo. Thus movements in the water level in the ring had no effect on the amount of surface area that was exposed to the liquid, and thus the size of the liquid modes remained consistent. In this way the reliability of the system was vastly improved.

5. *Inconsistencies in the sample*

As a sample is loaded in the tube, a bubble can easily be trapped in sample. This offers a disturbance to the acoustic system and thus reduces the size of the liquid mode. Also if the sample is depressurized, size of the bubble will increase and as such further impede the acoustic system. This creates a system that fluctuates with changes of pressure, making it difficult to track. Since the tube transmits all ultrasound towards its centre, the centre is the most sensitive to disturbances.

6. *Mechanical loading of the piezo*

External loading of the Piezo will cause a voltage to be induced on the piezo. This by itself has no effect on the phase spectrum. However, the loading could cause a reduction in the size of the thickness mode by damping the system. Thus with a smaller thickness mode the liquid modes will be less amplified and also smaller.

By careful design of the system and selection of the liquid modes used, all the negative effects mentioned above can be overcome or avoided. Thus having selected a reliable liquid mode, of constant size, that changes its resonant frequency linearly with changes in sound speed, a system needed to be designed to accurately measure the relative movements of the mode. The way that was achieved was through a transmission phase locked loop.

## Design of the Phase Lock Loop

In a phase locked loop the frequency from a voltage controlled oscillator (VCO) is applied to the piezo tube. The frequency is then adjusted by a control loop in such a way that the phase between the input voltage, applied to the piezo tube, and the output, which in this case is the current flowing through the piezo, equals a control value.

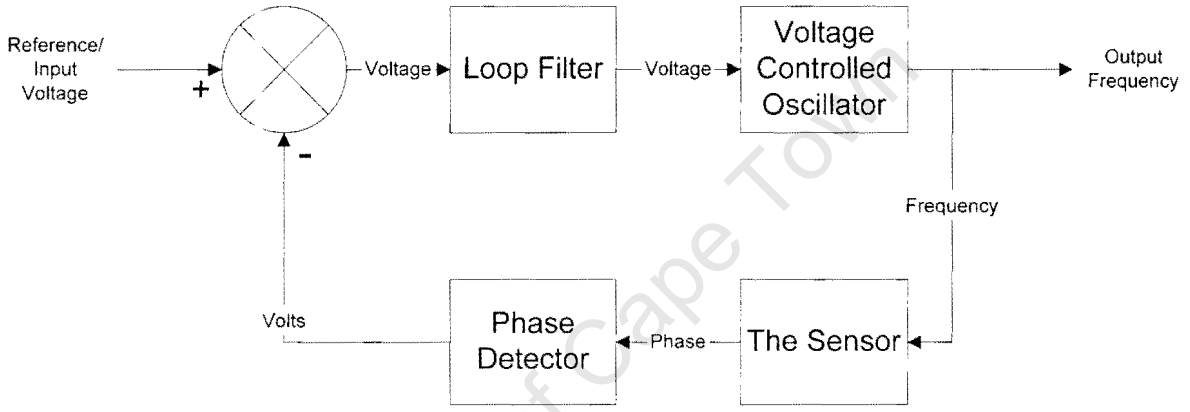


*Fig 6.6: Block Diagram of a generic Phase Locked Loop*

The phase angle is adjusted, by changing the control voltage for the phase lock loop, so that the loop and the frequency span over which the voltage controlled oscillator operates is adjusted so that the phase lock loop tracks a slope of one of the liquid modes. There will be a slight frequency offset between the locked frequency point and the actual resonant frequency, since the phase locked loop simply locks onto the side of the liquid mode. However as long as the liquid mode does not change size, the offset will remain constant and any changes in the position of the mode will be precisely tracked.

A phase lock loop consists of the following 4 components: the voltage controlled oscillator, the sensor, the phase detector and the loop filter, as can be seen in figure 6.6. The accuracy of the system will be dependent on how well each of these factors is implemented.

## 1. *The sensor*

Obviously, for this application, the sensor is the piezo tube. The phase lock loop needs to be locked to one of the liquid modes. Issues affecting its accuracy were discussed in detail in the sections above.

An additional external effect that caused some difficulty in this application was the length of the wire that connected to the tube. Since the tube was encased in the thermal jacket and submerged in the thermal bath, the cable that came out to the phase lock loop needed to be at least 1 m long. Thus the cable's own resonant mode fell very close to that of the tube, since the tube was so thin. This caused some distortion of the impedance spectra of the piezo.

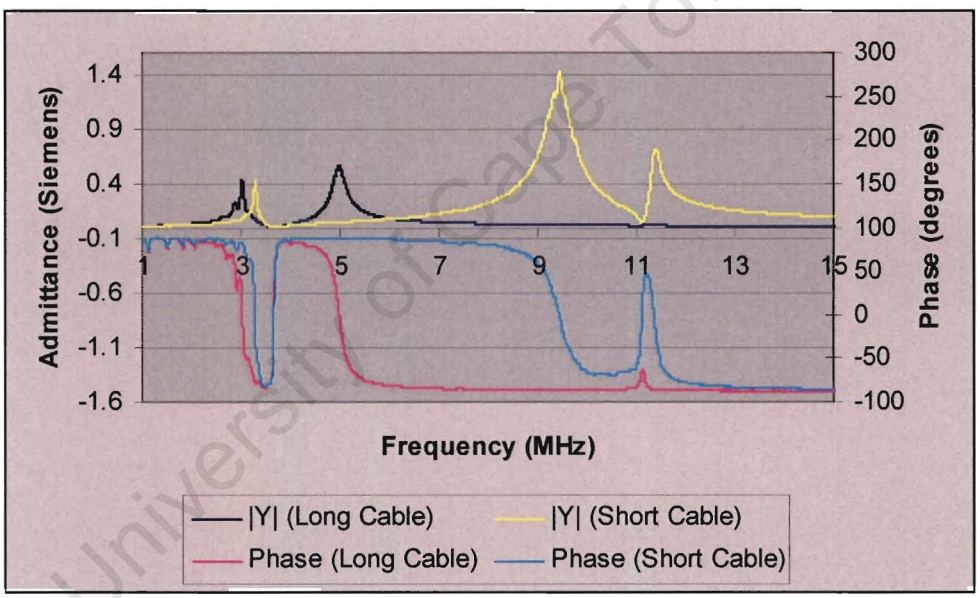




*Fig 6.7: Impedance spectra of an empty cylinder connected with different lengths of cables. The thickness mode occurs at about 3.5MHz. From the long wire spectrum it can be seen that its wire mode occurs at 5MHz, whereas the short wire mode is at 9MHz. With the long wire's mode being so close to the thickness mode it affect the movement of liquid modes that will occur in that area.*

The problem was overcome by laying out a small printed circuit board that contained a drive opamp and a current to voltage conversion circuit. This enabled the PCB to be placed into the

thermal jacket and thus permitted only a very short cable to be used to drive the piezo tube. Consequently the cable mode was moved far enough away from the tube's resonant mode.

## 2. *The Phase Detector*

This phase detector is designed to produce a voltage proportional to the phase difference between the voltage and current waveforms of the piezo tube. However phase detectors are used to calculate the phase difference between any two waveforms.

Several techniques can be used; many are digital, such as using a comparator to create two digital waveforms from the current and voltage sine waves. Then, one uses an XOR gate to compare the two signals together, and taking the average of the output, the phase can be calculated. This is a linear method; however, like most digital methods, it tends to add noise to the ground plane and also requires relatively fast components with small bias voltages to prevent switching delay problems and offset problems.

The analogue technique that was implemented uses a simple trigonometric identity. If the drive signal is considered to be the reference signal and the current is seen as a signal of the same frequency, as the reference, but at a different magnitude and phase, the multiple of those waveforms will contain a component that is related to phase.

$$\text{So } V_d = |V_d|\cos(\omega_0 t) \text{ and } I_r = |I_r|\cos(\omega_0 t + \theta) \qquad (6.3, 6.4)$$

$$\text{Thus } V_d I_r = |V_d||I_r|\cos(\omega_0 t)\cos(\omega_0 t + \theta) = |V_d||I_r|\{\cos(\theta) + \cos(2\omega_0 t + \theta)\} \qquad (6.5)$$

The equation consists of two terms, a DC value that is proportional to the cosine of the phase and an AC value at twice the drive frequency. The frequency component is filtered away. As long as the phase angle is close to 90 degrees the cosine wave can be assumed to be linear. Thus the equation can be simplified to:

$$V_d I_r \approx |V_d||I_r|\theta \qquad (6.6)$$

It should be noted that in order to ensure phase measurement accuracy the amplitudes of the drive voltage and input current must remain constant. This is consistent with the tube system as long as the mode size remains constant.

### 3. *The Voltage Controlled Oscillator*

This block converts the voltage from a controller, to the drive signal for the sensor. It needs to be able to run at a very stable frequency with very little phase noise. Also since the phase detector needs a constant voltage in order to reduce its noise, the magnitude of the voltage produced must be very stable as well. The ideal VCO can be modelled as a perfectly linear relationship between the input voltage and the output frequency.

From the graphs previously displayed (figure 6.3) it can be observed that there are several possible liquid modes that the loop could lock onto, but only some of these modes will produce correct results. Thus the VCO must have the ability to be set over a specific frequency span. Due to the requirement that this detector be used in several measurements of different liquids, the need existed that the centre frequency location and the span over which the VCO operates should be easily adjustable.

The most simple and robust technique that was available to implement the VCO was to use a function generator in RF mode. The device that was used was a HP8656. This device is very robust, it can work to high frequencies with very low noise, and it has a spectral purity of 1 part in $10^8$ [21]. Also it has the ability to create these accurate frequencies at a very low voltage. The implemented system functioned at 20mV to reduce the effect of heating of the piezo. Another advantage is that the frequency span of the VCO can be set down to 1 kHz at any frequency in the required range.

### 4. *Loop Filter*

This component can be seen as the controller of the feedback system. Its function is to ensure that the output frequency will tend in a direction so that the loop locks onto the correct phase angle. The input into the filter is obtained by subtracting the phase voltage from an input reference.

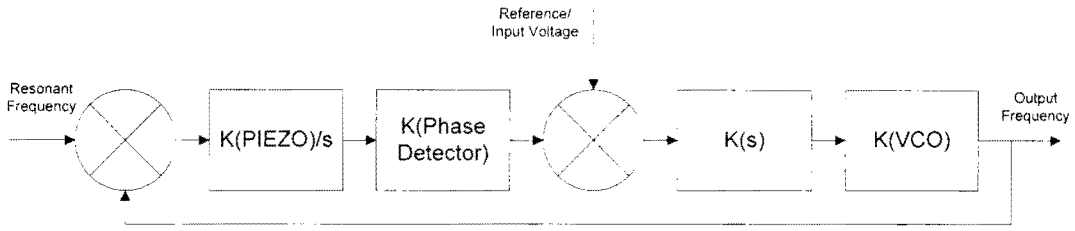


*Fig 6.8: Block Diagram of the phase locked loop for the piezo tube from the perspective of a moving resonant mode rather than from the locking phase. The emphasis here is on how well the loop handles movements in the resonant frequency, rather than how fast the loop locks onto the phase angle.*

The system can be simplified by assuming that both the phase detector and the VCO are linear. The piezo can be simplified as well, on the basis that if the locked phase is in the middle of the phase curve, it is in an almost linear region. Thus the piezo converts frequency to phase and there is a linear change in phase for movement of the resonant frequency. As can be seen from the block diagram (figure 6.6), if the phase angle that is locked onto is made the subject of the equation, it can show how well the system tracks changes in phase angle. However this system must track changes in frequency. The resonant frequency is modelled as a disturbance between the VCO and the sensor. If the resonant frequency is made the subject of the block diagram, the feedback loop link has a gain of one, as is seen in figure 6.8. All the other terms can be grouped to create g(s). The offset value subtracted from the phase is assumed constant.

$$\text{Thus } f(s) = 1 \text{ and } g(s) = \frac{K_{vco} K_{phase} K_{piezo}}{s} \tag{6.7}$$

Thus the system has a pole on the imaginary axis. The controller that was used needed to drive the root locus back into the negative real half-plane. The controller that was used was a lead-lag circuit. The circuit has the characteristic equation:

$$h(s) = K\frac{1+\tau_z s}{1+\tau_p s} \tag{6.8}$$

$$\text{Where } \tau_p = (R1)*(C1) \text{ and } \tau_z = \frac{(R1)*(R2)}{(R1)+(R2)}(C1) \tag{6.9, 6.10}$$

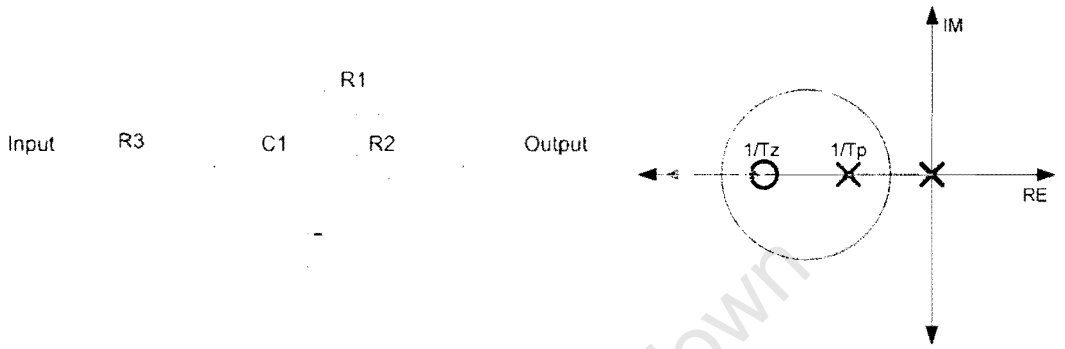


*Fig 6.9 & 6.10: Circuit diagram and root locus diagram for lead-lag controller such as was implemented for this filter design. As can be seen from equation 6.7, the system has an open loop pole at zero. The lead circuit ensures that the system remains stable, fast and non-oscillatory [13] [10].*

The time constants are determined by the resistor and capacitor values in the circuit. The characteristic equation (6.7) of the circuit shows that the pole is always at a smaller negative value than the zero. This circuit makes the system stable and it can be shown that, as long as a reasonable pole, zero and gain value is chosen, the system has a fast speed of response with adequately low noise.

The locked frequency from the function generator was also connected to a frequency counter. It was capable of resolving a frequency input accurate to 0.001 Hz and capable of sampling at high enough frequencies.

## The Pressure Sensor

The other measurement that needs to be taken simultaneously with the speed of sound of the sample is the pressure that is applied to the sample. Examining the equation for B/A, it can be seen

that the pressure measurement does not need to be as accurate as the measurement of the frequency. The resolution that was settled on was 1% of the full scale change of pressure that will be used with a standard test. Since the magnitude of the pressure waves that were implemented was 20kPa to -20kPa gauge pressure, the pressure circuit would need to measure accurately to a resolution of 400 Pa.

The sensor that was used is an MPX100. It is a piezoresistive pressure transducer that has a full scale range of 100kPa [29]. The reason for the large size of full scale pressure is that the system produces pressure manually with a piston and can produce much more pressure that what was required. Thus, especially in the development stage of the project, it proved valuable to be able to pressurize over a larger range without damaging the sensor. The transducer is not fully temperature compensated, but since it will be used in a thermal bath, temperature will not be fluctuating. It has a linearity of 0.25% of its full scale pressure. Thus the maximum error on the device will be around 250 Pa. However the calibration data from tests done on the sensor showed an error of less than 200Pa.

The electrical model for the sensor is a Wheatstone bridge. The circuit is implemented by placing a double regulated reference voltage to power the bridge, and grounding the base. The voltage difference between the other two terminals is proportional to the pressure. The accuracy of the system is dependent on ensuring a stable accurate reference voltage, and taking measurements of the differential voltage with little noise.



### *Temperature Sensor*

Although temperature is not a measurement required within the formula to calculate B/A, it is a fundamental measurement to be taken. The equation for B/A requires isentropic conditions, this means that the system must be under constant entropy. A technique for obtaining this condition is by keeping the temperature in the system constant.

The reason for this can be seen with a close analysis of the equations that determine entropy. Change in entropy is defined by the equation:

$$\Delta S = \int_1^2 \left( \frac{\delta Q}{T} \right)_{\text{int rev}} \tag{6.11}$$

If the system is held under isothermal conditions the equation simplifies to:

$$\Delta S = \frac{Q}{T_0} \tag{6.12}$$

For this reason, as long as the temperature is held constant in the system, the change in entropy is zero.

There are three different ways that heat is transferred: conduction, convection and radiation. All three of these transfer modes require changes in temperature. Thus as long as the temperature is held constant the system will be isentropic.

Consequently, careful monitoring of the temperature in the system is required to obtain results that are accurate. Although the temperature is controlled by the thermal bath, an accurate temperature sensor is required within the thermal jacket in order to see when the sample has reached thermal equilibrium. The need for accurate measurement of temperature can most easily be seen in the following comparison. For a sample liquid of FC75, if the pressure changes 1kPa the fundamental frequency will change 27Hz, whereas if there is a one degree Celsius change in temperature there is a 15 kHz change in temperature.

The sensor that was implemented inside the thermal jacket was a PT100 $1/10th$ Din resistance temperature detector (RTD). It consists of a platinum wire that has been designed to have a nominal resistance of 100Ω. The sensor works on the principle that the resistivity of platinum changes with temperature. The sensor is housed in a 3mm diameter sleeve to ensure that it does not get damaged. It is connected using the four wire technique; since this ensures that the resistance of the wiring does not offset the true result and also reduces connection resistance. The wiring works on the principle that two wires are connected to each sides of the platinum wire, two of the wires are used to drive a constant current through the platinum, and the others are used to measure the voltage across the platinum wire.

An HP34401A digital multimeter was used to calculate the resistance of the wire because it has the capability to take 4-wire resistance measurements, and since it can take resistance readings accurate to 100μΩ. This should give a temperature measurement accurate to $258\times10^{-6}$ °C.

It should be noted though that since the sensor is encased in a thin metallic sleeve surrounded with heat sink paste, it takes some time for the temperature changes from outside the sleeve to pass onto the platinum wire. Except for this nonlinearity, the sensor had no noticeable hysteresis and seemed very accurate.

All the Hewlett Packard devices used had the capability of being networked to a PC using a HPIB bus, thus allowing very accurate and relatively fast readings to be taken and stored on the computer. This especially helped to capture the frequency output from the phase lock loop, since these readings need to be so accurate. The voltage output from the pressure circuit was wired to an ADC card in the computer. The card was a PC30 ADC card produced by Eagle Electronics and was capable of taken readings at a faster rate than the data was received through the GPIB bus.

*Chapter 7*

# Implementing System

The previous chapter discussed the sensors that were used and the factors that affected their accuracy. In this chapter the methods for integrating the sensors to form a complete system will be discussed. This will include the implementation of a thermally regulated sample cavity, the design of the pressure source and the automation of the system through software.

Emphasis in the design was to create modular implementation especially for the pressure system and the thermal jacket that contained the sensors, to permit the systems to be separated without having to take both systems apart. Another emphasis was to keep the system simple and yet versatile enough to allow for implementation changes to be made without a complete redesign.

The mechanical systems design can be broken into 3 main components: the interferometer, the pressure system and the thermal bath. The performance of the interferometer is dependent on both the pressure system and the thermal bath.



## *The Pressure System*

This is one of the main differences between this execution and the previous designs where a pressurized cylinder was used. This implementation attempts to create a more flexible design that is capable of producing positive and negative pressures of relatively small amounts. Another requirement was to be able to change the size and frequency of the pressure that was applied to the sample.

Several options were available for cyclic pressure sources, such as using an acoustic speaker, but due to the difficulties of implementing a high frequency system, such as finding a pressure sensor with a small enough time constant, it was decided to use a piston-cylinder actuator.

Although the piston-cylinder system has the advantage of being very versatile with reference to being able to change the pressure wave size and offset without any difficulties, it has a thermodynamic disadvantage. When pressurizing the air, it tends to warm up, as discussed previously. These temperature fluctuations will be cancelled out during the time of the whole cycle, yet it will affect the instantaneous readings taken for speed of sound and especially the isentropic conditions in the sample.

Previous implementations have used a pressured gas cylinder as a pressure source. A pressure pulse was then passed through a restrictor which created a filtered affect on the pulse to allow for readings to be taken at different pressures. Although the system had already reached thermal equilibrium, the pulse of pressurized air is still a pressure disturbance in the system and will still create slight changes in temperature. The solution that was suggested and implemented to overcome this problem was to pulse the pressure at a high enough frequency that insuficient heat could be transferred into the sample over the time frame, to adversely affect the results. The time frame that was chosen was 2 seconds [9]. The same assumption was initially used in this design, and the effect of decision will be discussed in the next chapter.

The principle behind the piston and cylinder pressure source is that the system will have an initial volume in which a specific amount of air will be trapped. When the piston moves up or down, the volume in which the specific amount of gas is trapped either increases or decreases; from the ideal gas equation, $PV = nRT$, it can be seen that since $R$ is a constant and $n$ remains constant due to the sealed environment, the pressure and the temperature of the system will fluctuate. Thermal fluctuations can be considered to be minimal in comparison with the pressure changes, although it will have effects on the isentropic conditions. Thus the equation that can be used to describe the system can be simplified to $P = \frac{P_0 V_0}{V}$. Noticeable from this equation is that the relationship between changes in volume and changes in pressure are hyperbolic and not linear. This means that in order to produce sinusoidal pressure waves with the piston, the volume would need to be changed in a nonlinear way.

From this volumetric equation, the desired volume inside the cylinder can be approximated. The pressure system was designed that it could be used on the small interferometer whose design will be discussed later, and for a larger interferometer designed by Davies [9]. The internal volume of the larger interferometer was smaller than $50\times10^{-6}\,\mathrm{m}^3$. The cylinder dimensions were then chosen to ensure that it was of sufficient length to allow for a reasonable resolution on the movement of the piston compared to output pressure; and a large enough diameter to ensure that the volume was inside the cylinder was significantly larger than that inside the interferometer, to ensure that enough pressure could be created.

Another implication of the nonlinear relationship between the volume and pressure is that the actuator of the piston would need to be designed to allow for freedom in movement. A crank shaft mechanism was considered; however since the crank shaft does not create true sinusoidal pressure and also due to its rigidity, it would have limited the intended flexibility of the design. A worm drive was chosen instead. Here a motor drives a threaded rod. This rod is coupled to a slider that is connected to the piston. As the motor turns the thread, the slider will move up or down and in such a way the piston will pressurize or depressurize the interferometer.

The advantages of this technique include that the piston can be moved through the full range of the cylinder without restriction, and also that the piston cannot move the slider because the slider is held in place by the thread. Thus once the pressure is created in the cylinder, it is held constant without the motor needing to do any additional work. Disadvantages included that there is a zero pressure crossover distortion between the slider's thread and the threaded rod. This occurred because as the pressure changes sign, the slider is restricted by the opposite side of the thread. Another disadvantage is that the system was slower that a crank shaft system would have been.

A simple negative feedback system was implemented to control the motor. A function generator was used to create the required pressure reference signal. An audio opamp was used to drive the motor. An attempt was made to use a PWM system, but this introduced some noise to the ground plane and thus to the phase lock loop discussed in the previous chapter.

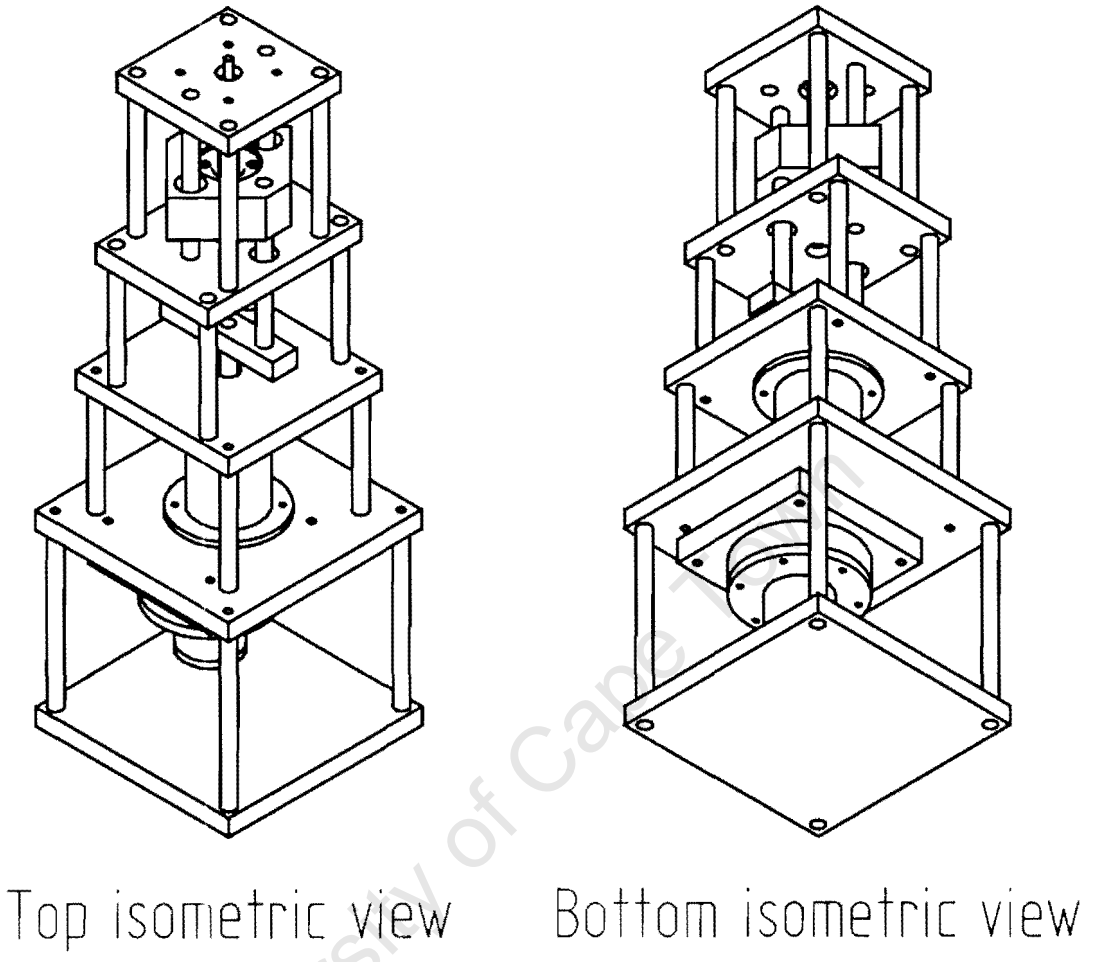


*Fig 7.1: Isometric views of pressure system*

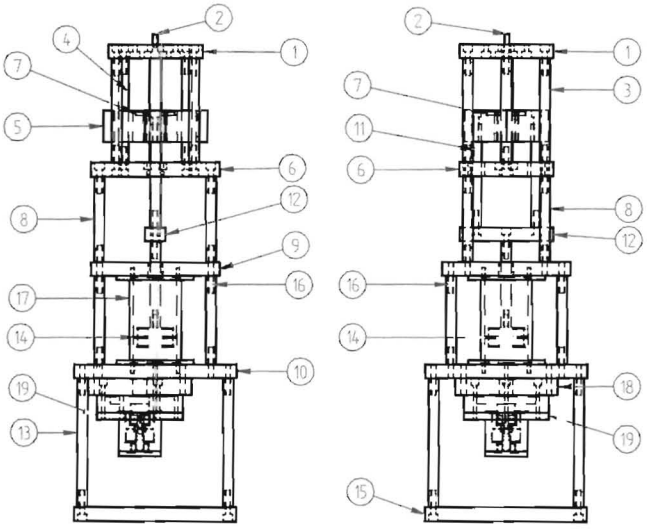


| Item Number | Title | Material | Quantity |
|---|---|---|---|
| 1 | Top plate | aluminum | 1 |
| 2 | Threaded rod | steel | 1 |
| 3 | Upper connecting rods | steel | 4 |
| 4 | Locating rods | steel | 2 |
| 5 | Slider | aluminum | 1 |
| 6 | Lower support plate for slider | aluminum | 1 |
| 7 | Insert for slider | brass | 1 |
| 8 | Middle connecting rods | steel | 5 |
| 9 | Plate above cylinder | PVC | 1 |
| 10 | Plate between cylinder and interferometer | PVC | 1 |
| 11 | Double piston rods | steel | 2 |
| 12 | Double connector | aluminum | 1 |
| 13 | Interferometer Connecting Rods | stainless steel | 4 |
| 14 | Pressure piston | brass | 1 |
| 15 | Base | PVC | 1 |
| 16 | Pressure connecting rods | stainless steel | 4 |
| 17 | Pressure Cylinder | brass | 1 |
| 18 | Inteferometer connection plate | PVC | 1 |
| 19 | Assembly of Inteferometer | | 1 |



*Fig 7.2: Front and left views of the pressure system and a table labelling each part*

## *The Interferometer*

The function of this component is to house the sensors in a sealed environment to allow for the sample to be pressurized, and to ensure that the water from the thermal bath does not leak into the cavities holding the sensors or sample. The other fundamental function of this interferometer is to act as a thermal jacket for the sample liquid.

The interferometer consists of several smaller components constructed from brass. Brass was chosen because it is a relatively good conductor of heat, it is easy to machine, and because it oxidizes very slowly in the water bath. A metal with good heat conduction properties ensures that the time taken for the system to settle will only be a few hours. The components form a sealed environment around the piezo tube. The piezo tube is siliconed onto a base. Initially the base had a hole that led to an external connector that permitted a liquid sample to be loaded through a pipe into the interferometer. Several problems were encountered when ensuring that the sample was loaded in such a way that no bubbles remain in the pipe (the bubbles would expand when the pressure is changed). This would make the level of liquid change in the tube, and the size of the water modes would change sufficiently to distort the location of the phase locked loop frequency. Later the piezo tube was siliconed on a base that could simply be removed and manually loaded to overcome this problem. The base also acts as the ground plane for connecting electrically to the inner plane of the piezo tube.



This base screws into an inner jacket. A lid is screwed into the jacket. The lid contains the temperature sensor, a port for the pressure sensor, and a thin copper wiper that was used to make electrical connection to the outer plane of the piezo. The temperature sensor was held into place and sealed with epoxy, as was the wire from the wiper. A copper tube, used for the pressure port, was silver soldered to the lid, to ensure that it was sealed and had a sturdy connection. A ridge was silver soldered onto the other end of the tube. A plastic pipe was pushed over the ridge and led to the pressure sensor. Total piping was less than 40mm thus keeping pressure path length to sensor minimal. The inner jacket had 1mm holes drilled from its outer wall into the cavity that held the piezo tube. This gave a path for the pressurized air to flow.

The inner thermal jacket screws into an outer thermal jacket with a 2mm gap between the inner and outer jacket diameters. The air gap was used to increase the time constant of the thermal jacket and as a path for the pressurized air to travel. The inner jacket has a thickness of 9mm brass and the outer jacket has a thickness of 15mm, this causes the thermal system to have a settling time of about 1.5 hours. A lid is bolted to the top of the outer thermal jacket. Its functions are to seal the air gap, to give a route for the pressurized air to the air gap, and to house the sensor electronics before the wiring gets removed to outside the thermal bath. The small interferometer is then bolted to the pressure system, making sure that the pressure port lines up and that the wiring can be removed. A base is added to the system to ensure that it will not tip over. The base is sufficiently far away from the interferometer to insure that piezo tube can be unscrewed without difficulties.

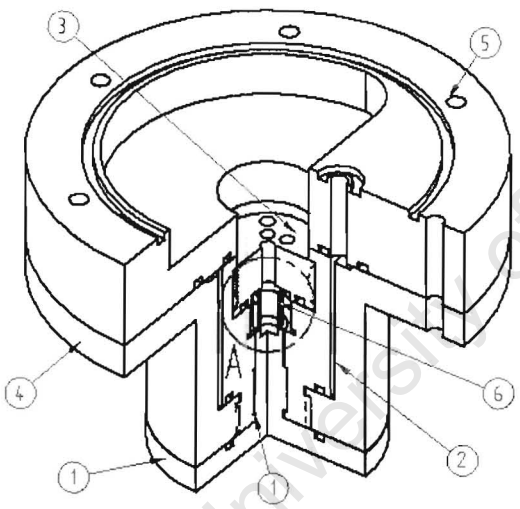


Thermal jacket with a cut out

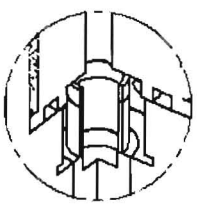

DETAIL A

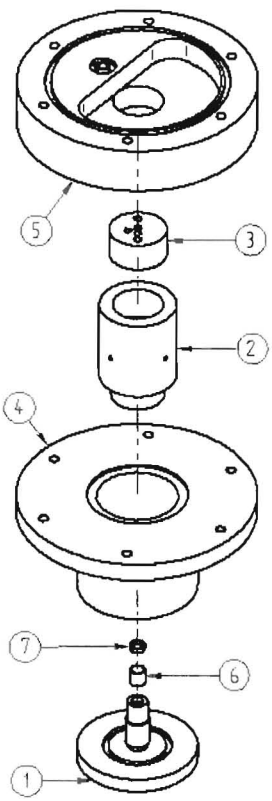


Exploded view of thermal jacket

| Item Number | Title | Material | Quantity |
|---|---|---|---|
| 1 | Base for Piezo Tube | brass | 1 |
| 2 | Inner Jacket | brass | 1 |
| 3 | Inner Lid | brass | 1 |
| 4 | Outer Jacket | brass | 1 |
| 5 | Outer Lid | brass | 1 |
| 6 | Tube Resonator | Piezo | 1 |
| 7 | Liquid level add-on | brass | 1 |

*Fig 7.3: Exploded and cutaway view of the interferometer. The Drawing also contains a table labelling all the parts*

## *The Thermal Bath*

A thermal bath attempts to control the external temperature that surrounds the thermal jacket to a specific value so as to reduce the amount of heat that flows through the thermal jacket once it has reached steady state. This is especially important with reference to creating a quasi-isentropic condition for sample liquid since the most abundant source for change in heat is thermal fluctuations in the surrounding environment.

The thermal bath that was used was designed by Davies [9]. The principle of the design is to surround the interferometer and the cylinder of the pressure system with water at a constant temperature. This was achieved by placing the combined system into a tank constructed from 5mm thick glass. The outside surface of the glass was covered with 25mm polystyrene foam sheets. The tank was then filled until the water level came to the top of the pressure cylinder. The surface area of water that was still exposed to the air was then covered with polystyrene foam packing chips. This ensured that the water was further isolated from the outside air.

Two 500W heating elements were placed into the water to allow the water to be heated above room temperature to a point where it could be controlled. No cooling was used since it is adds to the complexity and cost of the system without adequately improving the system's functionality. An LM35A silicon temperature sensor was used to measure the temperature of the bath; this was fed back to a controller that drove the heating elements. The controller was a proportional integrator and the elements where driven using triacs and diacs modulated at the controlled phase angle. The water in the bath was circulated to ensure that no hot spots would occur. This was achieved using a submersible pump.

The bath could be used to temperatures from 2°C above room temperature to in excess of 45°C, and has a noise of less than 0.003°C. Usually it was run at 30°C because most readings preformed in previous implementations used this temperature. The bath takes 2.5 minutes for every 1°C change in temperature change in water temperature.

All additional components that were used for structural purposes composed of PVC plates with stainless steel rods, if they were submerged in water; or made from aluminium plate with steel rods, if they were above the water line. The reason for the use of aluminium was because the author tried to ensure that the apparatus did not become top heavy. The cables were removed from the water bath using a plastic pipe "dam" to ensure that no water leaked into the interferometer.

## *Software*

Due to the speed of the system, and the accuracy and post processing needed on the readings, it was important to automate the system. As described in the previous Chapter, all the sensors that measure parameters directly affecting the sample were implemented in such a way that they eventually connected to a PC. The PC that was used was an Intel Pentium 150 with 16Mb of RAM. It had a Hewlett Packard HPIB card and a data capture card that was capable of doing analogue to digital conversions.



The software tool that was used to implement the system was HPVEE. It is a visual language, from Hewlett Packard, where software blocks are used to represent components of the system. By interconnecting the blocks, a flow of commands and data can be set up to form a program.

HPVEE was used because it connects well to Hewlett Packard instruments and due to its ease of implementation. Although panel drivers where available for most of the instruments used, a need existed to speed up the code, and thus some of the instruments, like the frequency counter and the function generator, were implemented using the GPIB commands found in the devices software implementation manuals.

The emphasis on the software implementation is to take fast readings of pressure and frequency and to ensure that the readings are taken simultaneously. This is achieved by initializing the Hewlett Packard instruments in such a way that they have all features disabled except the desired function so that the instruments can perform these functions at maximum efficiency and also by setting the device so that it only needed to be triggered to perform the measurements.

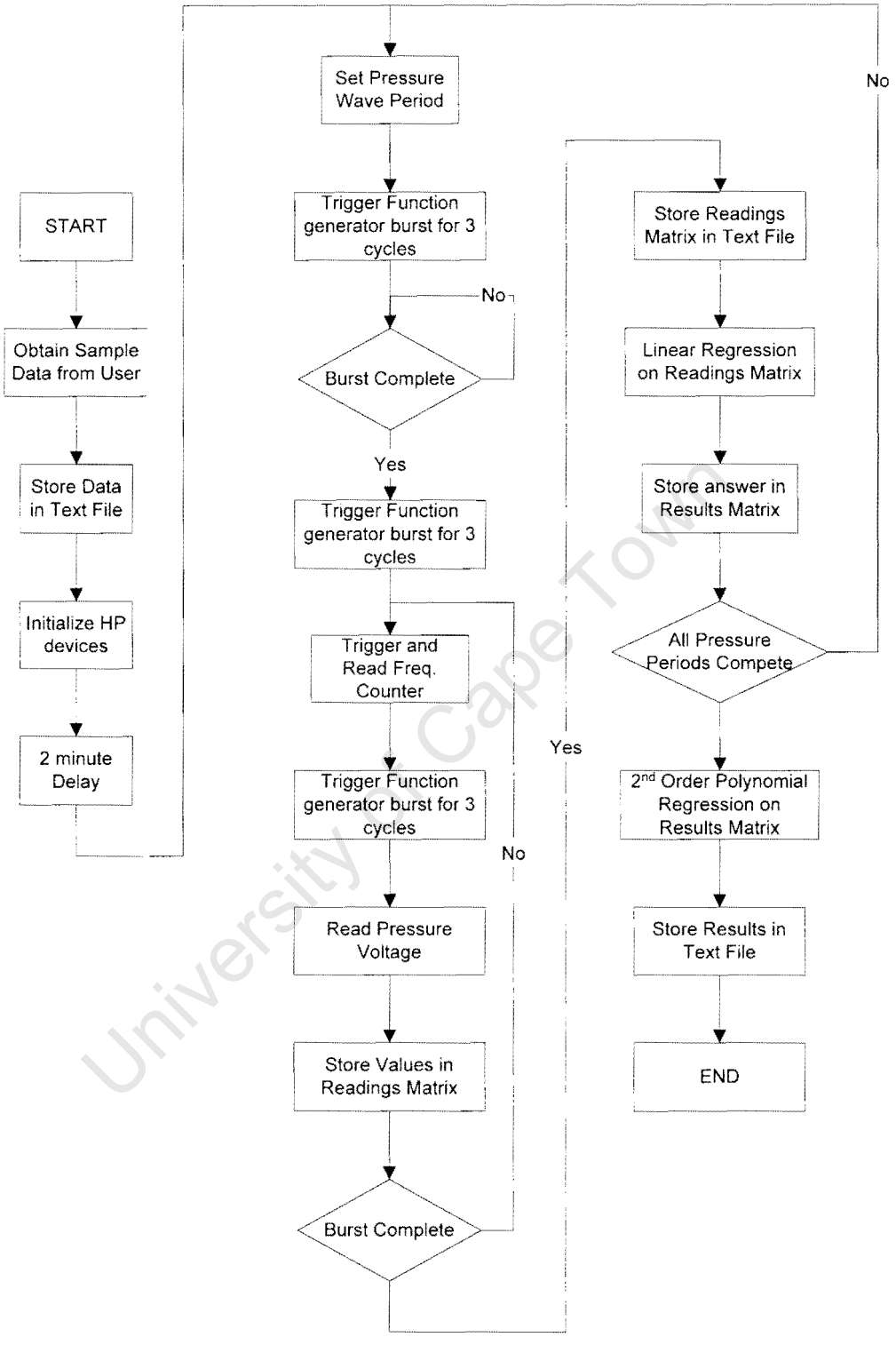




*Fig 7.4: Flow chart of software used to take readings from the instruments and calculate a value for B/A.*

The code started by loading the desired period, amplitude and number of cycles into the function generator. It was initialized into burst mode. The burst was triggered from the program and when

all the cycles where complete, a bit was set in its status register. This enables the pressure actuator to run without needing supervision from the code. A standard burst consisted of 3 waves.

The system first completed a couple of cycles at the desired frequency to ensure that the measurement cavity was at steady state. Once this first burst has completed a second burst is triggered. Until the completion of this burst, only the readings for pressure and frequency are taken and placed into an array. Once the burst was complete, a linear regression was performed on the collected data and the period, readings, result of the regression and sample details were written to file and displayed on the screen. Sampling rates of over 30 samples a second were achieved which was sufficient since the lowest period that was used was over 10s long. The reasons for using an extended time frame are discussed in the System Analysis Chapter (Chapter 8).

*Chapter 8*

# System Analysis

Before the system's results can be placed into context with reference to consistency and accuracy, the system's performance must be critically analyzed. The main focus of the analysis will be to determine whether the system is truly at steady state and to examine the affects of the slight temperature changes due to pressure being applied by the piston.

## *Analysis of Temperature Sensor Time Constant*

As discussed before, the temperature sensor is very precise, however the time it takes for its readings to stabilize has yet to be shown. This had a large impact on future results, and tests from pressure pulses and cycles showed that the time constant was between 10 and 15 seconds.

## *Settling Time of the Thermal Jacket*

The thermal jacket is designed to act as a thermal filter to the fluctuations in the temperature of the thermal bath. It has to be designed in such a way that thermal noise in the bath does not effect the sample liquid, while the jacket still takes a reasonable time to reach steady state.

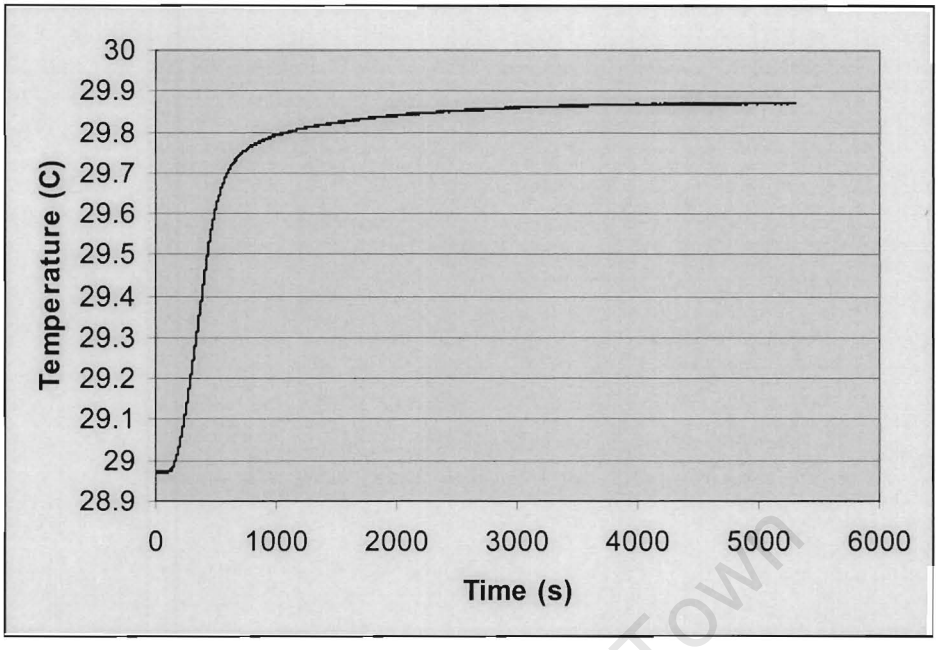


*Fig 8.1: Graph representing the temperature readings from inside the measurement cavity after the thermal bath was increased by one degree. The thermal bath took about 2 minutes to achieve this change; however it took nearly 1.5 hours for sufficient heat to travel into the measurement cavity for the system to reach steady state.*



From figure 8.1, it is difficult to obtain a time constant for the system since the thermal bath cannot create an instantaneous change in temperature, and due to the design of the jacket it is unlikely to resemble a first order system. However the settling time of the system can be seen from the graph to be about 1.5 hours. This should be sufficient to filter out the slight temperature disturbances in the thermal bath.

## *Effect of Heat Generated by Piezo Tube*

Obviously as the piezo tube is being made to oscillate it produces heat. This has an effect on the system which needs to be investigated to see whether or not it is negligible. The results of that test can be seen in figure 8.2.

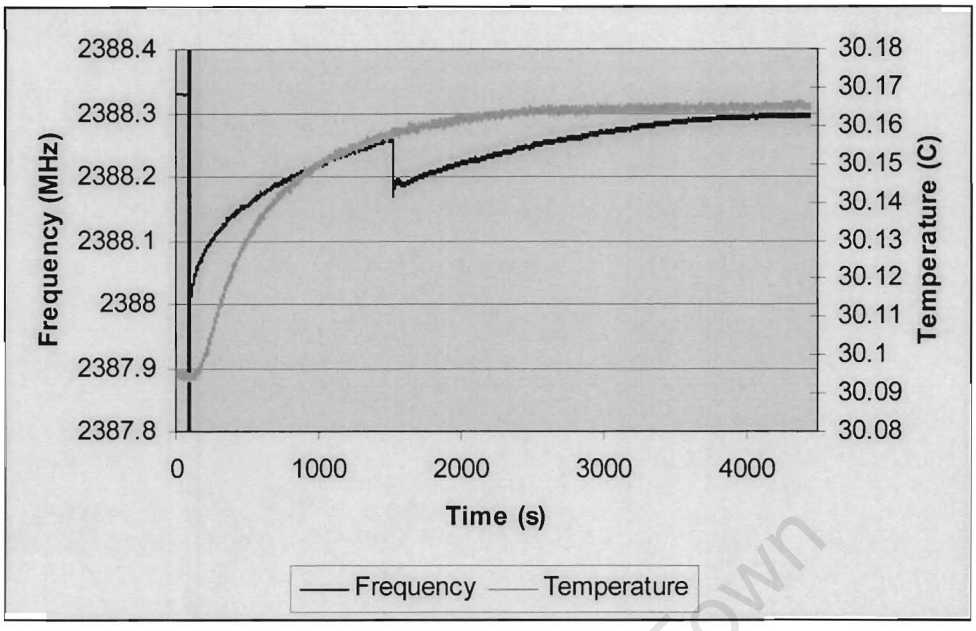


*Fig 8.2: Graph of locked frequency and temperature inside measurement cavity immediately after the piezo tube was activated. The piezo tube was activated at about 60 sec. At this time the frequency readings spiked out the top and bottom of the graph. The system was then allowed to start settling. At 1300 seconds the phase reference signal of the PLL was changed to investigate if there would be a significant thermal change.*

The phase lock loop circuit is switched on at the point when the frequency saturates to the top and bottom of the graph; before this point the piezo tube had no signal connected to it. After that point the temperature of the inner cavity increases, due to the heat produced from the piezo tube, until it reaches steady state. Also note that the frequency increases due to the thermal effects. The phase reference was slightly adjusted during the experiment to see whether small movements of the locked point would have a noticeable temperature effect. As can be seen there was no noticeable effect. This implies that, as long as the phase locked loop is locked and enough time is allowed for the system to reach steady state, the piezo itself will not introduce thermal fluctuations to the sample during readings.

## *Temperature Effects on Locked Frequency*

As mentioned in chapter 5, there is a relationship between the temperature of the sample and the speed of sound in the liquid. The size of this proportionality is dependent on the properties of the sample liquid. The values for the change of sound speed with temperature for the liquids measured in this study are documented. An interesting observation is that some of these values are positive and some are negative.

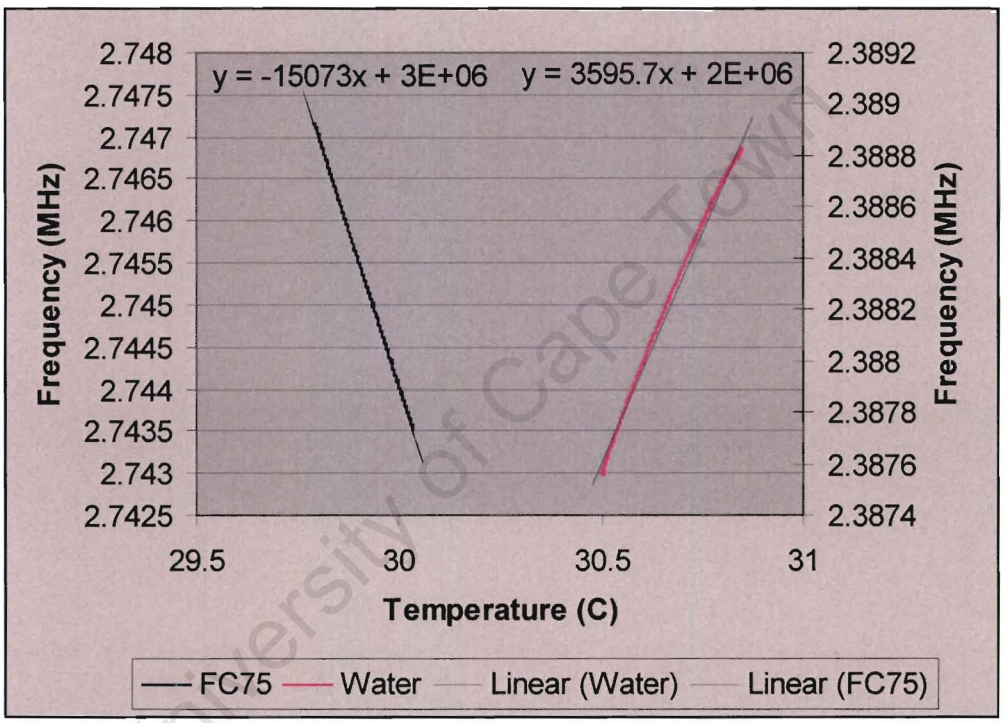




*Fig: 8.3: Graph showing the relationship between locked frequency and temperature for FC75 and Water, showing how the sound speeds of the samples are dependent on temperature. The measurement of the frequency is proportional the sound of sound, the mode number that is being measured and diameter of the tube, however the fractional change in the frequency will be the same as the fractional change in sound speed due to changes in temperature.*

Both of these readings where taken by varying the temperature of the thermal both and monitoring the frequency. The two plots are on different axis so their gradients are distorted. By converting

the frequency to the sound speed within the sample, the relationship between sound speed and temperature was calculated to be: FC75 = -3.12 $m.s^{-1}{}^{o}C^{-1}$; Water = 2.27 $m.s^{-1}{}^{o}C^{-1}$.

## *Pressure Effects on Locked Frequency*

This of course is the effect that is to be measured to obtain B/A and the accuracy and linearity of this reading is fundamental to accuracy of the system.

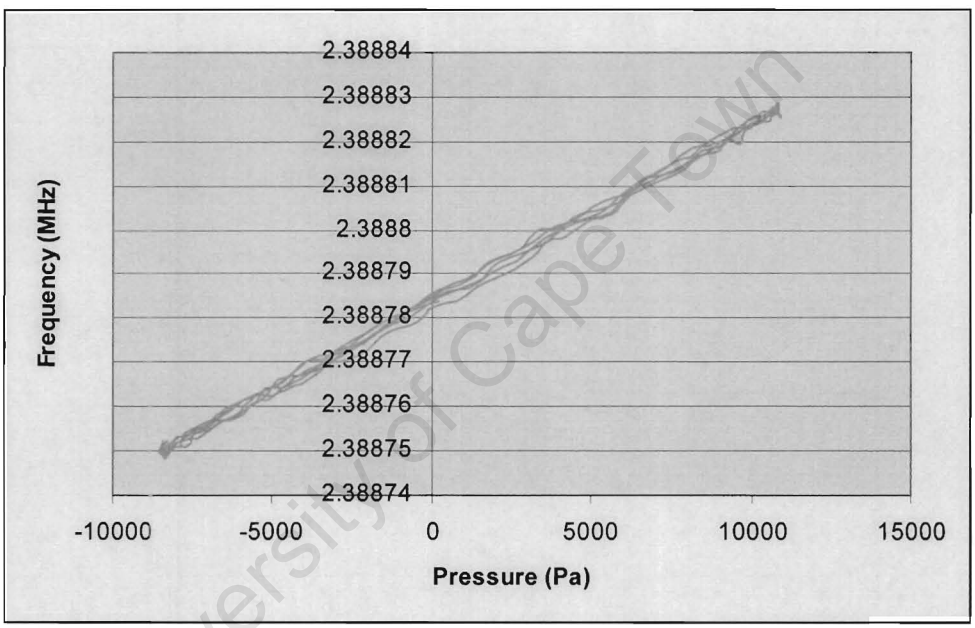




*Fig: 8.5: Graph showing the relationship between frequency and pressure for a sample of water being pressurized by a 20kPa peak to peak sine wave at a period of 60 seconds. The gradient of this line is the value required for B/A measurements*

Figure 8.5 is a plot showing the effect that pressure has on sound speed of water. The pressure source was a sinusoidal waveform with a period of 60s. It should be noted that there is a thermal effect along with the pressure wave and thus the gradient of the line will not give an exact answer for B/A calculation.

## Pressure Effects on Temperature

As discussed previously, there is a definite temperature effect to changing the pressure with the piston device. To show the existence of this effect, a 1 bar pressure change was produced by the piston and the temperature sensor's output was measured.

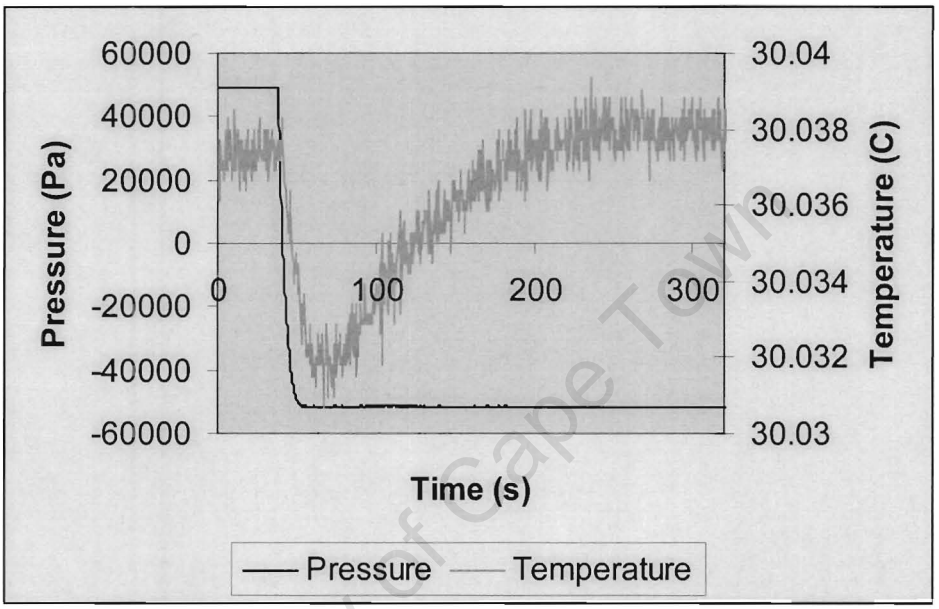


*Fig 8.6: The change in temperature in the sample cavity due to a 1 bar change in pressure*

As can be seen the change in pressure results in a definite change in temperature. The effect of this change is actually understated by the graph, since the sensor has a relatively slow time constant. Also note that it takes about 3 minutes for the additional heat in the air to be absorbed by the inner thermal jacket wall.

## Analysis of Thermal Effects Within a Pressure Wave

As the temperature in the air surrounding the sample changes sinusoidally, the temperature of the sample is affected. This obviously has an effect on the frequency waveform. Due to the difficulty in obtaining accurate real-time temperature readings from the sensor, a different approach for examining the effect was needed.

A retrospective approach was taken. From previous detection techniques, the B/A of the FC75 sample we used was well characterised. The expected frequency waveform was compared to the measured waveform, and the component from changes in temperature could be extracted.

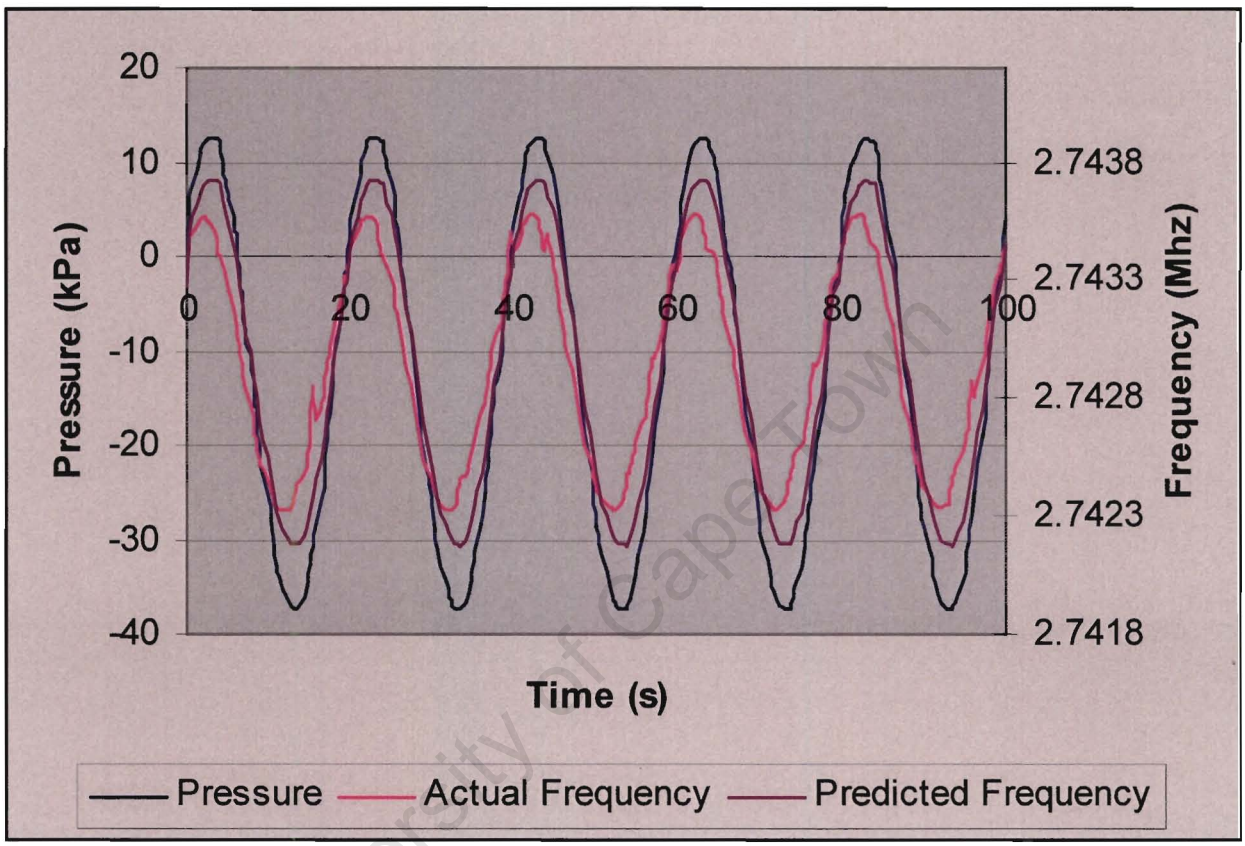


*Fig 8.7: Pressure and frequency readings taken for a sample of FC75 at 30 degrees. Using B/A measurements from literature, a plot of predicted frequencies was added to allow for a comparison.*



The difference between the actual waveform and the expected waveform is assumed to be caused by thermal effects. Thus using the relationship between changes in temperature and frequency discussed in the previous sections, the difference converted to changes in temperature.

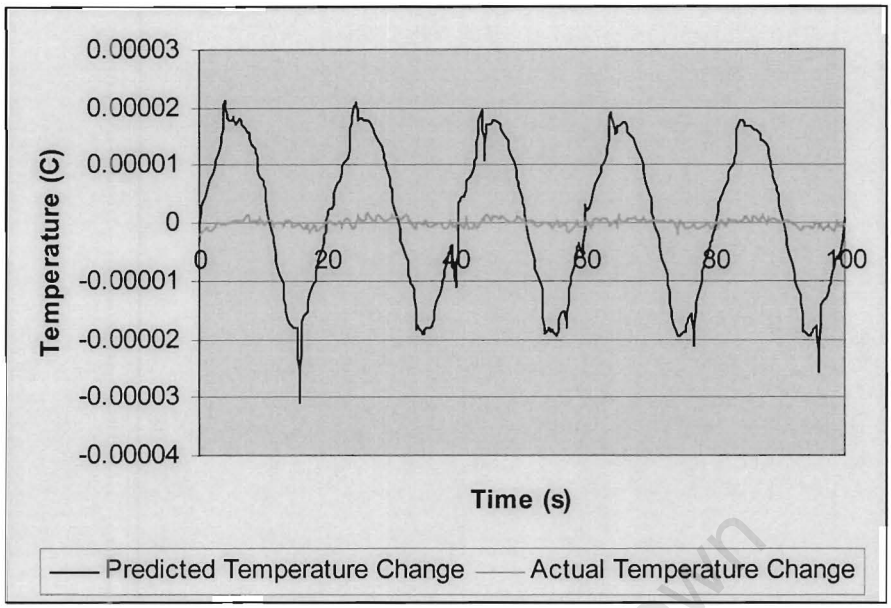


*Fig 8.8: Plot of temperature sensor measurements and the predicted temperature change in the FC75 obtained by subtracting the real and predicted frequencies, shown in figure 8.7, from each other, and using the sound speed to temperature relationship obtained in figure 8.3. There is a noticeable difference between these two graphs which is accounted for by the time constant of the temperature sensor.*



As can be seen there is still a vast difference between the projected temperature change and the actual readings (fig 8.8). However fluorocarbons conduct heat quite well, whereas the temperature sensor has a time-constant of between 10s and 15s. If the projected temperature waveform of the fluorocarbon is assumed to be equal to that of the air in the cavity, then linear control theory can be applied to a sine wave of the same magnitude and phase as the projected temperature waveform.

A first order system was assumed for the temperature sensor with a characteristic equation of $g(s) = \frac{1}{1+s\tau}$, where $\tau$ is the time constant. Thus the amplitude ratio will be $|g(s)| = \frac{1}{\sqrt{1+\omega^2\tau^2}}$ and the phase angle will be $\phi = -\tan^{-1}(\omega\tau)$ [5], where $\omega$ is the frequency of the pressure waveform. The time constant of the sensor was assumed to be 13 s, and the transfer function was applied to a sine wave representation of the predicted temperature change equation from figure 8.8. The results are shown in figure 8.9.

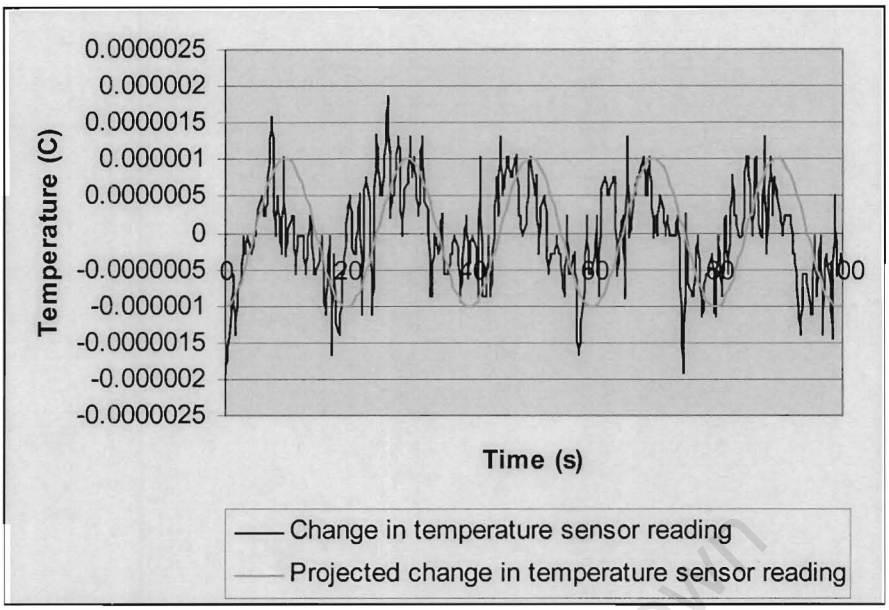


*Fig 8.9: Plot of measurements taken from the temperature sensor, and the projected temperature sensor readings obtained by applying a first order characteristic equation, with a time constant of 13s, to the predicted temperature change in figure 8.8. This chart shows that although only a small temperature change was read by the sensors, there is a far larger temperature change happening in the sample itself.*



As can be seen the magnitude of the projected waveform diminishes substantially. Although the magnitudes of both readings now seem to be similar, there still seems to be a slight error in the phase. This can be attributed to the error in the assumption that the sample liquid has no time constant, and that the temperature sensor is a first order system. However, these calculations and graphs show that there is a definite error that can be associated with the temperature of the sample, and that this error will introduce a phase shift and an amplitude change to the pressure waveform. The effect on water seems even more apparent since it has a much higher thermal time constant than FC75.

*Chapter 9*

# Describing and Compensating for the Thermal Effect

The results and demonstration shown in chapter 8 indicates a definite thermal effect on the sound speed measurements. The exact impact that this will have on the readings will vary according to sample and system parameters. One of these parameters is the change in sound speed with temperature of the sample, and was discussed in chapter 8; however there are several more such as the thermal resistance and capacity of the sample, the time constant of the inner wall of the thermal jacket, and the change in air temperature with pressure.

## *Analysis of Thermal Effect*

Due to the sinusoidal change in pressure of the air around the sample, there is a sinusoidal heat flux in the air. The amount of heat that is produced and absorbed by the air will be consistent in each cycle. However, it will take a couple of cycles for the system to reach steady state once it is activated. The heat produced by the air flows into the brass walls and tube extension, the piezo tube, and the sample itself. The rate of flow, and thermal effect from this flow, is dependent on each individual material's thermal properties.

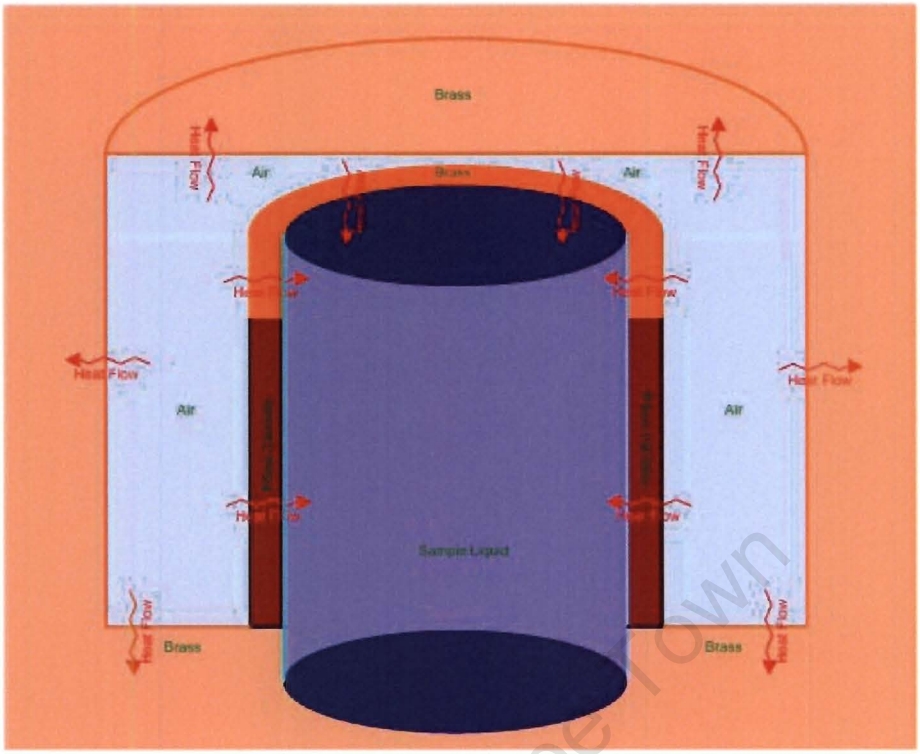


*Fig 9.1: Illustration of the flow of heat into the sample liquid from the pressurized air. Since different materials have different thermal characteristics, the effect they have on the thermal system is different. The heat that flows into the brass outer walls, base, and lid removes the amount of excess heat in the air and thus reduces the thermal effect at larger pressure cycle periods. Heat that affects the measurement of the sound speed must either pass through the piezo tube into the sample liquid, or travel though the excess liquid above measurement zone of the piezo tube.*



The area of interest for the thermal effect is the volume of sample liquid that is within the range of the piezo. Assuming that the piezo tube produces perfect waves only within its range, this suggests that heat changes in the liquid that is contained by the brass ring above the piezo tube, and in the recess below the piezo tube will not effect the sound speed measurements. Changes to its temperature affect the sound speed of the sample and thus directly affect the accuracy of the readings.

The system properties that are most likely to affect the temperature of the sample are listed below:

1. *Heat produced due to the change in pressure of the air*

This is the source of the problem. With an increase in pressure, the air particles are forced closer together and this change produces heat. This effect is assumed to be linear and thus for every sine wave of pressure, the temperature of the air will change sinusoidally in phase with the pressure waveform.

2. *The rate of heat flow into or out of the liquid sample*

Each sample will have different values for specific heat (which determines the capacity of a substance to retain its heat) and the thermal conduction (which determines how fast heat can flow though the substance). Thus for different samples it will take different amounts of time for heat to be absorbed. For water the rate of heat flow is much smaller than for FC75 and FC43.

3. *The geometry of the measurement chamber*

The initial design for the size of the piezo, the size of the chamber wherein it sits, the amount of air available around the sample liquid, and the size of open air available at the top surface of the sample liquid, affect the amount of heat that is produced due to the change in pressure, and also the paths that are available for the heat to flow. Since the piezo was so small in size, a proportionally larger amount of air was needed, in comparison with Davies [9] design, around the sample liquid, to allow the design to be practical. This meant that proportionally more heat would be produced around the liquid and thus the thermal effect would be more extreme.

4. *The thermal characteristics of the measurement chamber*

The thermal characteristics of the brass and the piezo tube determine their affect on the distribution of heat in the chamber. The less heat that the piezo tube allows to pass into the liquid, the better the readings will be and the more heat the brass absorbs away from the chamber, the less heat will be available to make it into the sample.

5. *The frequency of the pressure wave*

Since heat takes time to travel through a material, the faster the heat is removed from the air the less heat will have had time to penetrate the liquid. Thus the faster the pressure wave the less temperature change there will be in the sample.

Since the sound speed measurements will be affected by the average thermal effect within the sample, and every point in the sample will have sinusoidal temperature change proportional to its position and parameter mentioned above, the thermal effect on the sound speed measurements will be the sum of many sine waves of the same frequency and thus sinusoidal in shape. A vector diagram can thus be used to illustrate the thermal effect, pressure effect and actual reading taken.

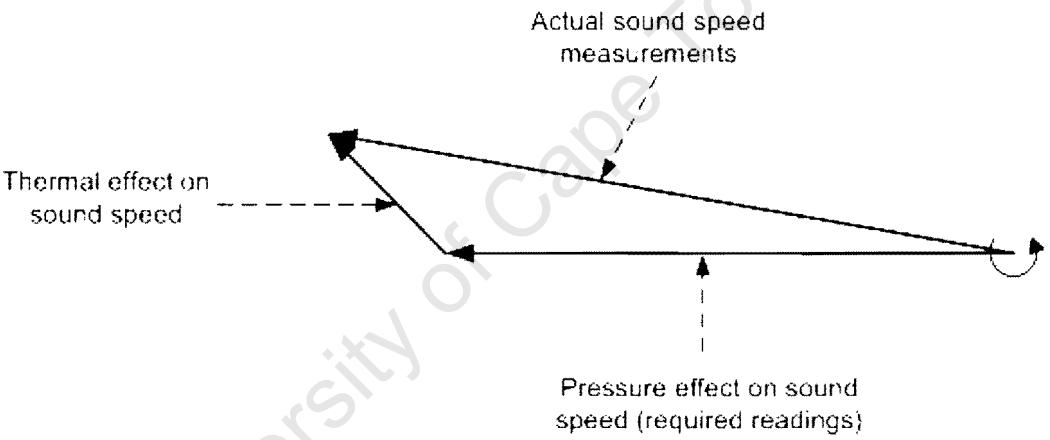




*Fig 9.2: Vector diagram illustrating the how the thermal effect distorts the actual sound speed measurement away from the required results. As the phase angle and the magnitude of the thermal component changes at different pressure waveform frequencies, so will the error between the actual and required measurements.*

Although the pressure effect on sound speed should remain constant for all frequencies and in phase with the pressure waveform, the temperature effect will vary both with magnitude and phase shift. This added heat affects the sound speed measurements taken by introducing a phase shift and a magnitude change to the sound speed measurement. Since the vector of the thermal effect is unknown, the pressure effects vector can not simply be calculated using the vector relationship. However from the trend, created from varying the frequency, a value for B/A can be extrapolated.

This can be done since the desired condition, at which the B/A readings should be taken, is isothermal. And if the pressure wave period was vanishingly small, there would not be any time for heat to be transferred into the liquid and thus isothermal conditions would be in effect. Thus a compensation technique, to remove the thermal effect, should attempt to calculate what the value for B/A would be at a period of zero seconds.

## *The Thermal Component's Influence on B/A Readings*

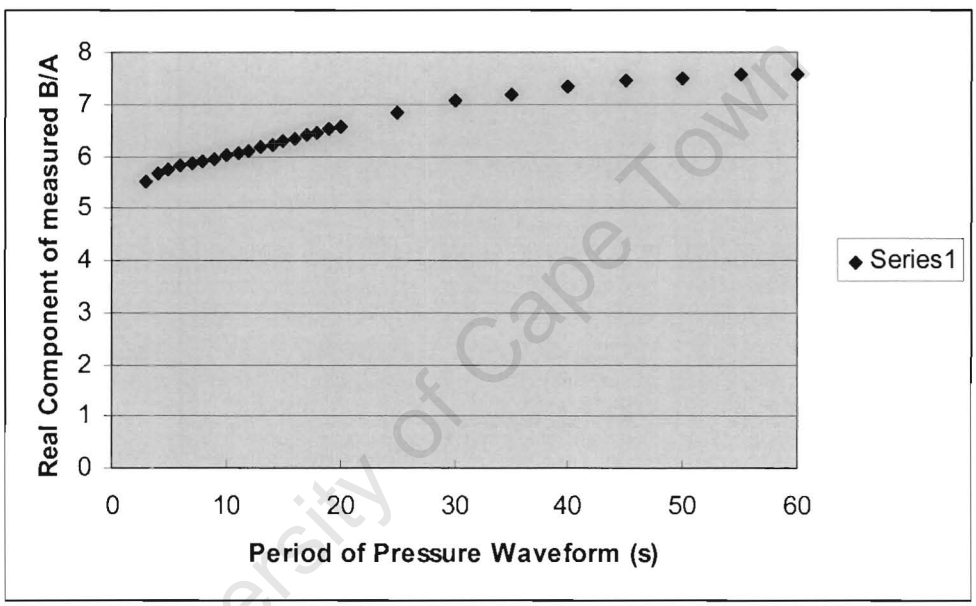




*Fig 9.3: Measurements of the real component of B/A for water at 30 degrees at various pressure periods. Note that the measured B/A are inflated at slower periods since the sound speed of water increases with increases in temperature. The graph tends towards the true value, however as the period becomes very small the heat flux within the sample liquid no longer is homogeneous and a noise component starts to become apparent.*

A sample of water was placed in the system and was pressurized at different frequencies. A linear regression was done on relationship between pressure and sound speed to obtain the real component of the temperature affected $\frac{\partial F}{\partial P}$ and thus B/A, and the results were plotted in figure 9.3. While the period of the pressure waveform is large (say longer that 20s, depending on the

liquid) the heat is rather uniformly absorbed in the liquid. Noticeably as the period decreased, less heat has time to be absorbed and thus there is a downward trend in the values, as expected.

It takes time for the heat to pass though the sample, and thus as the period is decreased even more, there is not enough time for the heat to remain uniformly distributed in the sample liquid, so the system becomes nonlinear. The start of this effect can be seen in figure 9.3 when the period is less than 10 seconds.

## *Attempts at Modelling Measurement Cavity*

The effect of the heat is proportional to the several parameters mentioned at the start of this chapter. All, but one, of these parameters are sample liquid independent. The only parameter that is dependant on the sample liquid is the rate of heat flow into the sample. Thus if a model could be produced that would only depend on this parameter and the frequency of the pressure wave, then readings for the sound velocity can be used to predict what the B/A readings would be at a period of zero.

From the vector relationship, shown in figure 9.2, it can be seen that the thermal vector causes the actual sound speed readings vector to change in magnitude and phase. From the measurements taken, both the magnitude and the phase angle of the actual sound speed vector, at a specific pressure wave period, can be calculated. However since the thermal vector is unknown, the real readings can not simply be calculated. Thus a couple of models for this vector were attempted and compared to real results to see whether they reflected what actually happened inside the sample liquid.

The primary assumption for these techniques was that the system changed as a function of only one variable, being related to the thermal characteristics of the sample liquid, as to avoid ambiguities. Also it was assumed that, in comparison to heat entering through the top of the sample, the heat entering via the piezo into the sample liquid would be negligible.

The initial attempt was a first order system, with a single pole due to the thermal time constant of the sample liquid. This was improved to a second order system due to the time constant of the outer walls. The effect of this time constant can be seen in figure 8.6, where the temperature drops back down to zero after sufficient time. The proposed characteristic equations were manipulated to obtain the analytical relationship between phase angles of the temperature vectors and frequency of the pressure waveforms. The imaginary component of the temperature vector and the actual readings taken (refer to figure 9.2) are equal. Thus only the phase angles of the models were needed to obtain to calculate the predicted pressure effect on sound speed.

| Model | Characteristic Equation |
|---|---|
| First order | $g(s) = \frac{k_f}{s + 1/T_C}$ |
| Second order | $g(s) = \frac{k_s(1/T_w)}{(s + (1/T_w))(s + (1/Tc))}$ |

*Table 9.1: Characteristic equations of the first and second order models attempted. In the equations $T_c$ and $T_w$ are the thermal time constant of the liquid and the walls respectively.*

These models proved ineffective to obtain accurate results. The model trends did not follow the actual data accurately and the time constants that gave best results were unrealistic. Also these models tended to underestimate the size of the thermal vector.

A standard heat conduction model was also attempted. The model is a semi-infinite solid in which conduction occurs due to a periodic surface temperature variation [28]. The model is similar to the actual system, assuming that the brass below the sample has little effect and that no heat penetrates though the piezo ceramic. The temperature profile that the equation defined was then integrated, for the range in which the piezo was active, to obtain an equation defining the average value of the temperature with respect to time. The thermal time constant on the wall was taken into account by adjusting the size of the surface temperature variation.

| Description | Equation | Variables |
|---|---|---|
| Surface temperature variation | $(T_s - T_0) = (T_S^* - T_0)\sin(\omega t)$ | *Where $T_2^*$ is the magnitude of the surface temperature wave.* |
| Temperature profile in liquid | $\left(\frac{T - T_0}{T_s^* - T_0}\right) = e^{-x(\omega/s\alpha)^{1/2}} \sin\left[\omega t - x(\omega/2\alpha)^{1/2}\right]$ | *Where α is thermal diffusivity* |
| Average temperature in sample at a specific time | $\lvert T_{ave}\rvert = \frac{\sqrt{2}T_s^*(e^{-x_2(\omega/2\alpha)^{1/2}} - e^{-x_1(\omega/2\alpha)^{1/2}})\sin\left(\frac{x_2 - x_1}{2}(\omega/2\alpha)^{1/2}\right)}{(x_2 - x_1)(\omega/2\alpha)^{1/2}}$ <br> $Phase = \pi + \frac{3x_2 - x_1}{2}(\omega/2\alpha)^{1/2}$ | *Where $x_1$ and $x_2$ distance to top and bottom of piezo from surface of liquid* |

*Table 9.2: Equations governing the heat transfer model using periodic surface temperature variation. As can be seen there is a component in the average temperature magnitude which fluctuates sinusoidally due to changes in frequency. This offers an explanation for the variations seen in figure 9.3 with a period less than 10 seconds.*

This model produced result that followed the actual measurements much more accurately than the previous attempts, and gave insight into what the thermal distribution would be inside the sample. The equation from this model also has similar variations in the thermal effect at low periods, as is apparent in the actual readings taken, refer to figure 9.3. However results that used this technique still underestimated the thermal effect. Thus to understand what is actually happening in the measurement cavity, a finite element analysis was done and it showed that the system deviated from the assumptions that the models were based upon.

## *Finite Element Analysis of Measurement Cavity*

To illustrate the how the heat is absorbed into the sample liquid, a finite element analysis was done for a sample of water. A simplified model was generated for the interferometer. The air

surrounding the piezo and the sample was subjected to a sinusoidal change in heat flux. The model that was used is shown below.

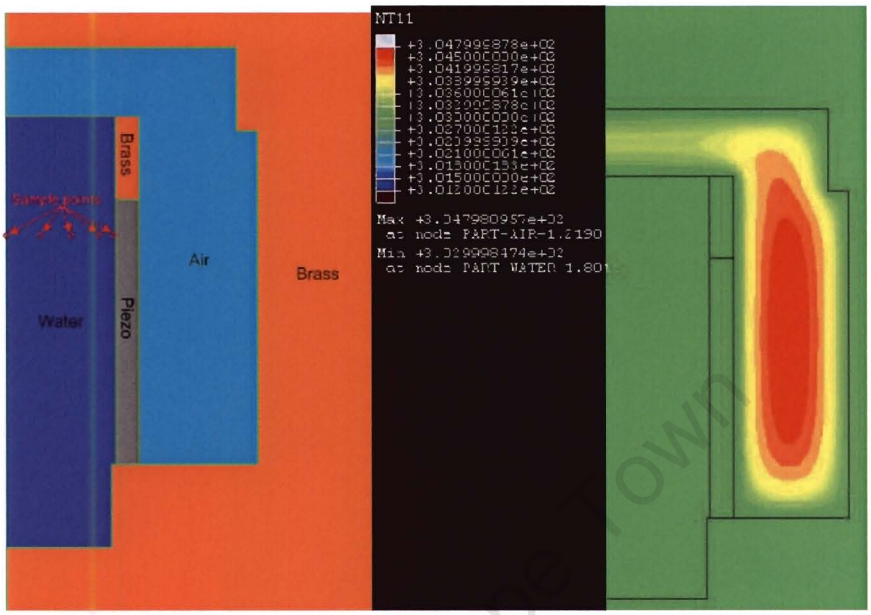


*Fig 9.4: Illustration on the left is the simplified model that was implemented for the Finite Element analysis. Some of the brass section was cut away to allow the inner cavity to be seen. The system was reduced to 2D and that section was cut in half to reduce the size of the model. The outside walls of the brass were set to a temperature of 303 K. Sample points were placed inside the liquid section to act as reference points when comparing the heat profile at different pressure wave frequencies. The nodes represent the following colours from left to right: red, green, orange, purple and blue. On the right is the highest temperature point of the air due to the change in heat flux. As can be seen the point of highest temperature is the side of the piezo. This is because the heat gets dissipated faster above the liquid, where the gap is smaller.*

Although the thermal parameters of the brass, water and air are well documented, the piezo ceramics properties were not known. A generic value for a ceramic was used. Since this test was done primarily to observe how the temperature profile would change with frequency, the error that would accompany this inaccuracy is acceptable.

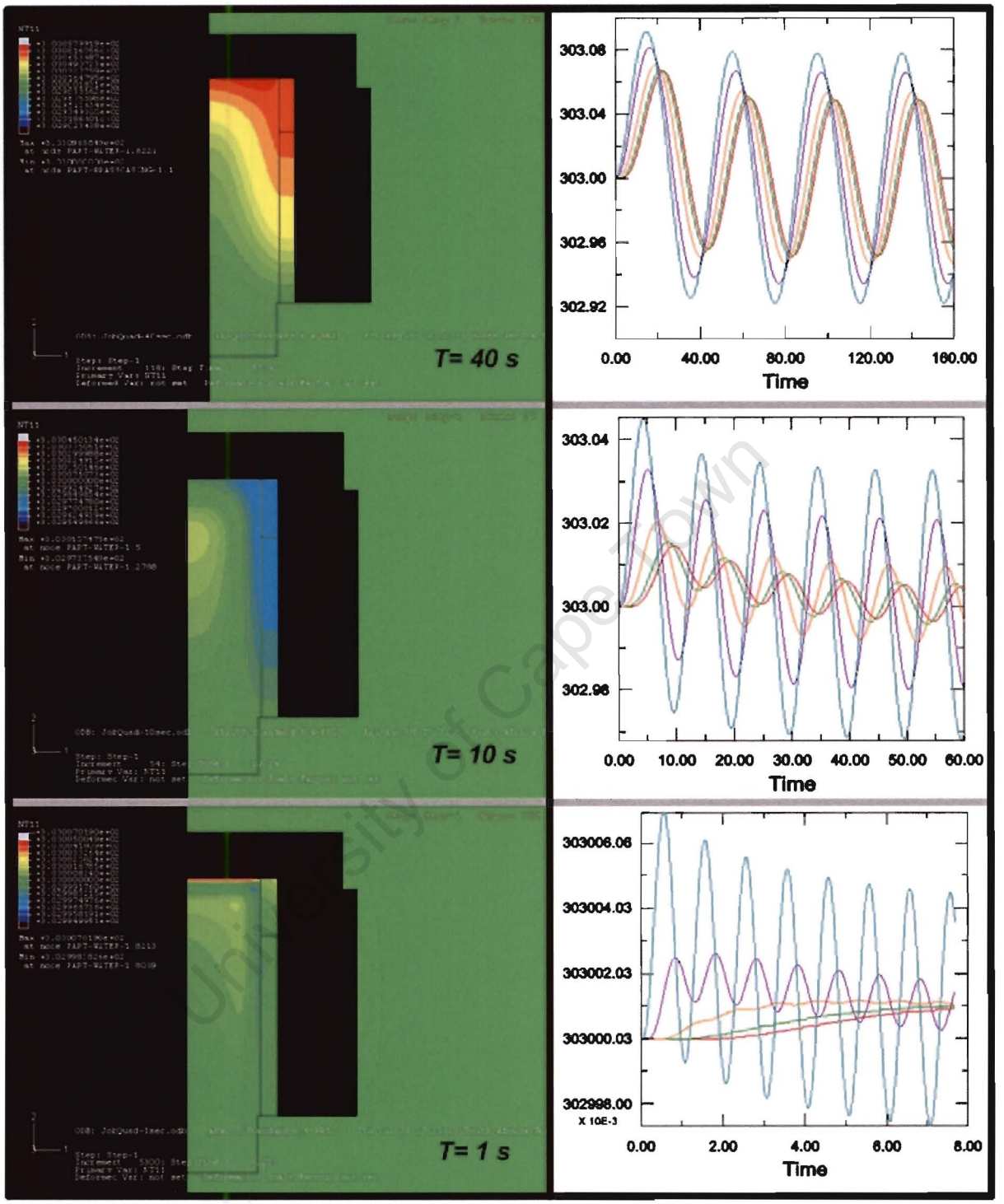


*Fig 9.5: Results from Finite Element analysis. On the left are temperature maps of selected times for each of 3 periods the simulation was run for. On the right are the temperature waveforms with respect to time of the selected nodes shown in figure 9.4. As the period drops, less heat gets absorbed into the liquid and also the phase shift between the nodes increases. At a period of 1 sec the temperature profiles show mainly a surface effect.*

As can be seen in figure 9.5, the amount of temperature variation within the liquid is dependant on the frequency of the pressure waveforms. As the simulation is started from steady state, with the whole system at 30 degrees, the start of the simulation was a disturbance and the system will need to return to steady state again. From the 10 second waveforms in figure 9.5 it can be seen that this takes about 40 seconds.

Comparing the waveforms for each sample point, one can see that with the 40s period the waveforms are similar in size and phase shift. As the period becomes smaller, the temperature of the sample points that are nearer to the centre of the liquid drop in magnitude and increase in the phase shift. With a one second period, the liquid that is far from the sides and top of the sample hardly gets affected at all.

As the pressure period decreases, there is not enough time for all the energy from the previous wave to dissipate before the next wave arrives. Thus the energy from previous parts of the wave lags inside the liquid. This can be seen in figure 9.5 where with a 10 second period there is still a warmer section in the centre of the liquid while the outside of the liquid is already cold. The section of sample liquid in the middle of the cylinder will have smaller transients than the section on the outside, as can be seen in the accompanying graphs. This effect is what causes the B/A readings (in figure 9.3), that are taken with a period of less than 10 seconds, to seem to have a transient component added to the downward trend.



## *Interpolation to Obtain Results*

Several techniques were attempted to mathematically equate the path that the readings from figure 9.3 take, to the actual value of B/A. These include simplifying the problem to a first order or a second order problem, or simplifying the problem to a standard heat flow problem [28] as is discussed earlier in this chapter. However due to the number of variables that affect the actual heat pattern, as became apparent with the finite element analysis, this was not viable, and the results, from these attempts, were not very robust.

The technique that obtained the best results was a second order polynomial regression on the results obtained for each of the tested liquids. The readings were only taken with pressure wave periods of between 12s and 40s. This ensured that the readings were still in the homogenous heat distribution range for materials with less thermal inertia than water. The results and correlation are listed below:

| *Liquid* | *Temperature* | *Density* | *Sound Speed* | *B/A* | *$R^2$ error* | *Literature results* |
|---|---|---|---|---|---|---|
| Water | 30°C | 995.7 | 1509.1 | 5.22 | 0.9991 | 5.28[12]<br>5.18[35]<br>5.21[8]<br>5.19[9]<br>5.13[9] |
| FC43 | 30°C | 1861 | 638 | 13.16 | 0.9962 | 13.19[9]<br>12.85(20°C)[26] |
| FC75 | 30°C | 1768 | 567 | 12.48 | 0.9979 | 12.83[9]<br>12.19(20°C)[26] |

*Table 9.3: B/A results using 2nd order polynomial regression.*

Although these results compare well with results found in literature, it is difficult to determine how well the regression reflects on the true trend that the temperature path will take. This could be an area for future research.

*Chapter 10*

# Conclusions

The initial aim of this project was to create a system to measure the B/A of small samples of liquid, using a low pressure wave without needing to take thousands of readings for statistical purposes. Although these aims were achieved, the thermal effect in the results added an error that adversely affected the confidence in the results obtained. However, a comparison of the results that were obtained using this technique with results from literature shows that the regression used does give accurate results. Based on these results, and the implementation of the system, the following conclusions can be drawn:

- Using sinusoidal waves as the pressure source is a vast improvement over using square pulses. It allows for a study in the thermal effects within the sample and keeps the measurement cavity under more stable conditions.
- The assumptions on which the isentropic phase technique are based are correct, as long as the measurement cavity is specifically designed to reduce the flow of heat into the liquid, and the pressure source can operate at a high enough frequency.
- The small piezo tubes used in the measurement of sound speed produce accurate results, as long as they have been correctly implemented in such a way to reduce possible surface effects and pressure loading.
- There is a definite thermal effect on the sample liquid due to the change in pressure in the air surrounding the sample, especially with such a small sample volume. However by careful design of the measurement chamber this effect can be minimised. Also mathematical methods can be used to reduce this effect; however the accuracy of the mathematical technique is unknown.
- The technique of the second order polynomial regression to obtain a thermally unaffected B/A result gives answers that compare well with literature results.
- Results for a sample can be obtained within 15 minutes of a sample reaching thermal steady state.

*Chapter 11*

# Recommendations

The following recommendations can be made for future work based on this project:

- The measurement cavity should be designed to have as little as possible air surrounding the sample liquid to ensure that the amount of heat that is produced is minimal. Yet the design should ensure that there is sufficient space for the pressurised air to flow unimpeded, to insure that the piezo tube is not loaded, and that the exact pressure of the sample is known.
- The phase locked loop can be replaced with a design whereby the capacitance of the liquid modes is subtracted and the system is made to self oscillate. Such a system is immune to changes in the magnitude of the acoustic mode. This will facilitate in taking measurements in samples where the acoustic properties change with pressure, such as ultrasonic contrast agents.
- Further work should be done on understanding the exact path that the heat flow takes with changes in the pressure wave frequency. If the mathematical model was known, then the true value for B/A can be determined by measuring B/A at only one or two pressure frequencies.
- The work done with the small piezo ceramic tube showed some interesting phenomena in the behaviour of the liquid modes, specifically with changes in level of the sample liquid, and these should be studied in greater detail.

# References

[1] R. Apfel. Prediction of tissue composition from ultrasonic measurements and mixture rules. J. Acoust. Soc. Am., 79(1):148-152, 1986.

[2] R. Beyer. Nonlinear acoustics. Naval Ship Systems Command, 1974.

[3] R. Beyer. Nonlinear acoustics in fluids. Van Nostrand Reinhold Co., Berkshire, England, 1984.

[4] R. Beyer. Parameter of nonlinearity in fluids. J. Acoust. Soc. Am., 32(6):719-721, 1960.

[5] M. Braae. Control Theory for Electrical Engineers. UCT Press, Cape Town, South Africa, 1994.

[6] W. N. Cobb. Finite amplitude method for determination of the acoustic nonlinearity parameter B/A. J. Acoust. Soc. Am., 73(5):1525-1531, 1983.

[7] A. Coleman, T. Kodama, M. Choi, T. Adams and J. Saunders. The cavitation threshold of human tissue exposed to 0.2 MHz pulsed ultrasound: Preliminary measurements based on a study of clinical lithotripsy. Ultrasound in Med. And Biol., 21(3):405-417, 1995.

[8] A. Coppens, R. Beyer, M. Seyden, J. Donohue, F. Guepin, R. Hodson, asnd C. Townsend. Parameter of nonlinearity in fluids II. J. Acoust. Soc. Am., 38:797-804, 1965.

[9] J. Davies. Continuous wave mode locking for the determination of the acoustic nonlinearity parameter B/A. PhD Thesis, University of Cape Town, South Africa, 2001

[10] W. F. Egan. Phase-lock Basics. John Wiley & sons, inc. New York, 1998.

[11] E.C. Everbach. Tissue Composition Determination via Measurement of the Acoustic Nonlinearity Parameter. PhD thesis, Yale University, New Haven, CT., 1989.

[12] E. C. Everbach, and R. E. Apfel. An interferometric technique for B/A measurement. J. Acoust. Soc. Am., 98(6):3428-3438, 1995.

[13] F. M. Gardner. Phaselock Techniques, Second Edition. John Wiley & sons, inc. New York, 1979.

[14] M. Greenspan and C. E. Tschiegg. Sing-around ultrasonic velocimeter for liquids. Rev. Sci. Inst., 28(11):897-901, 1957.

[15] X. Gong, Z. Zhu, T. Shi, and J. Huang. Determination of the acoustic nonlinearity parameter in biological media using FAIS and ITD methods. J. Acoust. Soc. Am., 86(1):1-5, 1989.

[16] M. Hagelberg, G. Holton, and S. Kao. Calculation of B/A for water from measurements of ultrasonic velocity versus temperature and pressure to 10000kg/cm$^2$. J. Acoust. Soc. Am., 41(3):564-567, 1966.

[17] D. Halliday, R. Resnick and J. Walker. Fundamentals of Physics, Fifth Edition. John Wiley and Sons, USA, 1997.

[18] B. Hartmann. Potential energy effect on sound speed in liquids. J. Acoust. Soc. Am., 65:1392-1396, 1979.

[19] E. Heidemann. Ultraschallforshung. De Gruyter, 1939

[20] E. Heidemann and K. Zankel. The study of ultrasonic waveform by optical methods. Acustica, 11:213-223, 1961.

[21] HP8656 User Manual. Hewlett Packard. USA, 1987.

[22] http://www.ferroperm-piezo.com/Definitions.html, 2003-08-13.

[23] H. Kashkooli, P. Dolan, and C. Smith. Measurement of the acoustic nonlinearity parameter in water, methanol, liquid nitrogen, and liquid helium-II by two different methods: A comparison. J. Acoust. Soc. Am., 82(6):2086-2089, 1987.

[24] L. Kinsler, R. Austin, P. Coppens, and R. Sanders. Fundamentals of Acoustics. John Wiley and Sons, New York, 1982.

[25] M. S. Korman, and J. M. Sabatier. Nonlinear Acoustic Techniques for land mine detection. www.demine.org/SCOT/Papers/sabatier.pdf , 2003-08-06.

[26] W. Madigosky, I Rosenbaum, and R. Lucas. Sound velocities and B/A of fluorocarbon fluids and in several low density solids. J. Acoust. Soc. Am., 69(6):1639-1643, 1981.

[27] H. McSkimin. Variations of the ultrasonic pulse-superposition method for increasing the sensitivity of delay-time measurements. J. Acoust. Soc. Am., 37(5):864-871, 1965.

[28] A. F. Mills. Heat Transfer. Richard D. Irwin, Inc. USA, 1992.

[29] MPX100/D datasheet, rev 3. Motorola, 1995.

[30] S. Poisson. Memoir on the theory of sound. J. Ec. Poltech., 7:364:370, 1808

[31] I. Rudnick. On the attenuation of finite amplitude waves in liquids. J. Acoust. Soc. Am., 30(6):564-567, 1958.

[32] C. Sehgal, R. Bahn, and J. Greenleaf. Measurement of the acoustic nonlinearity parameter B/A in human tissue by a thermodynamic method. J. Acoust. Soc. Am., 76(4):1023-1029, 1984.

[33] G. Stokes. On the difficulty in the theory of sound. Philos. Mag., 33.349-356, 1848

[34] J. Strutt (Lord Rayleigh). The Theory of Sound, volume 1 and 2. Macmillan and Co., New York, 2nd Ed., 1894.

[35] J. Zhang, and F. Dunn. Small volume thermodynamic system for B/A measurement. J. Acoust. Soc. Am., 89(1):73-79, 1991.

[36] Z. Zhu, M. Roos, W. Cobb, and K. Jensen. Determination of the acoustic nonlinearity parameter B/A from phase measurements. J. Acoust. Soc. Am., 74(5):1518-1521, 1983.

# Appendixes

The appendixes consist of the following sections:

- *Mechanical Drawings*

  The design drawings for each part in the thermal jacket are included as well as assembly drawings for the thermal jacket, the threaded oscillator and the complete system. Some pictures of the system are also included.

- *Electrical Circuit Diagrams*

  Contains the circuit diagrams for the phase locked loop and the pressure control system. It should be noted that some parts of the phase lock loop circuit design are present due to the evolution from other design topologies. This section also includes the layout of the top and bottom layers of the printed circuit board used to drive the piezo.

- *HPVEE code*

  This is the code used to take send instructions and take readings from the instruments. The Flow Chart of the code is shown in figure 7.4.

- *Abaqus input file*

  The input file is a text file that Abaqus uses to complete the finite element analysis. Usually this file is extremely long, thus the lines showing information about individual nodes have been removed.

*Appendix A*

# Mechanical Drawings

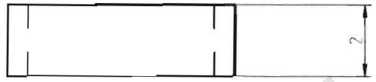


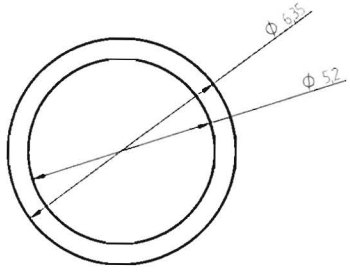


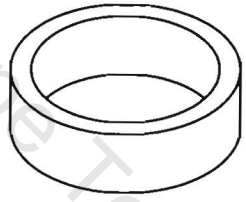



Material: Brass

| | | | | | | | |
|---|---|---|---|---|---|---|---|
| Björn Prenzlow<br>University of Cape Town | | | Part: Piezo Level Addon | | | | |
| | | | Quantity: | | 1 | | |

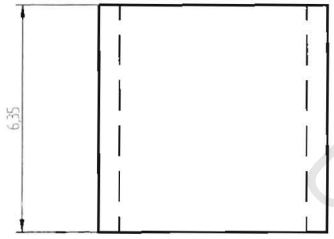


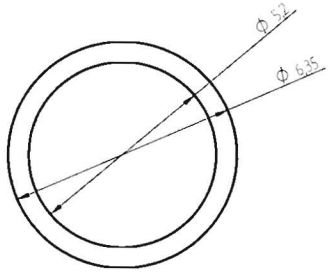


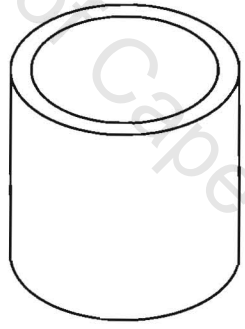



| | |
|---|---|
| Bjorn Prenzlow<br>University of Cape Town | Piezo Ceramic Tube |
| | Quantity: 1 |

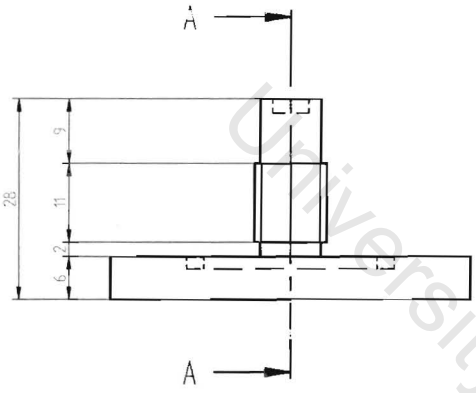


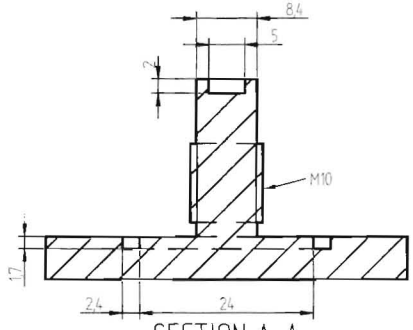


SECTION A-A

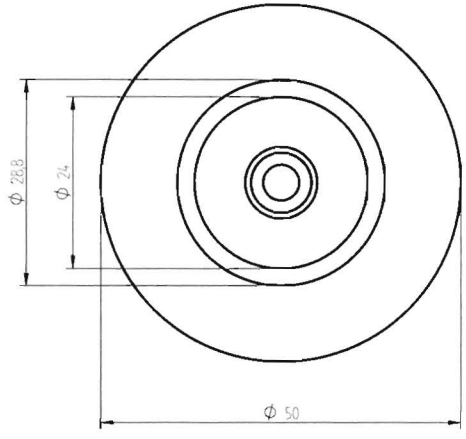


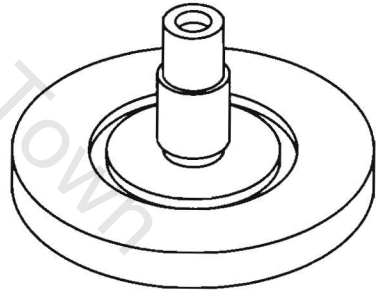

Material: Brass



| | |
|---|---|
| Björn Prenzlow<br>University of Cape Town | Removable Base<br>Quantity: 1 |

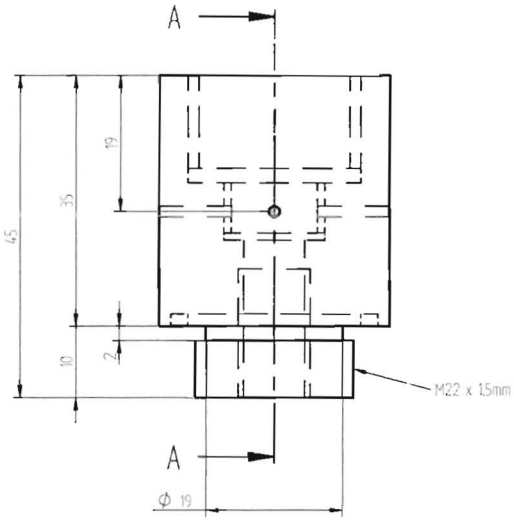


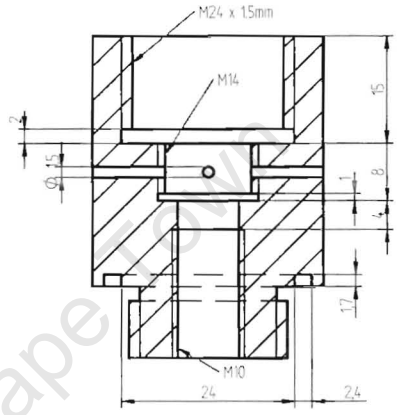


SECTION A-A

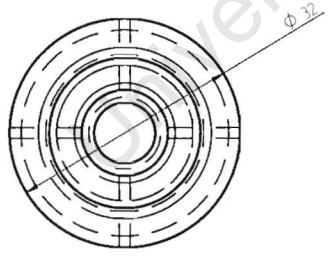


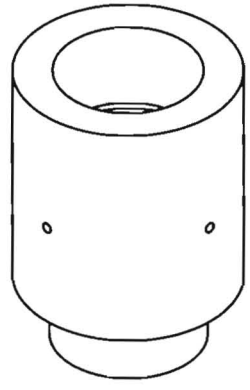



Material: Brass

| | |
|---|---|
| Björn Prenzlow<br>University of Cape Town | Inner Thermal Jacket (removeable base)<br>Quantity: 1 |


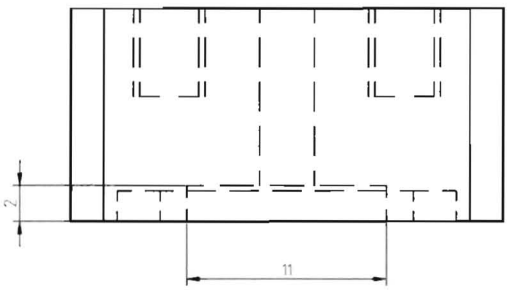


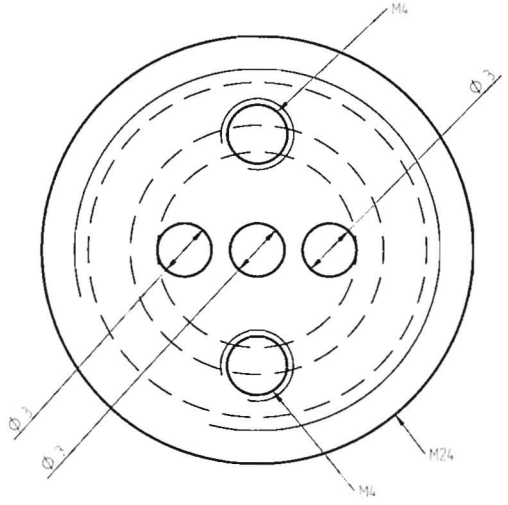


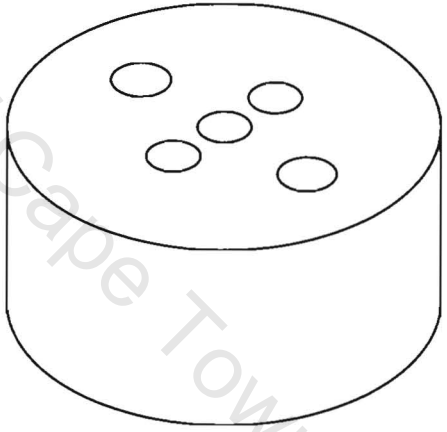



| | |
|---|---|
| Björn Prenzlow<br>University of Cape Town | Part: Inner Lid |
| | Quantity: 1 |

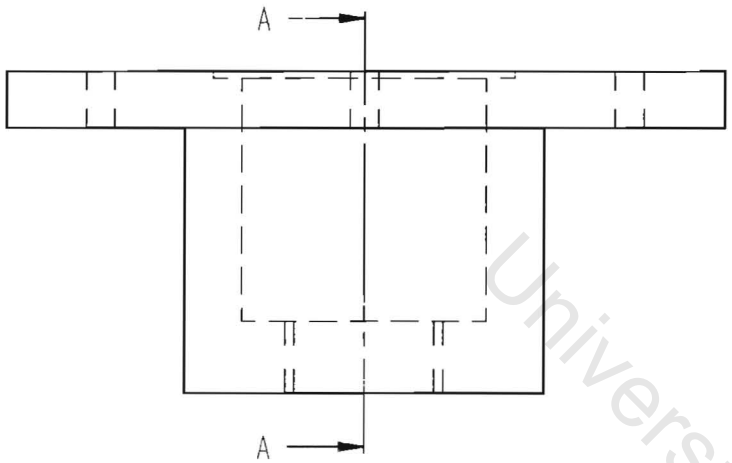


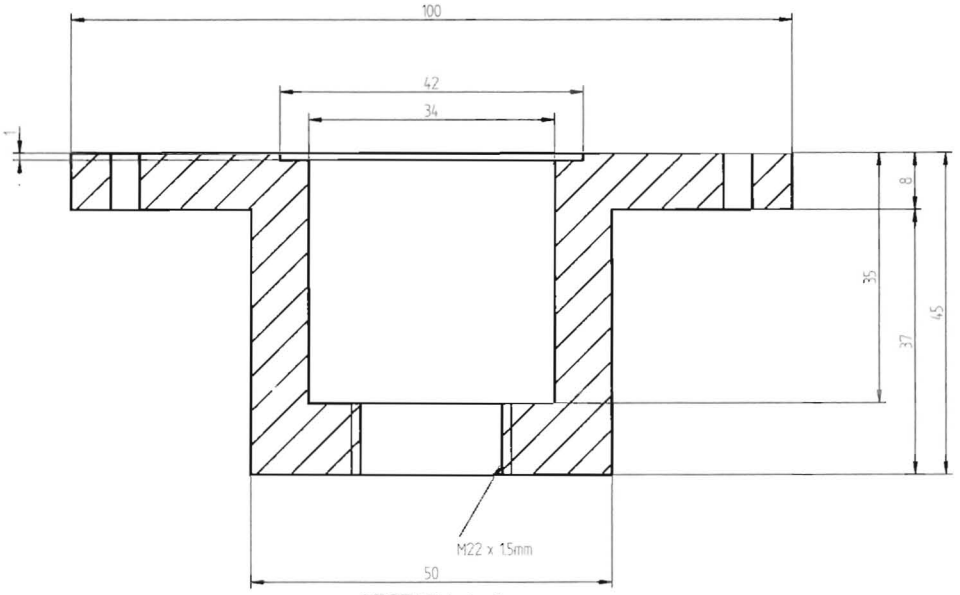


SECTION A-A

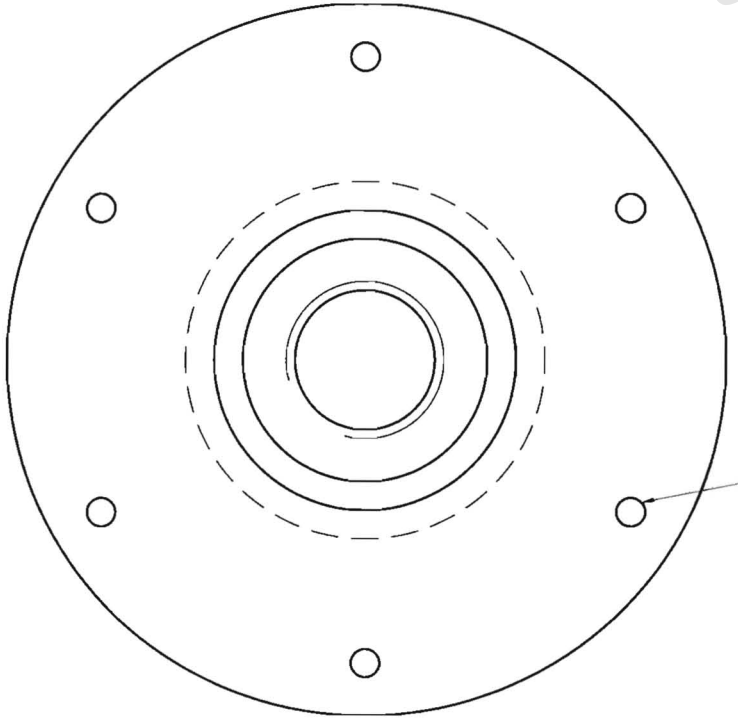

Φ 4mm
6 Holes equally spaced on Φ 85 mm

Material: Brass



| | |
|---|---|
| Björn Prenzlow<br>University of Cape Town) | Part: Outer Jacket (D) |
| | Quantity: 1 |

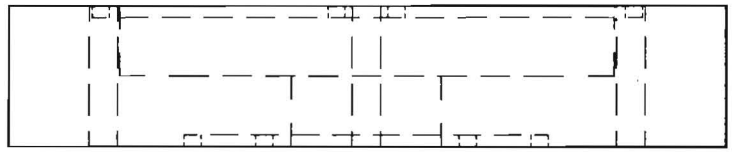

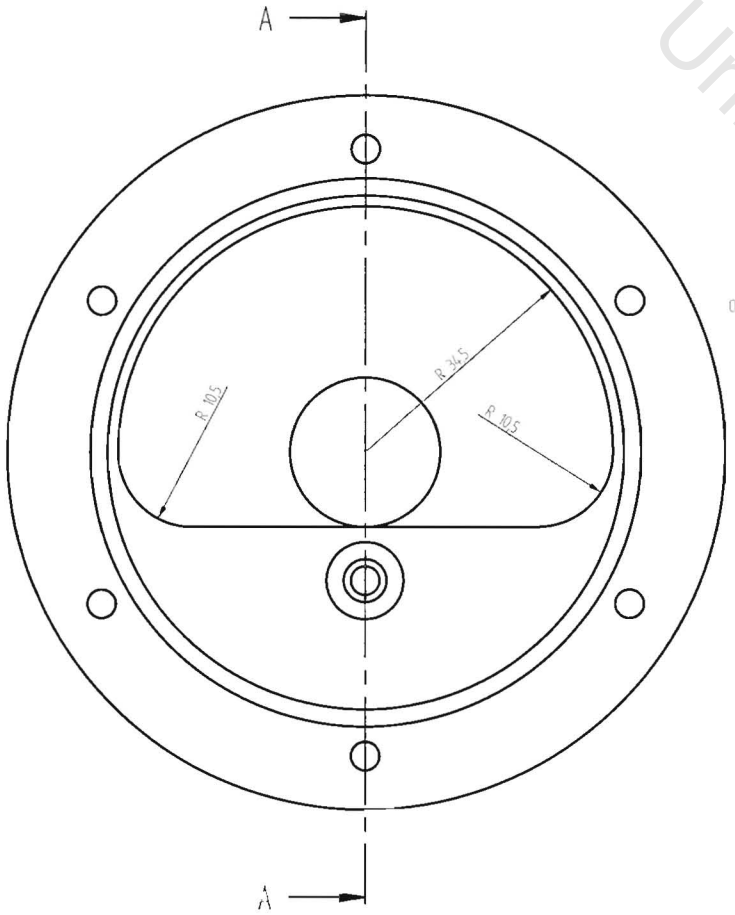


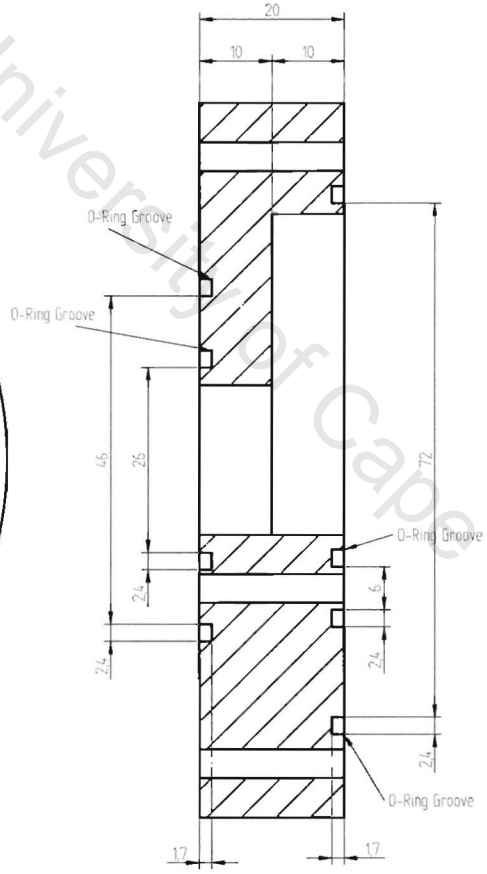


SECTION A-A

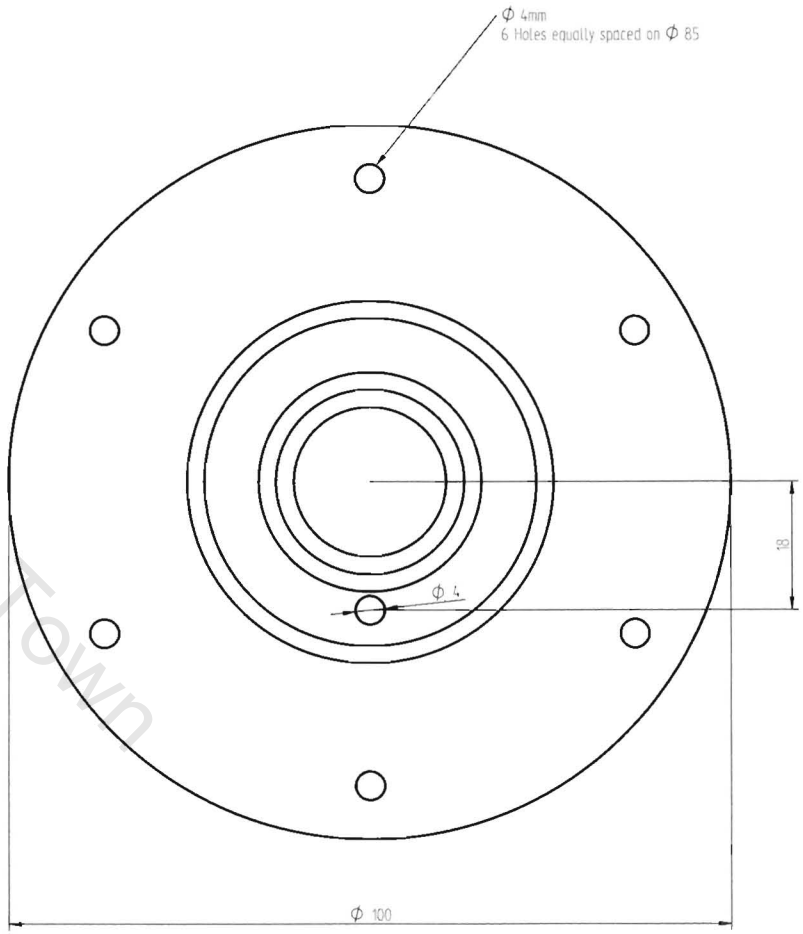




Material: Brass

| | | | | | | |
|---|---|---|---|---|---|---|
| Björn Prenzlow<br>University of Cape Town | | | Part: Outer Lid (E) | | | |
| | | | Quantity: | 1 | | |

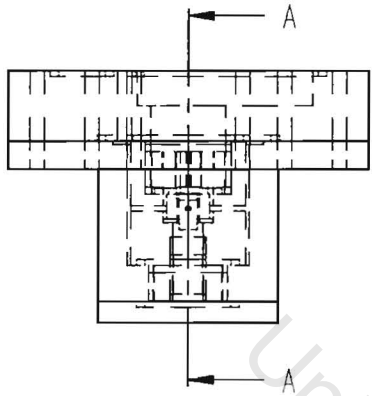


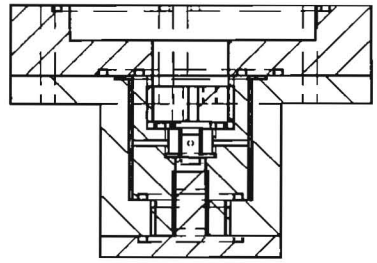

SECTION A-A

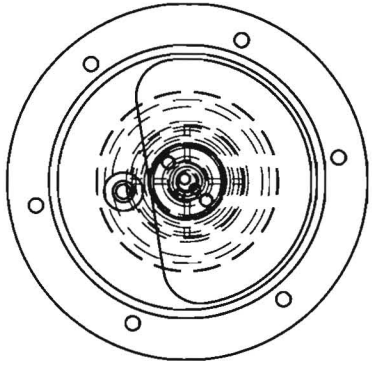

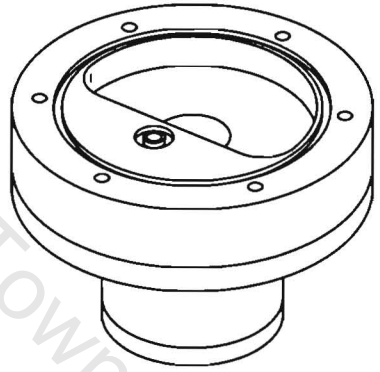



| | |
|---|---|
| Björn Prenzlow<br>University of Cape Town | Assembly Of Parts (Thermal Jacket) |
| | Quantity: 1 |

| | |
|---|---|
| Title: Threaded Oscillator | Quantity: 1 |
| Bjorn Prenzlow<br>University of Cape Town | |

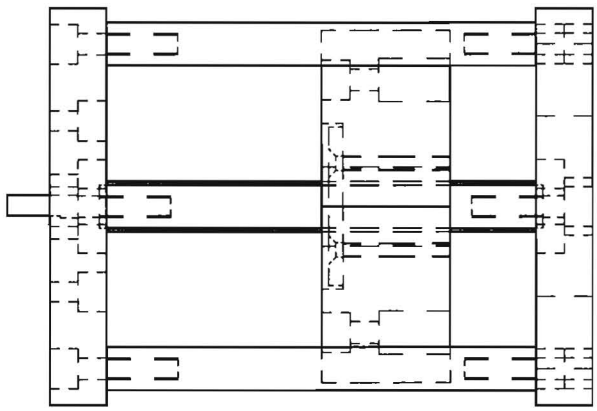

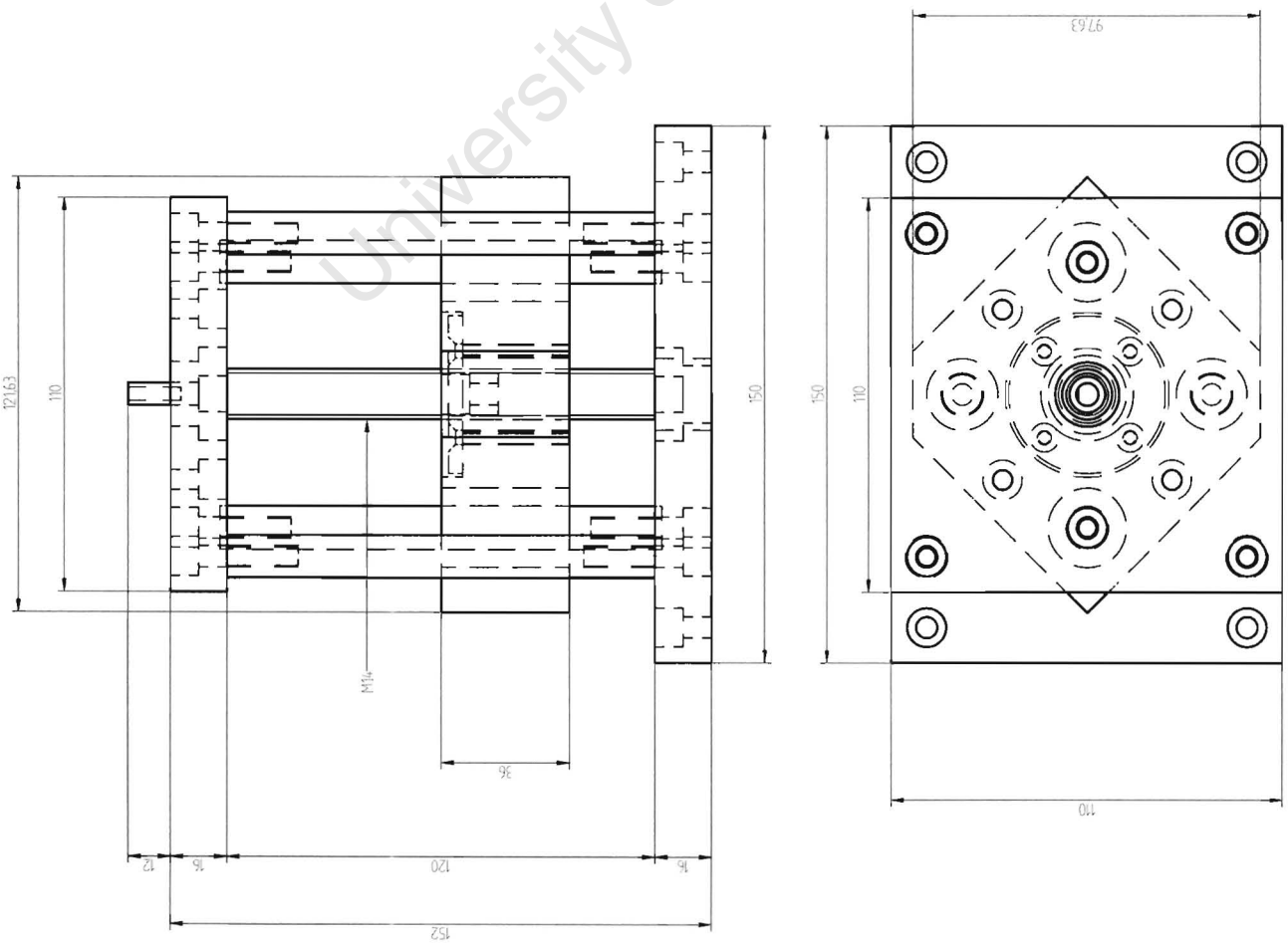

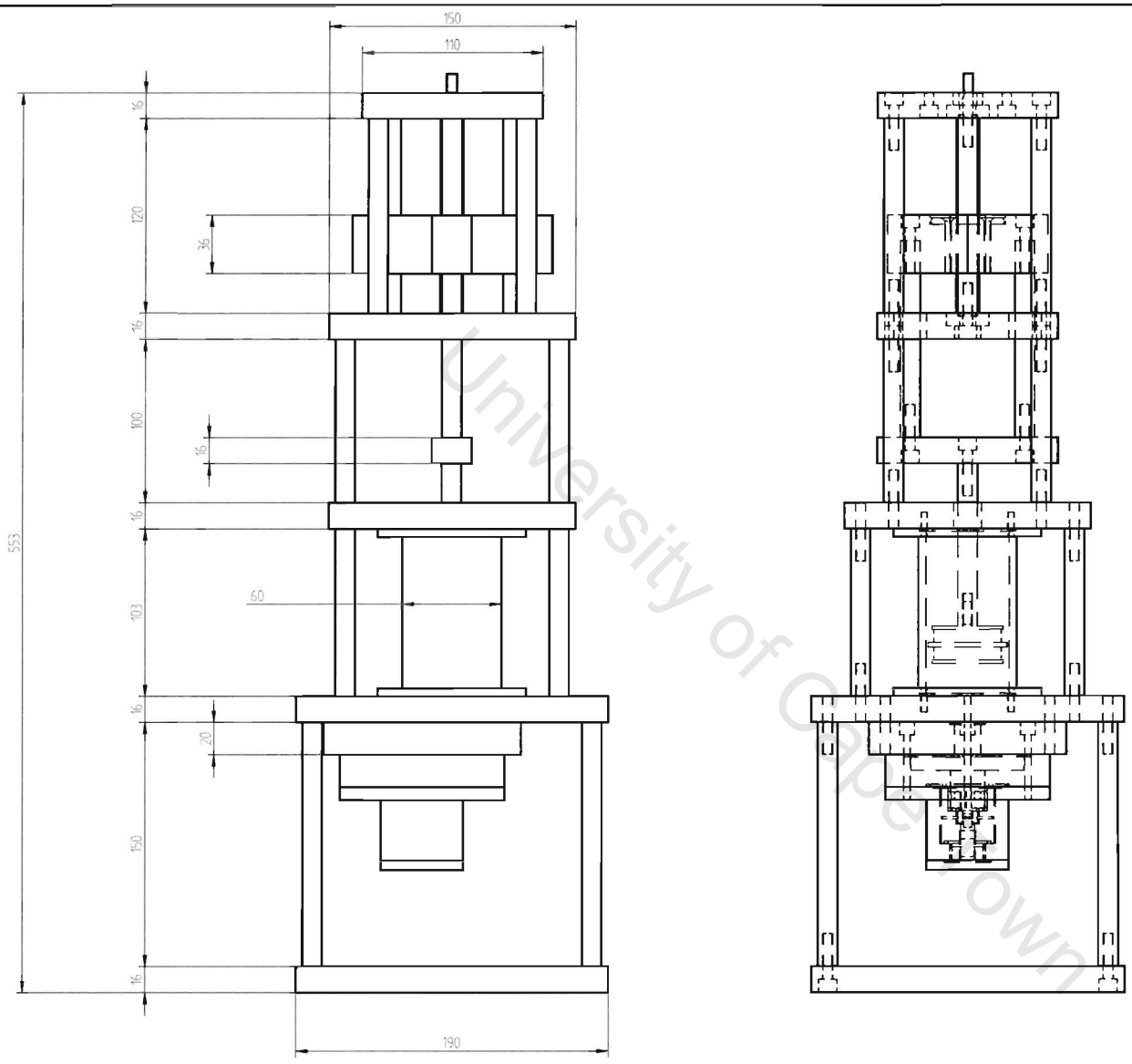




| | |
|---|---|
| Björn Prenzlow<br>University of Cape Town | Title: Assembly of Pressure System<br>Quantity: 1 |

*Picture of piezo tube siliconed onto base*

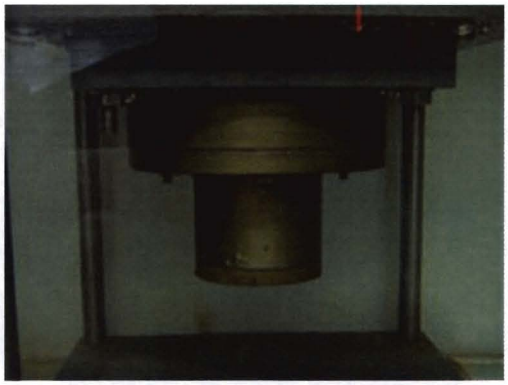

Picture of submerged thermal jacket

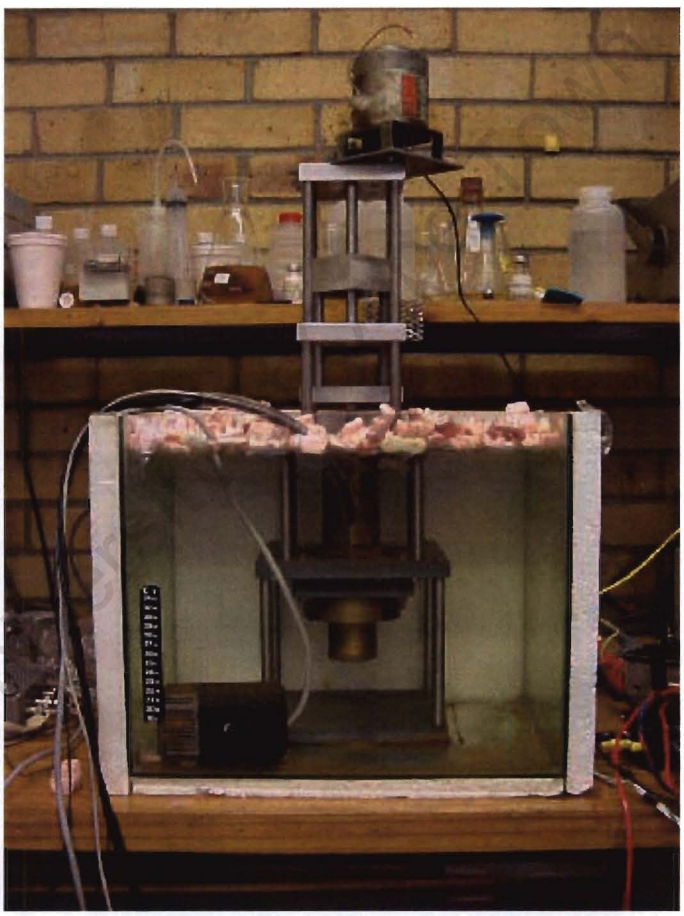

*Picture of complete system submerged in the bath (Front Polystyrene panel removed)*

## Pictures of the mechanical system

*Appendix B*

# *Electrical Circuit Diagrams*

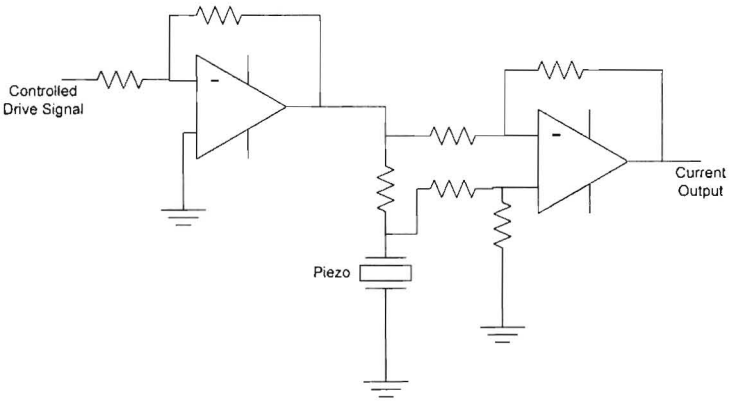


Circuit of the PCB used to drive the Piezo

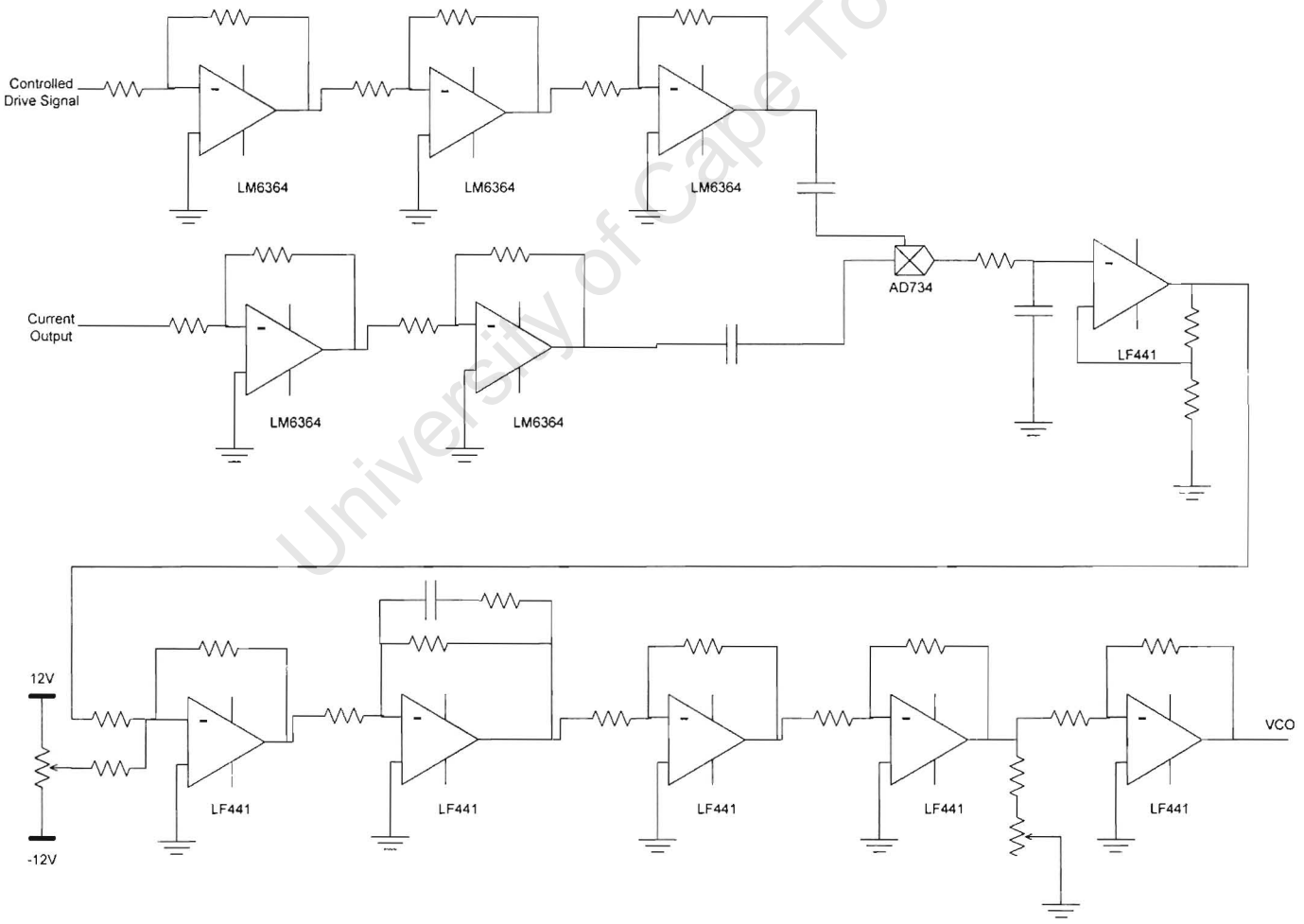




Circuit for the Phase Locked Loop

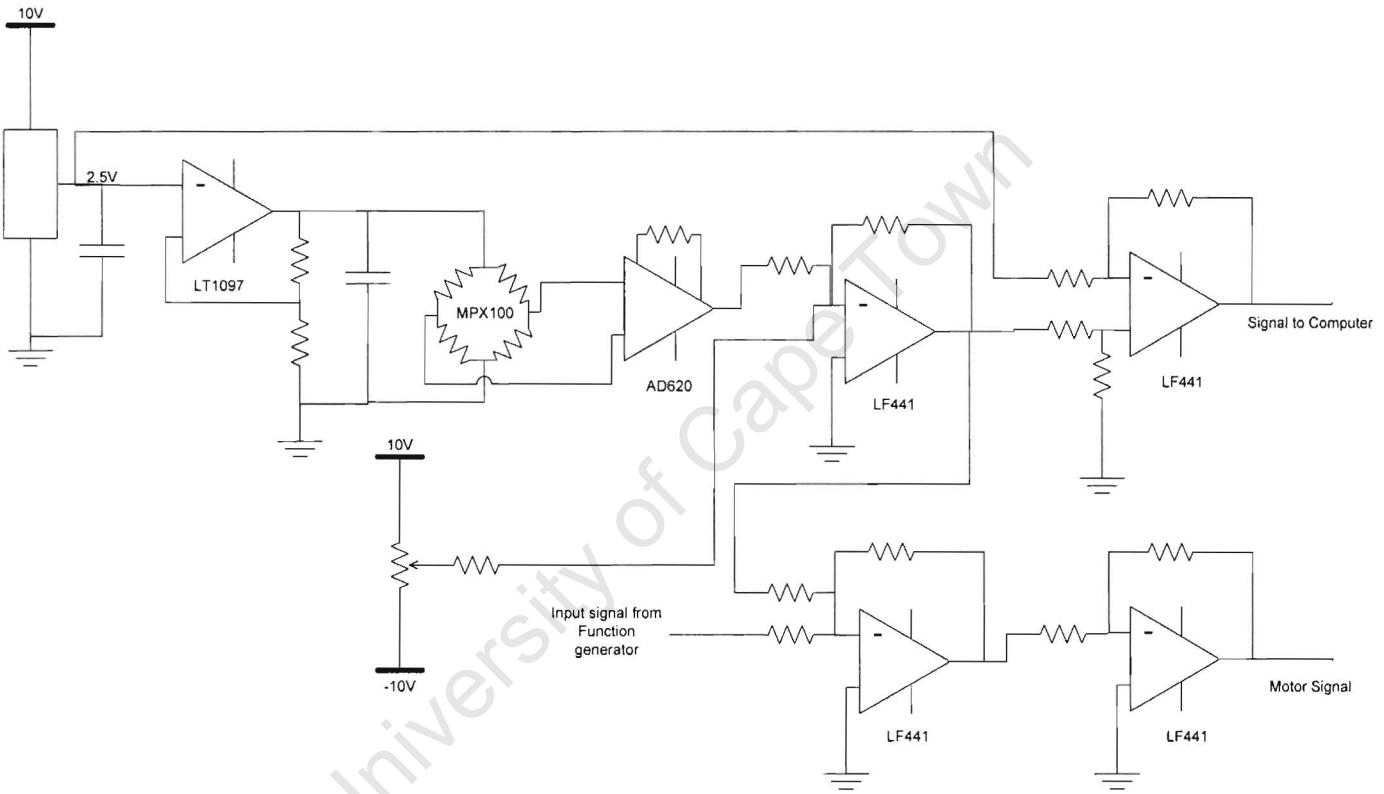




Circuit for the Pressure Controller


Top Layer (Scale 1:1)


Bottom Layer (Scale 1:1)

*PCB for the piezo drive circuit that was placed inside the thermal jacket*

*Appendix C*

## HPVEE Code

```
(saveFormat "2.3")
(date "Tue 18/Feb/2003 21:42:12 ")
(veerev "4.01")
(platform "PC")
(execMode fast)
(filterNAN 0)
(workspaceStackingOrder M.191 M)
(SaveCF no)
(device 0 ROOTCONTEXT
(properties
(trigMode deg)
(nextID 236)
(popupTitleText "Untitled")
(popupMoveable 1))
(deviceList
(UserFunctions
(nextID 1)
(context 0
(properties
(name "UserFunction1")
(trigMode deg)
(nextID 0)
(popupMoveable 1))
(deviceList
(configuration))
(contextCarrier
(active detail)
(detail
(extent 432 348)
(anchorPt 0 0)
(configuration)))))
(device 0 CALL
(properties
(name "Call e.GetBoardName")
(callFunc "e.GetBoardName")
(parmMode rev30))
(interface
(input 1
(name "bh")
(requires
(datatype Int32)
(shape "Scalar"))
(optional yes))
(output 1
(name "Name")
(lock name constraints)
(optional yes))))
(device 1 CONTEXT
(properties
(name "Call Edr Libraries")
(trigMode deg)
(nextID 2)
(popupTitleText "UserObject")
(popupMoveable 1))
(deviceList
(device 0 IMPORT
(properties
(name "Import Library")
(libType DLL)
(libName "edr")
(fileName
"c:\\WINDOWS\\SYSTEM\\EDR32.DLL")
(defnFileName
"c:\\Eagle\\HPVEE\\EDR32VEE.H"))
(implementation))
(device 1 IMPORT
(properties
(name "Import Library")
(libType userFunction)
(libName "e")
(fileName "c:\\Eagle\\HPVEE\\EDR.VEE"))
(implementation))
(configuration
(connect D0:0 D1:0)))
(contextCarrier
(active detail)
(detail
(extent 350 297)
(anchorPt -146 -68)
(configuration
(devCarrierFor 0
(active open)
(icon)
(open
(extent 252 113))
(pinCenter 340 150))
(devCarrierFor 1
(active open)
(icon)
(open
(extent 250 85))
(pinCenter 350 310))
(connect D0:0 D1:0
(points 4 340 209 340 230 350 230 350 247)))
(stackingOrder 0 1))))
(device 2 START25)
(device 5 CONSTANT
(properties
(name "Board Handler"))
(interface
(output 1
(name "Int32")
(lock name constraints)))
(implementation
(value Int32
(data 1))
(initValue Int32
(data 0))))
(device 6 CONSTANT
(properties
(name "Channel"))
(interface
(output 1
(name "Int32")
(lock name constraints)))
(implementation
(value Int32
(data 0))
(initValue Int32
(data 0))))
(device 93 IODEVICE
(properties
(name "FreqCounter ( @ 703)")
(transactions 24 "WRITE TEXT \"*RST\" EOL"
"WRITE TEXT \"*CLS\" EOL"
"WRITE TEXT \"*SRE 0\" EOL" "WRITE
TEXT \"*ESE 0\" EOL"
"WRITE TEXT \":STAT:PRES\" EOL" "WRITE
TEXT \":FORMAT ASCII\" EOL"
"WRITE TEXT \":FUNC \\\"FREQ 1\\\"\" EOL"
"WRITE TEXT \":EVENT1:LEVEL 0\" EOL"
"WRITE TEXT \":FREQ:ARM:STAR:SOUR
IMM\" EOL"
"WRITE TEXT \"FREQ:ARM:STOP:SOUR
TIM\" EOL"
"WRITE TEXT \":FREQ:ARM:STOP:TIM .01\"
EOL" "WRITE TEXT \":ROSC:SOUR INT\"
EOL"
"WRITE TEXT \":DAIG:CAL:INT:AUTO
OFF\" EOL" "WRITE TEXT \":DISP:ENAB
OFF\" EOL"
"WRITE TEXT \":CALC:MATH:STATE OFF\"
EOL"
"WRITE TEXT \":CALC2:LIM:STATE OFF\"
EOL"
"WRITE TEXT \":CALC3:AVER:STATE OFF\"
EOL" "WRITE TEXT \":HCOPY:CONT OFF\"
EOL"
"WRITE TEXT \"*DDT #15FETC?\" EOL"
"WRITE TEXT \"READ:FREQ?\" EOL"
"READ TEXT x REAL" "WRITE TEXT
\":FREQ:EXP1 \"" "WRITE TEXT x EOL"
"WRITE TEXT \":INIT:CONT ON\" EOL"))
(interface
(output 1
(name "X")
(optional yes)))
(implementation
(iopath "FreqCounter")))
(device 130 INPUTDLG
(properties
(name "Sample Name")
(prompt "Enter Liquid Sample\'s Name:")
(initialValue "FC75")
(valueConstraint "strLen(value)>0")
(vErrorMessage "Don\'t be such a reject!"))
(interface
(output 1
(name "Value")
(lock name constraints))
(output 2
(name "Cancel")
(lock name constraints)))
(implementation
(inputType "text")))
(device 131 INPUTDLG
(properties
(name "Density")
(popupTitle "Text Input")
(prompt "Enter Density:")
(initialValue "1768")
(valueConstraint "0<value")
(vErrorMessage "Negetive Densities?"))
(interface
(output 1
(name "Value")
(lock name constraints))
(output 2
(name "Cancel")
(lock name constraints)))
(implementation
(inputType "real")))
(device 132 INPUTDLG
(properties
(name "Sound Speed")
(popupTitle "Text Input")
(position 201 201)
(prompt "Enter Speed of Sound:")
(initialValue "567")
(valueConstraint "0<=value")
(vErrorMessage "Sound moving toward
source?"))
(interface
(output 1
(name "Value")
(lock name constraints))
(output 2
(name "Cancel")
(lock name constraints)))
(implementation
(inputType "real")))
(device 133 INPUTDLG
(properties
(name "Tempreture")
(popupTitle "Text Input")
(prompt "Tempreture:")
(initialValue "30")
(vErrorMessage ""))
(interface
(output 1
(name "Value")
(lock name constraints))
(output 2
(name "Cancel")
(lock name constraints)))
(implementation
(inputType "real")))
(device 134 INPUTDLG
(properties
(name "Filename")
(position 200 201)
(prompt "Enter Filename:")
(initialValue "c:\\Bjorn\\hpvee\\b_over_a\\")
(vErrorMessage ""))
(interface
(output 1
(name "Value")
(lock name constraints))
(output 2
(name "Cancel")
```

```
(lock name constraints)))
(implementation
(inputType "text")))
(device 135 TOFILE
(properties
(transactions 4 "WRITE TEXT \"Sample : \", A
EOL"
"WRITE TEXT \"Density : \", B EOL"
"WRITE TEXT \"Speed of Sound : \", C EOL"
"WRITE TEXT \"Tempreture : \", D EOL"))
(interface
(input 1
(name "A")
(optional yes))
(input 2
(name "B")
(optional yes))
(input 3
(name "C")
(optional yes))
(input 4
(name "D")
(optional yes))
(input 5
(type control)
(name "File Name")
(requires
(datatype Text)
(shape "Scalar"))
(lock name constraints)
(optional yes)))
(implementation
(attr iopath file write
"c:\\Bjorn\\hpvee\\b_over_a\\FC43_30deg_autor
un_d10"
(readTerm "\n")
(fs "\r\n")
(eol "\r\n")
(multiField fullSyntax)
(arrayFormat block))))
(device 149 IODEVICE
(properties
(name "funcgen (hp33120a @ 710)")
(transactions 18 "WRITE TEXT \"*RST\" EOL"
"WRITE TEXT \"*CLS\" EOL"
"WRITE TEXT \"OUTPUT:STATE OFF\"
EOL" "WRITE TEXT \"OUTPUT:SYNC OFF\"
EOL"
"WRITE TEXT \"*ESE 1\" EOL" "WRITE
TEXT \"*SRE 32\" EOL"
"WRITE TEXT \"FUNC SIN\" EOL" "WRITE
TEXT \"FREQ 0.1 HZ\" EOL"
"WRITE TEXT \"VOLT 1 VPP\" EOL" "WRITE
TEXT \"VOLT:OFFS 0\" EOL"
"WRITE TEXT \"BURS:MODE TRIG\" EOL"
"WRITE TEXT \"BURS:NCYC \", A EOL"
"WRITE TEXT \"BURS:INT:PER MAX\" EOL"
"WRITE TEXT \"BURS:PHAS 0\" EOL"
"WRITE TEXT \"TRIG:SOUR BUS\" EOL"
"WRITE TEXT \"BURST:STATE ON\" EOL"
"WRITE TEXT \"OUTPUT:STATE ON\" EOL"
"WRITE TEXT \"OUTPUT:SYNC ON\" EOL"))
(interface
(input 1
(name "A")
(optional yes)))
(implementation
(iopath "funcgen")))
(device 191 CONTEXT
(properties
(name "init_cycles")
(trigMode deg)
(nextID 7)
(popupTitleText "UserObject")
(popupMoveable 1))
(interface
(input 1
(name "A")
(optional yes))
(input 2
(name "B")
(optional yes))
(output 1
(type data)
(name "X")
(lock constraints)
(optional yes)))
(deviceList
(device 0 BREAK)
(device 1 IFTHENELSE
(properties
(cases 1 "A==1"))
(interface
(input 1
(name "A")
(optional yes))
(output 1
(name "Then")
(lock name constraints))
(output 2
(name "Else")
(lock name constraints))))
(device 2 FORMULA
(properties
(name "bit(x,n)")
(expr 1 "bit(x, n)"))
(interface
(input 1
(name "x")
(optional yes))
(input 2
(name "n")
(optional yes))
(output 1
(name "Result")
(tag "Result")
(lock name constraints)
(optional yes))))
(device 3 CONSTANT
(properties
(name "Integer"))
(interface
(output 1
(name "Int32")
(lock name constraints)))
(implementation
(value Int32
(data 6))
(initValue Int32
(data 0))))
(device 4 IODEVICE
(properties
(name "funcgen (hp33120a @ 710)")
(transactions 2 "WRITE TEXT \"*stb?\" EOL"
"READ TEXT x REAL"))
(interface
(output 1
(name "X")
(optional yes)))
(implementation
(iopath "funcgen")))
(device 5 REPEATUNTILBREAK
(interface
(output 1
(name "Continuous")
(lock name constraints))))
(device 6 IODEVICE
(properties
(name "funcgen (hp33120a @ 710)")
(transactions 4 "WRITE TEXT \"BURS:NCYC
\", A EOL" "WRITE TEXT \"*CLS\" EOL"
"EXECUTE TRIGGER" "WRITE TEXT
\"*OPC\" EOL"))
(interface
(input 1
(name "A")
(optional yes)))
(implementation
(iopath "funcgen")))
(configuration
(connect D1:1 D0:0)
(connect D2:1 D1:1)
(connect D4:1 D2:1)
(connect D3:1 D2:2)
(connect D5:1 D4:0)
(connect D6:0 D5:0)
(connect I1:1 D6:0)
(connect I2:1 D6:1)
(connect D5:0 O1:1)))
(contextCarrier
(wndOrigin 22 22)
(wndState res)
(active detail)
(detail
(extent 350 300)
(anchorPt 0 0)
(configuration
(devCarrierFor 0
(active icon)
(icon
(extent 41 16))
(open)
(terminals on)
(pinCenter 390 390))
(devCarrierFor 1
(active icon)
(icon
(extent 82 25))
(open
(extent 65 53))
(terminals on)
(pinCenter 340 350))
(devCarrierFor 2
(active icon)
(icon
(extent 47 25))
(open
(extent 81 42))
(terminals on)
(pinCenter 340 270))
(devCarrierFor 3
(active open)
(icon
(extent 48 16))
(open
(extent 84 30)
(showFormat int))
(pinCenter 250 290))
(devCarrierFor 4
(active icon)
(icon
(extent 192 52)
(iconImage "io.icn"))
(open
(extent 254 78))
(terminals on)
(pinCenter 350 210))
(devCarrierFor 5
(active icon)
(icon
(extent 74 52)
(iconImage "loop.icn"))
(open)
(terminals on)
(pinCenter 170 210))
(devCarrierFor 6
(active open)
(icon
(extent 192 52)
(iconImage "io.icn"))
(open
(extent 254 78))
(terminals on)
(pinCenter 190 130))
(connect D1:1 D0:0
(points 3 383 340 390 340 390 379))
(connect D2:1 D1:1
(points 6 366 270 390 270 390 320 290 320 290
350 296 350))
(connect D4:1 D2:1
```

```
(points 8 448 210 470 210 470 260 390 260 390
250 300 250 300 260 314 260))
(connect D3:1 D2:2
(points 4 294 290 290 290 290 280 314 280))
(connect D5:1 D4:0
(points 7 209 210 230 210 230 170 300 170 300
160 350 160 350 181))
(connect D6:0 D5:0
(points 4 190 171 190 170 170 170 170 181))
(connect I1:1 D6:0
(points 5 0 69 10 69 10 84 190 84 190 70))
(connect I2:1 D6:1
(points 4 0 229 10 229 10 130 30 130))
(connect D5:0 O1:1
(points 5 170 238 170 420 480 420 480 149 349
149)))
(stackingOrder 0 1 2 3 4 5 6))))
(device 192 CONTEXT
(properties
(name "Take_Readings")
(trigMode deg)
(nextID 23)
(popupTitleText "UserObject")
(popupMoveable 1))
(interface
(input 1
(name "Start")
(optional yes))
(input 2
(name "Board")
(optional yes))
(input 3
(name "Channel")
(optional yes))
(input 4
(name "No Cycles")
(optional yes))
(output 1
(type data)
(name "End")
(lock constraints)
(optional yes))
(output 2
(type data)
(name "Co-ord")
(lock constraints)
(optional yes))
(output 3
(type data)
(name "Array")
(lock constraints)
(optional yes))
(output 4
(type data)
(name "Voltage")
(lock constraints)
(optional yes))
(output 5
(type data)
(name "Pressure")
(lock constraints)
(optional yes))
(output 6
(type data)
(name "Frequency")
(lock constraints)
(optional yes))
(output 7
(type data)
(name "Read_next")
(lock constraints)
(optional yes)))
(deviceList
(device 0 BREAK)
(device 1 IFTHENELSE
(properties
(cases 1 "A==1"))
(interface
(input 1
(name "A")
(optional yes))
(output 1
(name "Then")
(lock name constraints))
(output 2
(name "Else")
(lock name constraints))))
(device 2 FORMULA
(properties
(name "bit(x,n)")
(expr 1 "bit(x, n)"))
(interface
(input 1
(name "x")
(optional yes))
(input 2
(name "n")
(optional yes))
(output 1
(name "Result")
(tag "Result")
(lock name constraints)
(optional yes))))
(device 3 CONSTANT
(properties
(name "Integer"))
(interface
(output 1
(name "Int32")
(lock name constraints)))
(implementation
(value Int32
(data 6))
(initValue Int32
(data 0))))
(device 4 COLLECTOR
(properties
(output1D 0))
(interface
(input 1
(name "Data")
(tag "Data"))
(input 2
(type control)
(name "Clear")
(lock name constraints)
(optional yes))
(input 3
(type trigger)
(name "XEQ")
(lock name constraints))
(output 1
(name "Array")
(tag "Array"))))
(device 5 COLLECTOR
(properties
(output1D 0))
(interface
(input 1
(name "Data")
(tag "Data"))
(input 2
(type control)
(name "Clear")
(lock name constraints)
(optional yes))
(input 3
(type trigger)
(name "XEQ")
(lock name constraints))
(output 1
(name "Array")
(tag "Array"))))
(device 6 IODEVICE
(properties
(name "funcgen (hp33120a @ 710)")
(transactions 2 "WRITE TEXT \"*stb?\" EOL"
"READ TEXT x REAL"))
(interface
(output 1
(name "X")
(optional yes)))
(implementation
(iopath "funcgen")))
(device 7 TORECORD
(properties
(outputType scalar))
(interface
(input 1
(name "A")
(optional yes))
(input 2
(name "B")
(optional yes))
(output 1
(name "Record"))))
(device 8 TOCOORDINATE
(interface
(input 1
(name "X Data")
(tag "X")
(requires
(datatype Real))
(lock constraints))
(input 2
(name "Y Data")
(tag "Y")
(requires
(datatype Real))
(lock constraints))
(output 1
(name "Coord")
(tag "Coord"))))
(device 9 FORMULA
(properties
(expr 1 "( -A)*19.6995*1000+50000"))
(interface
(input 1
(name "A")
(optional yes))
(output 1
(name "Result")
(tag "Result")
(lock name constraints)
(optional yes))))
(device 10 CALL
(properties
(name "Call e.VoltageIn")
(callFunc "e.VoltageIn")
(parmMode rev30))
(interface
(input 1
(name "Board")
(requires
(datatype Int32)
(shape "Scalar"))
(optional yes))
(input 2
(name "Channel")
(requires
(datatype Int32)
(shape "Scalar"))
(optional yes))
(output 1
(name "Voltage")
(lock name constraints)
(optional yes))))
(device 11 IODEVICE
(properties
(name "FreqCounter ( @ 703)")
(transactions 2 "EXECUTE TRIGGER" "READ
TEXT x REAL"))
(interface
(output 1
(name "X")
(optional yes)))
(implementation
(iopath "FreqCounter")))
(device 12 IODEVICE
(properties
```

```
(name "funcgen (hp33120a @ 710)")
(transactions 4 "WRITE TEXT \"BURS:NCYC
\", A EOL" "WRITE TEXT \"*cls\" EOL"
"EXECUTE TRIGGER" "WRITE TEXT
\"*OPC\" EOL"))
(interface
(input 1
(name "A")
(optional yes)))
(implementation
(iopath "funcgen")))
(device 13 REPEATUNTILBREAK
(interface
(output 1
(name "Continuous")
(lock name constraints))))
(device 18 TEXTDISPLAY
(properties
(name "Voltage"))
(interface
(input 1
(name "Data")))))
(device 19 TEXTDISPLAY
(properties
(name "pressure"))
(interface
(input 1
(name "Data"))))
(device 20 TEXTDISPLAY
(properties
(name "frequency"))
(interface
(input 1
(name "Data"))))
(configuration
(connect D1:1 D0:0)
(connect D2:1 D1:1)
(connect D6:1 D2:1)
(connect D3:1 D2:2)
(connect D7:0 D4:0)
(connect D7:1 D4:1)
(connect D12:0 D4:2)
(connect D1:1 D4:3)
(connect D7:0 D5:0)
(connect D8:1 D5:1)
(connect D12:0 D5:2)
(connect D1:1 D5:3)
(connect D7:0 D6:0)
(connect D9:0 D7:0)
(connect D9:1 D7:1)
(connect D11:1 D7:2)
(connect D9:0 D8:0)
(connect D9:1 D8:1)
(connect D11:1 D8:2)
(connect D10:0 D9:0)
(connect D10:1 D9:1)
(connect D11:0 D10:0)
(connect I2:1 D10:1)
(connect I3:1 D10:2)
(connect D13:1 D11:0)
(connect I1:1 D12:0)
(connect I4:1 D12:1)
(connect D12:0 D13:0)
(connect D7:0 D14:0)
(connect D10:1 D14:1)
(connect D14:0 D15:0)
(connect D9:1 D15:1)
(connect D15:0 D16:0)
(connect D11:1 D16:1)
(connect D13:0 O1:1)
(connect D5:1 O2:1)
(connect D4:1 O3:1)
(connect D10:1 O4:1)
(connect D9:1 O5:1)
(connect D11:1 O6:1)
(connect D7:0 O7:1)))
(contextCarrier
(active detail)
(panel
(extent 435 83)
(widget 14 detail
(relativeOrigin 10 20)
(title on)
(borderStyle flat)
(extent 131 28))
(widget 15 detail
(relativeOrigin 150 20)
(title on)
(borderStyle flat)
(extent 131 28)
(formatter
(realFormat standard)
(realSigDigits 7)
(realRadixSpec 4)
(integerBase decimal)))
(widget 16 detail
(relativeOrigin 290 20)
(title on)
(borderStyle flat)
(extent 131 28)
(formatter
(realFormat standard)
(realSigDigits 9)
(realRadixSpec 4)
(integerBase decimal))))
(detail
(extent 350 297)
(anchorPt -591 -78)
(configuration
(devCarrierFor 0
(active icon)
(icon
(extent 41 16))
(open)
(terminals on)
(pinCenter 760 540))
(devCarrierFor 1
(active icon)
(icon
(extent 82 25))
(open
(extent 65 53))
(terminals on)
(pinCenter 660 540))
(devCarrierFor 2
(active icon)
(icon
(extent 47 25))
(open
(extent 81 42))
(terminals on)
(pinCenter 570 540))
(devCarrierFor 3
(active open)
(icon
(extent 48 16))
(open
(extent 84 30)
(showFormat int))
(pinCenter 400 540))
(devCarrierFor 4
(active icon)
(icon
(extent 61 34))
(open
(extent 109 56))
(terminals on)
(pinCenter 730 300))
(devCarrierFor 5
(active icon)
(icon
(extent 61 34))
(open
(extent 109 56))
(terminals on)
(pinCenter 720 220))
(devCarrierFor 6
(active icon)
(icon
(extent 192 52)
(iconImage "io.icn"))
(open
(extent 254 78))
(terminals on)
(pinCenter 480 450))
(devCarrierFor 7
(active icon)
(icon
(extent 89 52)
(iconImage "build.icn"))
(open
(extent 113 56))
(terminals on)
(pinCenter 530 300))
(devCarrierFor 8
(active icon)
(icon
(extent 81 52)
(iconImage "build.icn"))
(open
(extent 17 50))
(terminals on)
(pinCenter 530 220))
(devCarrierFor 9
(active icon)
(icon
(extent 56 14))
(open
(extent 204 32))
(terminals on)
(pinCenter 400 300))
(devCarrierFor 10
(active icon)
(icon
(extent 108 25))
(open
(extent 196 53))
(terminals on)
(pinCenter 300 300))
(devCarrierFor 11
(active icon)
(icon
(extent 155 52)
(iconImage "io.icn"))
(open
(extent 254 78))
(terminals on)
(pinCenter 290 230))
(devCarrierFor 12
(active open)
(icon
(extent 192 52)
(iconImage "io.icn"))
(open
(extent 254 78))
(terminals on)
(pinCenter 140 70))
(devCarrierFor 13
(active icon)
(icon
(extent 74 52)
(iconImage "loop.icn"))
(open)
(terminals on)
(pinCenter 140 180))
(devCarrierFor 18
(active open)
(icon
(extent 52 0))
(open
(extent 131 28))
(pinCenter 250 400))
(devCarrierFor 19
(active open)
(icon
(extent 61 0))
(open
(extent 131 28)
(formatter
(realFormat standard)
```

```
(realSigDigits 7)
(realRadixSpec 4)
(integerBase decimal)))
(pinCenter 250 460))
(devCarrierFor 20
(active open)
(icon
(extent 69 0))
(open
(extent 131 28)
(formatter
(realFormat standard)
(realSigDigits 9)
(realRadixSpec 4)
(integerBase decimal)))
(pinCenter 250 530))
(connect D1:1 D0:0
(points 5 703 530 720 530 720 520 760 520 760
529))
(connect D2:1 D1:1
(points 2 596 540 616 540))
(connect D6:1 D2:1
(points 6 578 450 600 450 600 500 530 500 530
530 544 530))
(connect D3:1 D2:2
(points 4 444 540 460 540 460 550 544 550))
(connect D7:0 D4:0
(points 8 530 328 530 350 610 350 610 320 680
320 680 270 730 270 730 280))
(connect D7:1 D4:1
(points 4 577 300 600 300 600 290 697 290))
(connect D12:0 D4:2
(points 9 140 111 140 130 300 130 300 180 470
180 470 240 620 240 620 300 697
300))
(connect D1:1 D4:3
(points 8 703 530 720 530 720 520 780 520 780
260 670 260 670 310 697 310))
(connect D7:0 D5:0
(points 10 530 328 530 350 610 350 610 320 680
320 680 270 770 270 770 180 720
180 720 200))
(connect D8:1 D5:1
(points 4 573 220 590 220 590 210 687 210))
(connect D12:0 D5:2
(points 9 140 111 140 130 300 130 300 180 470
180 470 240 620 240 620 220 687
220))
(connect D1:1 D5:3
(points 8 703 530 720 530 720 520 780 520 780
260 670 260 670 230 687 230))
(connect D7:0 D6:0
(points 4 530 328 530 370 480 370 480 421))
(connect D9:0 D7:0
(points 6 400 309 400 320 390 320 390 260 530
260 530 271))
(connect D9:1 D7:1
(points 4 430 300 460 300 460 290 483 290))
(connect D11:1 D7:2
(points 4 370 230 450 230 450 310 483 310))
(connect D9:0 D8:0
(points 6 400 309 400 320 390 320 390 170 530
170 530 191))
(connect D9:1 D8:1
(points 4 430 300 460 300 460 210 487 210))
(connect D11:1 D8:2
(points 2 370 230 487 230))
(connect D10:0 D9:0
(points 6 300 315 300 340 440 340 440 270 400
270 400 290))
(connect D10:1 D9:1
(points 2 356 300 369 300))
(connect D11:0 D10:0
(points 4 290 258 290 270 300 270 300 285))
(connect I2:1 D10:1
(points 4 591 186 10 186 10 290 243 290))
(connect I3:1 D10:2
(points 4 591 256 10 256 10 310 243 310))
(connect D13:1 D11:0
(points 3 179 180 290 180 290 201))
(connect I1:1 D12:0
(points 3 591 116 140 116 140 10))
(connect I4:1 D12:1
(points 6 591 326 -70 326 -70 390 -90 390 -90 70
-20 70))
(connect D12:0 D13:0
(points 4 140 111 140 124 140 124 140 151))
(connect D7:0 D14:0
(points 6 530 328 530 370 280 370 280 360 250
360 250 365))
(connect D10:1 D14:1
(points 6 356 300 380 300 380 350 160 350 160
400 182 400))
(connect D14:0 D15:0
(points 2 250 416 250 425))
(connect D9:1 D15:1
(points 8 430 300 460 300 460 380 340 380 340
570 160 570 160 460 182 460))
(connect D15:0 D16:0
(points 2 250 476 250 495))
(connect D11:1 D16:1
(points 8 370 230 450 230 450 360 290 360 290
340 150 340 150 530 182 530))
(connect D13:0 O1:1
(points 9 140 208 140 230 200 230 200 170 320
170 320 -10 310 -10 310 106 940
106))
(connect D5:1 O2:1
(points 4 753 220 780 220 780 146 940 146))
(connect D4:1 O3:1
(points 4 763 300 790 300 790 186 940 186))
(connect D10:1 O4:1
(points 6 356 300 380 300 380 350 520 350 520
226 940 226))
(connect D9:1 O5:1
(points 6 430 300 460 300 460 380 600 380 600
266 940 266))
(connect D11:1 O6:1
(points 6 370 230 450 230 450 390 610 390 610
306 940 306))
(connect D7:0 O7:1
(points 9 530 328 530 370 540 370 540 400 600
400 600 440 630 440 630 346 940
346)))
(stackingOrder 13 11 9 8 7 6 3 2 1 0 10 14 15 16
4 5 12))))
(device 193 TEXTDISPLAY
(properties
(name "B/A"))
(interface
(input 1
(name "Data"))))
(device 194 FORMULA
(properties
(expr 1 "2*A*(B^2)*D/C"))
(interface
(input 1
(name "A")
(optional yes))
(input 2
(name "B")
(optional yes))
(input 3
(name "C")
(optional yes))
(input 4
(name "D")
(optional yes))
(output 1
(name "Result")
(tag "Result")
(lock name constraints)
(optional yes))))
(device 195 TEXTDISPLAY
(properties
(name "dF / dP"))
(interface
(input 1
(name "Data"))))
(device 196 FROMARRAY
(properties
(expr 1 "Ary[1]"))
(interface
(input 1
(name "Ary")
(tag "Ary"))
(output 1
(name "SubAry")
(tag "Result"))
(output 2
(name "Type")
(tag "Type"))
(output 3
(name "NumDims")
(tag "NumDims"))
(output 4
(name "DimSizes")
(tag "DimSizes"))
(output 5
(name "TotSize")
(tag "TotSize"))))
(device 197 FROMARRAY
(properties
(expr 1 "Ary[0]"))
(interface
(input 1
(name "Ary")
(tag "Ary"))
(output 1
(name "SubAry")
(tag "Result"))
(output 2
(name "Type")
(tag "Type"))
(output 3
(name "NumDims")
(tag "NumDims"))
(output 4
(name "DimSizes")
(tag "DimSizes"))
(output 5
(name "TotSize")
(tag "TotSize"))))
(device 198 TOFILE
(properties
(transactions 7 "WRITE TEXT \" \" EOL"
"WRITE TEXT \"Frequency : \", B, \" ,Period :
\", F EOL"
"WRITE TEXT \"Frequency ,Pressure\" EOL"
"WRITE TEXT a EOL"
"WRITE TEXT \" \" EOL"
"WRITE TEXT \"dF/dP, \", C, \", F0, \", D, \"
,B/A ,\", E EOL"
"WRITE TEXT \" \" EOL"))
(interface
(input 1
(name "A")
(optional yes))
(input 2
(name "C")
(optional yes))
(input 3
(name "D")
(optional yes))
(input 4
(name "E")
(optional yes))
(input 5
(name "B")
(optional yes))
(input 6
(name "F")
(optional yes))
(input 7
(type control)
(name "File Name")
(requires
(datatype Text)
(shape "Scalar"))
(lock name constraints)
```

```
(optional yes)))
(implementation
(attr iopath file write
"c:\\Bjorn\\hpvee\\b_over_a\\FC43_30deg_autor
un_d10"
(readTerm "\n")
(fs "\r\n")
(eol "\r\n")
(multiField dataOnly)
(arrayFormat block))))
(device 199 REGRESSION
(properties
(fit LIN))
(interface
(input 1
(name "Point List")
(tag "InCoords")
(requires
(datatype Coord))
(lock name constraints))
(output 1
(name "Fitted Data")
(tag "OutCoords")
(lock name constraints))
(output 2
(name "Coeffs")
(tag "Coeffs")
(lock name constraints))
(output 3
(name "Goodness")
(tag "Goodness")
(lock name constraints))))
(device 200 YPLOT
(properties
(name "XY Trace"))
(interface
(input 1
(name "Trace1")
(lock constraints))
(input 2
(type control)
(name "Auto Scale X")
(lock name constraints)
(optional yes))
(input 3
(type control)
(name "Auto Scale Y")
(lock name constraints)
(optional yes)))
(implementation
(tracePin 1)
(graphMode rectangular)))
(device 206 TEXTDISPLAY
(interface
(input 1
(name "Data"))))
(device 207 IODEVICE
(properties
(name "funcgen (hp33120a @ 710)")
(transactions 1 "WRITE TEXT \"FREQ \", A, \"
HZ\" EOL"))
(interface
(input 1
(name "A")
(optional yes)))
(implementation
(iopath "funcgen")))
(device 208 FORMULA
(properties
(expr 1 "1/(A+(B*C))"))
(interface
(input 1
(name "A")
(optional yes))
(input 2
(name "B")
(optional yes))
(input 3
(name "C")
(optional yes))
(output 1
(name "Result")
(tag "Result")
(lock name constraints)
(optional yes))))
(device 210 CONSTANT
(properties
(name "Start Period"))
(interface
(output 1
(name "Real")
(lock name constraints)))
(implementation
(value Real
(data 10))
(initValue Real
(data 0))))
(device 211 CONSTANT
(properties
(name "Period Increment"))
(interface
(output 1
(name "Real")
(lock name constraints)))
(implementation
(value Real
(data 0.25))
(initValue Real
(data 0))))
(device 212 FORMULA
(properties
(expr 1 "1/A"))
(interface
(input 1
(name "A")
(optional yes))
(output 1
(name "Result")
(tag "Result")
(lock name constraints)
(optional yes))))
(device 213 TORECORD
(properties
(outputType scalar))
(interface
(input 1
(name "A")
(optional yes))
(input 2
(name "B")
(optional yes))
(output 1
(name "Record"))))
(device 214 TOCOORDINATE
(interface
(input 1
(name "X Data")
(tag "X")
(requires
(datatype Real))
(lock constraints))
(input 2
(name "Y Data")
(tag "Y")
(requires
(datatype Real))
(lock constraints))
(output 1
(name "Coord")
(tag "Coord"))))
(device 215 YPLOT
(properties
(name "XY Trace"))
(interface
(input 1
(name "Trace1")
(lock constraints))
(input 2
(type control)
(name "Auto Scale X")
(lock name constraints)
(optional yes))
(input 3
(type control)
(name "Auto Scale Y")
(lock name constraints)
(optional yes)))
(implementation
(tracePin 1)
(graphMode rectangular)))
(device 216 REGRESSION
(properties
(fit POLY)
(order 2))
(interface
(input 1
(name "Point List")
(tag "InCoords")
(requires
(datatype Coord))
(lock name constraints)
(optional yes))))
(device 217 TEXTDISPLAY
(properties
(name "Poly Terms(Projected B/A)' ))
(interface
(input 1
(name "Data"))))
(device 218 TEXTDISPLAY
(properties
(name "Goodness"))
(interface
(input 1
(name "Data"))))
(device 219 COLLECTOR
(properties
(output1D 0))
(interface
(input 1
(name "Data")
(tag "Data"))
(input 2
(type control)
(name "Clear")
(lock name constraints)
(optional yes))
(input 3
(type trigger)
(name "XEQ")
(lock name constraints))
(output 1
(name "Array")
(tag "Array"))))
(device 220 FORRANGE
(properties
(from 0)
(thru 80)
(step 1))
(interface
(output 1
(name "Data")
(lock name constraints))))
(device 223 COLLECTOR
(properties
(output1D 0))
(interface
(input 1
(name "Data")
```

```
(tag "Data"))
(input 2
(type trigger)
(name "XEQ")
(lock name constraints))
(output 1
(name "Array")
(tag "Array"))))
(device 224 FROMARRAY
(properties
(expr 1 "Ary[0]"))
(interface
(input 1
(name "Ary")
(tag "Ary"))
(output 1
(name "SubAry")
(tag "Result"))
(output 2
(name "Type")
(tag "Type"))
(output 3
(name "NumDims")
(tag "NumDims"))
(output 4
(name "DimSizes")
(tag "DimSizes"))
(output 5
(name "TotSize")
(tag "TotSize"))))
(device 225 TOFILE
(properties
(transactions 6 "WRITE TEXT \" \" EOL"
"WRITE TEXT \"Period , Tempreture Affected
B/A\" EOL" "WRITE TEXT a EOL"
"WRITE TEXT \" \" EOL" "WRITE TEXT
\"Projected B/A\", B EOL"
"WRITE TEXT \"R^2 Error : \", C EOL"))
(interface
(input 1
(name "A")
(optional yes))
(input 2
(name "B")
(optional yes))
(input 3
(name "C")
(optional yes))
(input 4
(type control)
(name "File Name")
(requires
(datatype Text)
(shape "Scalar"))
(lock name constraints)
(optional yes)))
(implementation
(attr iopath file write
"c:\\Bjorn\\hpvee\\b_over_a\\FC43_30deg_autor
un_d10"
(readTerm "\n")
(fs "\r\n")
(eol "\r\n")
(multiField fullSyntax)
(arrayFormat block))))
(device 226 CONSTANT
(properties
(name "No. of Cycles"))
(interface
(output 1
(name "Int32")
(lock name constraints)))
(implementation
(value Int32
(data 2))
(initValue Int32
(data 0))))
(device 228 CONSTANT
(properties
(name "Init Cycles"))
(interface
(output 1
(name "Int32")
(lock name constraints)))
(implementation
(value Int32
(data 2))
(initValue Int32
(data 0))))
(device 229 CONSTANT
(properties
(name "Run Cycles"))
(interface
(output 1
(name "Int32")
(lock name constraints)))
(implementation
(value Int32
(data 3))
(initValue Int32
(data 0))))
(device 235 DELAY
(properties
(delay 120))
(interface
(output 1
(name "Done"))))
(configuration
(connect D1:0 D0:0)
(connect D3:1 D0:1)
(connect D12:0 D1:0)
(connect D11:0 D5:0)
(connect D2:0 D6:0)
(connect D6:0 D7:0)
(connect D7:0 D8:0)
(connect D8:0 D9:0)
(connect D9:0 D10:0)
(connect D10:0 D11:0)
(connect D6:1 D11:1)
(connect D7:1 D11:2)
(connect D8:1 D11:3)
(connect D9:1 D11:4)
(connect D10:1 D11:5)
(connect D5:0 D12:0)
(connect D40:1 D12:1)
(connect D24:0 D13:0)
(connect D24:0 D13:1)
(connect D41:1 D13:2)
(connect D13:1 D14:0)
(connect D13:1 D14:1)
(connect D3:1 D14:2)
(connect D4:1 D14:3)
(connect D42:1 D14:4)
(connect D16:0 D15:0)
(connect D16:1 D15:1)
(connect D19:0 D16:0)
(connect D7:1 D16:1)
(connect D8:1 D16:2)
(connect D19:1 D16:3)
(connect D18:1 D16:4)
(connect D21:0 D17:0)
(connect D18:1 D17:1)
(connect D21:0 D18:0)
(connect D21:2 D18:1)
(connect D18:0 D19:0)
(connect D21:2 D19:1)
(connect D16:0 D20:0)
(connect D14:3 D20:1)
(connect D19:1 D20:2)
(connect D18:1 D20:3)
(connect D16:1 D20:4)
(connect D25:1 D20:5)
(connect D28:1 D20:6)
(connect D10:1 D20:7)
(connect D14:1 D21:0)
(connect D14:2 D21:1)
(connect D14:1 D22:0)
(connect D14:2 D22:1)
(connect D22:0 D22:2)
(connect D22:0 D22:3)
(connect D36:1 D23:1)
(connect D25:0 D24:0)
(connect D25:1 D24:1)
(connect D36:1 D25:0)
(connect D26:1 D25:1)
(connect D27:1 D25:2)
(connect D36:1 D25:3)
(connect D25:0 D28:0)
(connect D25:1 D28:1)
(connect D16:0 D29:0)
(connect D28:1 D29:1)
(connect D16:1 D29:2)
(connect D16:0 D30:0)
(connect D28:1 D30:1)
(connect D16:1 D30:2)
(connect D30:0 D31:0)
(connect D30:1 D31:1)
(connect D31:0 D31:2)
(connect D31:0 D31:3)
(connect D36:0 D32:0)
(connect D35:1 D32:1)
(connect D38:0 D33:0)
(connect D38:1 D33:1)
(connect D32:0 D34:0)
(connect D32:3 D34:1)
(connect D30:0 D35:0)
(connect D30:1 D35:1)
(connect D36:0 D35:3)
(connect D43:1 D36:0)
(connect D29:0 D37:0)
(connect D29:1 D37:1)
(connect D36:0 D37:2)
(connect D32:0 D38:0)
(connect D32:2 D38:1)
(connect D38:0 D39:0)
(connect D37:1 D39:1)
(connect D38:1 D39:2)
(connect D32:3 D39:3)
(connect D10:1 D39:4)
(connect D0:0 D43:0))
(ShowOnExecPanel))
(contextCarrier
(wndOrigin -18 51)
(wndState res)
(active detail)
(panel
(extent 622 417)
(widget 2 detail
(relativeOrigin 20 10)
(title off)
(borderStyle none)
(extent 47 21))
(widget 22 detail
(relativeOrigin 20 90)
(title on)
(borderStyle flat)
(extent 296 272)
(displayMode scrollGraph)
(graphType cartesian)
(gridType grid)
(scale 0
(name "Y name")
(domainName "X name")
(pen 9)
(show 1)
(range 2460000 2460900 4 linear))
(domain -20000 25000 4 linear)
(trace 0 onScale 0
(name "Trace1")
(pen 4)
(lineType 1)
(pointType 0)))
(widget 31 detail
(relativeOrigin 320 90)
(title on)
(borderStyle flat)
(extent 296 272)
(displayMode scrollGraph)
(graphType cartesian)
(gridType grid)
```

```
(scale 0
(name "Y name")
(domainName "X name")
(pen 9)
(show 1)
(range 12.5 12.75 4 linear))
(domain 10 18 4 linear)
(trace 0 onScale 0
(name "Trace1")
(pen 4)
(lineType 1)
(pointType 0)))
(widget 15 detail
(relativeOrigin 20 40)
(title on)
(borderStyle flat)
(extent 131 28))
(widget 23 detail
(relativeOrigin 160 40)
(title on)
(borderStyle flat)
(extent 96 28))
(widget 33 detail
(relativeOrigin 260 40)
(title on)
(borderStyle flat)
(extent 216 28))
(widget 34 detail
(relativeOrigin 480 40)
(title on)
(borderStyle flat)
(extent 131 28)))
(detail
(extent 491 345)
(anchorPt 14 15)
(configuration
(devCarrierFor 0
(active icon)
(icon
(extent 150 16))
(open
(extent 196 53))
(terminals on)
(pinCenter 260 140))
(devCarrierFor 1
(active icon)
(icon
(extent 119 16))
(terminals on)
(pinCenter 260 110))
(devCarrierFor 2
(active open)
(icon)
(open
(extent 47 21))
(title off)
(pinCenter 250 -320))
(devCarrierFor 5
(active icon)
(icon
(extent 100 16))
(open
(extent 136 30)
(showFormat int))
(pinCenter 90 320))
(devCarrierFor 6
(active icon)
(icon
(extent 58 16))
(open
(extent 94 30)
(showFormat int))
(pinCenter 100 360))
(devCarrierFor 93
(active icon)
(icon
(extent 155 52)
(iconImage "io.icn"))
(open
(extent 254 78))
(terminals on)
(pinCenter 260 -10))
(devCarrierFor 130
(active icon)
(icon
(extent 95 25))
(open
(extent 290 107))
(terminals on)
(pinCenter 180 -250))
(devCarrierFor 131
(active icon)
(icon
(extent 51 25))
(open
(extent 473 107))
(terminals on)
(pinCenter 140 -200))
(devCarrierFor 132
(active icon)
(icon
(extent 94 25))
(open
(extent 473 107))
(terminals on)
(pinCenter 130 -150))
(devCarrierFor 133
(active icon)
(icon
(extent 81 25))
(open
(extent 473 107))
(terminals on)
(pinCenter 260 -200))
(devCarrierFor 134
(active icon)
(icon
(extent 63 25))
(open
(extent 290 107))
(terminals on)
(pinCenter 190 -80))
(devCarrierFor 135
(active icon)
(icon
(extent 48 65))
(open
(extent 256 133))
(terminals on)
(pinCenter 530 -150))
(devCarrierFor 149
(active icon)
(icon
(extent 192 52)
(iconImage "io.icn"))
(open
(extent 254 78))
(terminals on)
(pinCenter 260 60))
(devCarrierFor 191
(active icon)
(icon
(extent 71 34))
(terminals on)
(pinCenter 280 460))
(devCarrierFor 192
(active icon)
(icon
(extent 110 74))
(open
(extent 480 297)
(carbonCopy))
(terminals on)
(bg "Light Blue Gray")
(pinCenter 430 490))
(devCarrierFor 193
(active open)
(icon
(extent 26 16))
(open
(extent 131 28))
(pinCenter 920 480))
(devCarrierFor 194
(active icon)
(icon
(extent 57 45))
(open
(extent 150 82))
(terminals on)
(pinCenter 850 290))
(devCarrierFor 195
(active icon)
(icon
(extent 50 16))
(open
(extent 131 28)
(formatter
(realFormat standard)
(realSigDigits 9)
(realRadixSpec 4)
(integerBase decimal)))
(pinCenter 670 220))
(devCarrierFor 196
(active icon)
(icon
(extent 77 54)
(iconImage "unbuild.icn"))
(open
(extent 111 110))
(terminals on)
(pinCenter 670 290))
(devCarrierFor 197
(active icon)
(icon
(extent 77 54)
(iconImage "unbuild.icn"))
(open
(extent 111 110))
(terminals on)
(pinCenter 680 360))
(devCarrierFor 198
(active icon)
(icon
(extent 48 74))
(open
(extent 256 157))
(terminals on)
(pinCenter 650 460))
(devCarrierFor 199
(active icon)
(icon
(extent 79 34))
(open
(extent 134 70))
(terminals on)
(pinCenter 520 300))
(devCarrierFor 200
(active icon)
(icon
(extent 68 52)
(iconImage "display.icn"))
(open
(extent 296 272)
(displayMode scrollGraph)
(graphType cartesian)
(gridType grid)
(scale 0
(name "Y name")
(domainName "X name")
(pen 9)
(show 1)
(range 2460000 2460900 4 linear))
(domain -20000 25000 4 linear)
(trace 0 onScale 0
(name "Trace1")
(pen 4)
(lineType 1)
(pointType 0)))
(pinCenter 510 370))
(devCarrierFor 206
```

```
(active icon)
(icon
(extent 95 16))
(open
(extent 131 28))
(pinCenter 420 160))
(devCarrierFor 207
(active icon)
(icon
(extent 192 52)
(iconImage "io.icn"))
(open
(extent 254 78))
(terminals on)
(pinCenter 300 370))
(devCarrierFor 208
(active icon)
(icon
(extent 57 34))
(open
(extent 107 62))
(terminals on)
(pinCenter 300 300))
(devCarrierFor 210
(active open)
(icon
(extent 82 16))
(open
(extent 148 30)
(showFormat real))
(pinCenter 80 240))
(devCarrierFor 211
(active icon)
(icon
(extent 117 16))
(open
(extent 183 30)
(showFormat real))
(pinCenter 50 280))
(devCarrierFor 212
(active icon)
(icon
(extent 57 16))
(open
(extent 72 32))
(terminals on)
(pinCenter 430 270))
(devCarrierFor 213
(active icon)
(icon
(extent 89 52)
(iconImage "build.icn"))
(open
(extent 113 56))
(terminals on)
(pinCenter 1040 380))
(devCarrierFor 214
(active icon)
(icon
(extent 81 52)
(iconImage "build.icn"))
(open)
(terminals on)
(pinCenter 970 260))
(devCarrierFor 215
(active icon)
(icon
(extent 81 58)
(iconImage "display.icn"))
(open
(extent 296 272)
(displayMode scrollGraph)
(graphType cartesian)
(gridType grid)
(scale 0
(name "Y name")
(domainName "X name")
(pen 9)
(show 1)
(range 12.5 12.75 4 linear))
(domain 10 18 4 linear)
(trace 0 onScale 0
(name "Trace1")
(pen 4)
(lineType 1)
(pointType 0)))
(pinCenter 1130 200))
(devCarrierFor 216
(active icon)
(icon
(extent 79 34))
(open
(extent 145 78))
(terminals on)
(pinCenter 1130 310))
(devCarrierFor 217
(active open)
(icon
(extent 183 0))
(open
(extent 219 28))
(pinCenter 1440 320))
(devCarrierFor 218
(active open)
(icon
(extent 71 0))
(open
(extent 131 28))
(pinCenter 1280 390))
(devCarrierFor 219
(active icon)
(icon
(extent 61 34))
(open
(extent 109 56))
(terminals on)
(pinCenter 1030 310))
(devCarrierFor 220
(active icon)
(icon
(extent 74 52)
(iconImage "loop.icn"))
(open
(extent 110 82))
(pinCenter 260 210))
(devCarrierFor 223
(active icon)
(icon
(extent 61 25))
(open)
(terminals on)
(pinCenter 1150 430))
(devCarrierFor 224
(active icon)
(icon
(extent 77 54)
(iconImage "unbuild.icn"))
(open
(extent 111 110))
(terminals on)
(pinCenter 1250 320))
(devCarrierFor 225
(active icon)
(icon
(extent 48 45))
(open
(extent 256 133))
(terminals on)
(pinCenter 1500 500))
(devCarrierFor 226
(active icon)
(icon
(extent 91 16))
(open
(extent 127 30)
(showFormat int))
(pinCenter 20 60))
(devCarrierFor 228
(active open)
(icon
(extent 70 16))
(open
(extent 106 30)
(showFormat int))
(pinCenter 150 540))
(devCarrierFor 229
(active open)
(icon
(extent 79 16))
(open
(extent 115 30)
(showFormat int))
(pinCenter 270 540))
(devCarrierFor 235
(active open)
(icon)
(open
(extent 76 32))
(pinCenter 160 170))
(connect D1:0 D0:0
(points 2 260 120 260 129))
(connect D3:1 D0:1
(points 6 142 320 180 320 180 180 160 180 160
140 182 140))
(connect D12:0 D1:0
(points 2 260 88 260 99))
(connect D11:0 D5:0
(points 4 530 -115 530 -90 260 -90 260 -39))
(connect D2:0 D6:0
(points 4 250 -307 250 -290 180 -290 180 -265))
(connect D6:0 D7:0
(points 4 180 -235 180 -220 140 -220 140 -215))
(connect D7:0 D8:0
(points 4 140 -185 140 -170 130 -170 130 -165))
(connect D8:0 D9:0
(points 6 130 -135 130 -110 200 -110 200 -220
260 -220 260 -215))
(connect D9:0 D10:0
(points 8 260 -185 260 -170 240 -170 240 -140
210 -140 210 -100 190 -100 190 -95
))
(connect D10:0 D11:0
(points 8 190 -65 190 -50 240 -50 240 -100 320 -
100 320 -200 530 -200 530 -185))
(connect D6:1 D11:1
(points 4 230 -260 340 -260 340 -170 503 -170))
(connect D7:1 D11:2
(points 4 168 -210 190 -210 190 -160 503 -160))
(connect D8:1 D11:3
(points 4 179 -160 190 -160 190 -150 503 -150))
(connect D9:1 D11:4
(points 4 303 -210 330 -210 330 -140 503 -140))
(connect D10:1 D11:5
(points 6 224 -90 230 -90 230 -70 470 -70 470 -
130 503 -130))
(connect D5:0 D12:0
(points 2 260 18 260 31))
(connect D40:1 D12:1
(points 2 68 60 161 60))
(connect D24:0 D13:0
(points 4 300 398 300 420 280 420 280 440))
(connect D24:0 D13:1
(points 5 300 398 300 420 230 420 230 450 242
450))
(connect D41:1 D13:2
(points 4 205 540 210 540 210 470 242 470))
(connect D13:1 D14:0
(points 5 318 460 360 460 360 430 430 430 430
450))
(connect D13:1 D14:1
(points 2 318 460 372 460))
(connect D3:1 D14:2
(points 8 142 320 170 320 170 480 220 480 220
490 330 490 330 480 372 480))
(connect D4:1 D14:3
(points 8 131 360 150 360 150 410 310 410 310
420 350 420 350 500 372 500))
(connect D42:1 D14:4
(points 4 330 540 350 540 350 520 372 520))
(connect D16:0 D15:0
```

(points 4 850 315 850 340 920 340 920 445))
(connect D16:1 D15:1
(points 8 881 290 890 290 890 320 900 320 900
390 830 390 830 480 852 480))
(connect D19:0 D16:0
(points 6 680 389 680 410 740 410 740 250 850
250 850 265))
(connect D7:1 D16:1
(points 8 168 -210 190 -210 190 -160 480 -160
480 -210 750 -210 750 270 819 270)
)
(connect D8:1 D16:2
(points 8 179 -160 190 -160 190 -150 250 -150
250 -80 730 -80 730 280 819 280))
(connect D19:1 D16:3
(points 4 721 340 750 340 750 290 819 290))
(connect D18:1 D16:4
(points 6 711 270 720 270 720 290 730 290 730
300 819 300))
(connect D21:0 D17:0
(points 8 520 319 520 340 570 340 570 280 590
280 590 200 670 200 670 209))
(connect D18:1 D17:1
(points 6 711 270 730 270 730 240 630 240 630
220 642 220))
(connect D21:0 D18:0
(points 10 520 319 520 340 570 340 570 280 590
280 590 230 620 230 620 250 670
250 670 260))
(connect D21:2 D18:1
(points 4 562 300 590 300 590 290 629 290))
(connect D18:0 D19:0
(points 2 670 319 680 330))
(connect D21:2 D19:1
(points 4 562 300 600 300 600 360 639 360))
(connect D16:0 D20:0
(points 8 850 315 850 350 820 350 820 420 670
420 670 410 650 410 650 420))
(connect D14:3 D20:1
(points 4 487 480 510 480 510 430 623 430))
(connect D19:1 D20:2
(points 6 721 340 730 340 730 400 610 400 610
440 623 440))
(connect D18:1 D20:3
(points 8 711 270 730 270 730 240 610 240 610
370 600 370 600 450 623 450))
(connect D16:1 D20:4
(points 12 881 290 890 290 890 320 900 320 900
390 830 390 830 480 820 480 820
510 600 510 600 460 623 460))
(connect D25:1 D20:5
(points 10 331 300 350 300 350 270 380 270 380
300 440 300 440 440 520 440 520
470 623 470))
(connect D28:1 D20:6
(points 12 461 270 470 270 470 290 430 290 430
410 520 410 520 420 530 420 530
520 610 520 610 480 623 480))
(connect D10:1 D20:7
(points 6 224 -90 230 -90 230 -70 570 -70 570
490 623 490))
(connect D14:1 D21:0
(points 5 487 460 580 460 580 260 520 260 520
280))
(connect D14:2 D21:1
(points 6 487 470 500 470 500 430 450 430 450
300 478 300))
(connect D14:1 D22:0
(points 5 487 460 580 460 580 330 510 330 510
341))
(connect D14:2 D22:1
(points 6 487 470 500 470 500 430 450 430 450
360 473 360))
(connect D22:0 D22:2
(points 5 510 398 510 420 460 420 460 370 473
370))
(connect D22:0 D22:3
(points 5 510 398 510 420 460 420 460 380 473
380))
(connect D36:1 D23:1
(points 4 299 210 350 210 350 160 370 160))
(connect D25:0 D24:0
(points 2 300 319 300 341))
(connect D25:1 D24:1
(points 8 331 300 350 300 350 260 190 260 190
330 180 330 180 370 201 370))
(connect D36:1 D25:0
(points 5 299 210 320 210 320 260 300 260 300
280))
(connect D26:1 D25:1
(points 4 156 240 200 240 200 290 269 290))
(connect D27:1 D25:2
(points 4 111 280 160 280 160 300 269 300))
(connect D36:1 D25:3
(points 6 299 210 320 210 320 260 250 260 250
310 269 310))
(connect D25:0 D28:0
(points 8 300 319 300 330 340 330 340 320 360
320 360 240 430 240 430 259))
(connect D25:1 D28:1
(points 4 331 300 350 300 350 270 399 270))
(connect D16:0 D29:0
(points 4 850 315 850 340 1040 340 1040 351))
(connect D28:1 D29:1
(points 8 461 270 480 270 480 190 900 190 900
310 930 310 930 370 993 370))
(connect D16:1 D29:2
(points 6 881 290 890 290 890 320 900 320 900
390 993 390))
(connect D16:0 D30:0
(points 6 850 315 850 340 910 340 910 210 970
210 970 231))
(connect D28:1 D30:1
(points 6 461 270 480 270 480 190 900 190 900
250 927 250))
(connect D16:1 D30:2
(points 4 881 290 890 290 890 270 927 270))
(connect D30:0 D31:0
(points 10 970 288 970 300 990 300 990 290
1010 290 1010 280 1030 280 1030 150
1130 150 1130 168))
(connect D30:1 D31:1
(points 4 1013 260 1040 260 1040 180 1087
180))
(connect D31:0 D31:2
(points 5 1130 231 1130 250 1070 250 1070 200
1087 200))
(connect D31:0 D31:3
(points 5 1130 231 1130 250 1070 250 1070 220
1087 220))
(connect D36:0 D32:0
(points 12 260 238 260 250 330 250 330 230 470
230 470 180 920 180 920 200 1050
200 1050 260 1130 260 1130 290))
(connect D35:1 D32:1
(points 2 1063 310 1088 310))
(connect D38:0 D33:0
(points 6 1250 349 1250 360 1190 360 1190 270
1440 270 1440 285))
(connect D38:1 D33:1
(points 4 1291 300 1310 300 1310 320 1328
320))
(connect D32:0 D34:0
(points 8 1130 329 1130 350 1180 350 1180 260
1300 260 1300 350 1280 350 1280
355))
(connect D32:3 D34:1
(points 4 1172 320 1200 320 1200 390 1212
390))
(connect D30:0 D35:0
(points 8 970 288 970 300 990 300 990 290 1010
290 1010 280 1030 280 1030 290))
(connect D30:1 D35:1
(points 6 1013 260 980 260 980 310 990 310 990
300 997 300))
(connect D36:0 D35:3
(points 11 260 238 260 250 330 250 330 230 470
230 470 180 920 180 920 300 940
300 940 320 997 320))
(connect D43:1 D36:0
(points 3 200 170 260 170 260 181))
(connect D29:0 D37:0
(points 6 1040 408 1040 430 1100 430 1100 400
1150 400 1150 415))
(connect D29:1 D37:1
(points 4 1087 380 1110 380 1110 420 1117
420))
(connect D36:0 D37:2
(points 13 260 238 260 250 330 250 330 230 470
230 470 180 920 180 920 300 940
300 940 430 1010 430 1010 440 1117 440))
(connect D32:0 D38:0
(points 6 1130 329 1130 350 1180 350 1180 260
1250 260 1250 290))
(connect D32:2 D38:1
(points 4 1172 310 1200 310 1200 320 1209
320))
(connect D38:0 D39:0
(points 10 1250 349 1250 360 1190 360 1190
400 1200 400 1200 480 1460 480 1460
470 1500 470 1500 475))
(connect D37:1 D39:1
(points 6 1183 430 1190 430 1190 490 1460 490
1460 480 1473 480))
(connect D38:1 D39:2
(points 8 1291 300 1310 300 1310 350 1370 350
1370 500 1460 500 1460 490 1473
490))
(connect D32:3 D39:3
(points 12 1172 320 1200 320 1200 390 1180
390 1180 410 1190 410 1190 420 1210
420 1210 510 1460 510 1460 500 1473 500))
(connect D10:1 D39:4
(points 12 224 -90 230 -90 230 -70 570 -70 570
490 590 490 590 530 620 530 620
520 1460 520 1460 510 1473 510))
(connect D0:0 D43:0
(points 8 260 150 260 160 210 160 210 150 190
150 190 120 160 120 160 133)))
(stackingOrder 2 10 6 7 9 8 3 4 16 18 19 21 17
15 30 29 22 32 34 20 24 5 1 0 23
11 31 37 35 33 38 39 40 13 12 28 25 42 41 26 14
27 36 43))
(numberFormats
(realFormat standard)
(realSigDigits 4)
(realRadixSpec 4)
(integerBase decimal))))

*Appendix D*

## *Abaqus Input File*

```
*Heading
** Job name: JobQuad-1sec Model name: Model-1
*Preprint, echo=NO, model=NO, history=NO, contact=NO
**
** PARTS
**
*Part, name=Part-Air
*End Part
*Part, name=Part-BrassCasing
*End Part
*Part, name=Part-PiezoDisk
*End Part
*Part, name=Part-TopPiezo
*End Part
*Part, name=Part-Water
*End Part
**
** ASSEMBLY
**
*Assembly, name=Assembly
**
*Instance, name=Part-BrassCasing-1, part=Part-BrassCasing
*Node
<<Lines removed to shorten document>>
*Element, type=DCAX8
<<Lines removed to shorten document>>
*Nset, nset=Set-1, generate
     1,  13282,      1
*Elset, elset=Set-1, generate
    1,  4275,     1
*Nset, nset=Set-BC
<<Lines removed to shorten document>>
*Elset, elset=Set-BC
<<Lines removed to shorten document>>
** Region: (Section-Brass:Set-1)
** Section: Section-Brass
*Solid Section, elset=Set-1, material=Material-Brass
1.,
*End Instance
**
*Instance, name=Part-PiezoDisk-1, part=Part-PiezoDisk
          0.,        0.028,           0.
*Node
<<Lines removed to shorten document>>
*Element, type=DCAX8
<<Lines removed to shorten document>>
*Nset, nset=Set-1, generate
    1,  1273,     1
*Elset, elset=Set-1, generate
   1,  378,     1
*Nset, nset=Set-water
<<Lines removed to shorten document>>
*Elset, elset=Set-water, generate
   1,  373,    6
*Nset, nset=Set-base
   1,   2,   3,   4,   5,   6,   7, 449, 453, 456, 459, 462, 465
*Elset, elset=Set-base, generate
 1,  6,  1
*Nset, nset=Set-air
<<Lines removed to shorten document>>
*Elset, elset=Set-air, generate
   6,  378,    6
*Nset, nset=Set-top
  442,  443,  444,  445,  446,  447,  448, 1262, 1265, 1267, 1269, 1271, 1273
```



```
*Elset, elset=Set-top, generate
 373,  378,     1
** Region: (Section-Piezo:Set-1)
** Section: Section-Piezo
*Solid Section, elset=Set-1, material=Material-PZT
1.,
*End Instance
**
*Instance, name=Part-TopPiezo-1, part=Part-TopPiezo
          0.,       0.03435,           0.
*Node
<<Lines removed to shorten document>>
*Element, type=DCAX8
<<Lines removed to shorten document>>
*Nset, nset=Set-1, generate
   1,  413,     1
*Elset, elset=Set-1, generate
   1,  120,     1
** Region: (Section-Brass:Set-1)
** Section: Section-Brass
*Solid Section, elset=Set-1, material=Material-Brass
1.,
*End Instance
**
*Instance, name=Part-Water-1, part=Part-Water
*Node
<<Lines removed to shorten document>>
*Element, type=DCAX8
<<Lines removed to shorten document>>
*Nset, nset=Set-1, generate
    1,  8233,      1
*Elset, elset=Set-1, generate
    1,  2658,      1
** Region: (Section-Water:Set-1)
** Section: Section-Water
*Solid Section, elset=Set-1, material=Material-H2O
1.,
*End Instance
**
*Instance, name=Part-Air-1, part=Part-Air
*Node
<<Lines removed to shorten document>>
*Element, type=DCAX8
<<Lines removed to shorten document>>
*Nset, nset=Set-1, generate
    1,  9926,      1
*Elset, elset=Set-1, generate
    1,  3203,      1
** Region: (Section-Air:Set-1)
** Section: Section-Air
*Solid Section, elset=Set-1, material=Material
1.,
*End Instance
*Elset, elset=_Surf-water2pzt_S2, internal, instance=Part-Water-1, generate
  26,  1638,    26
*Surface, type=ELEMENT, name=Surf-water2pzt
_Surf-water2pzt_S2, S2
*Elset, elset=_Surf-water2top_S2, internal, instance=Part-Water-1, generate
 2164,  2658,    26
*Surface, type=ELEMENT, name=Surf-water2top
_Surf-water2top_S2, S2
*Elset, elset=_Surf-water2base_S1, internal, instance=Part-Water-1
 26,
*Elset, elset=_Surf-water2base_S3, internal, instance=Part-Water-1, generate
```

```
 2114,  2138,     1
*Elset, elset=_Surf-water2base_S4, internal, instance=Part-Water-1, generate
 1639,  2114,    25
*Surface, type=ELEMENT, name=Surf-water2base
_Surf-water2base_S1, S1
_Surf-water2base_S3, S3
_Surf-water2base_S4, S4
*Elset, elset=_Surf-piezo2water_S4, internal, instance=Part-PiezoDisk-1, generate
   1,  373,    6
*Surface, type=ELEMENT, name=Surf-piezo2water
_Surf-piezo2water_S4, S4
*Elset, elset=_Surf-piezo2casing_S1, internal, instance=Part-PiezoDisk-1, generate
 1,  6,  1
*Surface, type=ELEMENT, name=Surf-piezo2casing
_Surf-piezo2casing_S1, S1
*Elset, elset=_Surf-piezo2air_S2, internal, instance=Part-PiezoDisk-1, generate
   6,  378,    6
*Surface, type=ELEMENT, name=Surf-piezo2air
_Surf-piezo2air_S2, S2
*Elset, elset=_Surf-piezo2top_S3, internal, instance=Part-PiezoDisk-1, generate
 373,  378,    1
*Surface, type=ELEMENT, name=Surf-piezo2top
_Surf-piezo2top_S3, S3
*Elset, elset=_Surf-top2water_S4, internal, instance=Part-TopPiezo-1, generate
   1,  115,    6
*Surface, type=ELEMENT, name=Surf-top2water
_Surf-top2water_S4, S4
*Elset, elset=_Surf-top2air_S2, internal, instance=Part-TopPiezo-1, generate
   6,  120,    6
*Elset, elset=_Surf-top2air_S3, internal, instance=Part-TopPiezo-1, generate
 115,  120,    1
*Surface, type=ELEMENT, name=Surf-top2air
_Surf-top2air_S2, S2
_Surf-top2air_S3, S3
*Elset, elset=_Surf-top2piezo_S1, internal, instance=Part-TopPiezo-1, generate
 1,  6,  1
*Surface, type=ELEMENT, name=Surf-top2piezo
_Surf-top2piezo_S1, S1
*Elset, elset=_Surf-casing2air_S3, internal, instance=Part-BrassCasing-1
    6,   29,   30,   37,   38,   39,   40,   41,   42,  114,  138,  433, 1019, 1067, 1
263, 1354
 2172, 2174, 2175, 2183, 2184, 2185, 2189, 2190, 2192, 2201, 2223, 2232, 2294, 2382, 2
383, 2386
 2387, 2426, 2427, 2446, 2474, 2478, 2479, 2480, 2482, 2484, 2485, 2487, 2489, 2492, 2
494, 2496
 2498, 2499, 2500, 2503, 2504, 2505, 2508, 2551, 2627, 2629, 2636, 3351
*Elset, elset=_Surf-casing2air_S4, internal, instance=Part-BrassCasing-1
    3,   28,   41,   43, 1015, 1016, 1020, 1024, 1025, 1026, 1027, 1030, 1038, 1040, 1
041, 1051
 1054, 1056, 1059, 1060, 1063, 1064, 1123, 1126, 2380, 2834
*Elset, elset=_Surf-casing2air_S , internal, instance=Part-BrassCasing-1
    5,   33,   34,   35,  127,  132,  137,  939, 1150, 2163, 2167, 2169, 2173, 2176, 2
178, 2179
 2180, 2186, 2187, 2228, 2235, 2238, 2240, 2372, 2384, 2385, 2388, 2425, 2447, 2450, 2
452, 2453
 2456, 2458, 2460, 2462, 2463, 2464, 2467, 2468, 2469, 2471, 2472, 2473, 2555, 2558, 2
561, 2567
 2569, 2570, 2573, 2576, 2578, 2581, 2583, 2587, 2589, 2596, 2611, 2633, 2634, 2639, 2
641, 2642
 2646, 2649
*Elset, elset=_Surf-casing2air_S2, internal, instance=Part-BrassCasing-1
  940,  954, 1023, 1028, 1029, 1032, 1033, 1034, 1036, 1042, 1045, 1047, 1048, 1049, 1
066, 1130
 1132, 1134, 1136, 1138, 1142, 1144, 1149, 1152, 1173, 1176, 1179, 1183, 1188, 1191, 1
```



```
684, 2421
 2422, 2423, 2507, 2594
*Surface, type=ELEMENT, name=Surf-casing2air
_Surf-casing2air_S3, S3
_Surf-casing2air_S4, S4
_Surf-casing2air_S2, S2
_Surf-casing2air_S1, S1
*Elset, elset=_Surf-casing2piezo_S1, internal, instance=Part-BrassCasing-1
 2166, 2199, 2200, 2245
*Elset, elset=_Surf-casing2piezo_S3, internal, instance=Part-BrassCasing-1
 2242, 2244
*Surface, type=ELEMENT, name=Surf-casing2piezo
_Surf-casing2piezo_S1, S1
_Surf-casing2piezo_S3, S3
*Elset, elset=_Surf-casing2water_S1, internal, instance=Part-BrassCasing-1
 1720, 1733, 1735, 1736, 1737, 1738, 1739, 1743, 1816, 1820, 1823, 1829, 1907, 1936, 2
155, 2162
 2164, 2165, 2194, 2197, 2198, 2205, 2243, 2248, 2250, 2292, 2293
*Elset, elset=_Surf-casing2water_S3, internal, instance=Part-BrassCasing-1
 1717, 1734, 1744, 1745, 1749, 1752, 1799, 2207, 2208, 2211, 2212, 2213, 2246
*Elset, elset=_Surf-casing2water_S4, internal, instance=Part-BrassCasing-1
 1741, 1751
*Elset, elset=_Surf-casing2water_S2, internal, instance=Part-BrassCasing-1
 1944, 2165, 2215, 2254
*Surface, type=ELEMENT, name=Surf-casing2water
_Surf-casing2water_S1, S1
_Surf-casing2water_S3, S3
_Surf-casing2water_S4, S4
_Surf-casing2water_S2, S2
*Elset, elset=_Surf-air2casing_S3, internal, instance=Part-Air-
  375,  376,  377,  378,  379,  380,  381,  382,  383,  384,  385,  386,  387,  388,
389,  390
  391, 3123, 3124, 3125, 3126, 3127, 3128, 3129, 3130, 3131, 3132, 3133, 3134, 3135, 3
136, 3137
 3138, 3139, 3140, 3141, 3142, 3143, 3144, 3145, 3146, 3147, 3148, 3149, 3150, 3151, 3
152, 3153
 3154, 3155, 3156, 3157, 3158, 3159, 3160, 3161, 3162, 3163, 3164, 3165, 3166, 3167, 3
168, 3169
 3170, 3171, 3172, 3173, 3174, 3175, 3176, 3177, 3178, 3179, 3180, 3181, 3182, 3183, 3
184, 3185
 3186, 3187, 3188, 3189, 3190, 3191, 3192, 3193, 3194, 3195, 3196, 3197, 3198, 3199, 3
200, 3201
 3202, 3203
*Elset, elset=_Surf-air2casing_S4, internal, instance=Part-Air-1
    1,   18,   35,   52,   69,   86,  103,  120,  137,  154,  171,  188,  205,  222,
239,  256
  273,  290,  307,  324,  341,  358,  375, 2799, 2880, 2961, 3042, 3123
*Elset, elset=_Surf-air2casing_S2, internal, instance=Part-Air-1
  408,  425,  442,  459,  476,  493,  510,  527,  544,  561,  578,  595,  612,  629,
646,  663
  680,  697,  714,  731,  748,  765,  782,  799,  816,  833,  850,  867,  884,  901,
918,  935
 1016, 1097, 1178, 1259, 1340, 1421, 1502, 1583, 1664, 1745, 1826, 1907, 1988, 2069, 2
150, 2231
 2312, 2393, 2474, 2555, 2636, 2717, 2798, 2879, 2960, 3041, 3122, 3203
*Surface, type=ELEMENT, name=Surf-air2casing
_Surf-air2casing_S3, S3
_Surf-air2casing_S4, S4
_Surf-air2casing_S2, S2
*Elset, elset=_Surf-air2water_S4, internal, instance=Part-Air-1, generate
 494,  919,   17
*Surface, type=ELEMENT, name=Surf-air2water
_Surf-air2water_S4, S4
*Elset, elset=_Surf-air2top_S3, internal, instance=Part-TopPiezo-1, generate
```

```
   6,  120,    6
*Elset, elset=_Surf-air2top_S3, internal, instance=Part-TopPiezo-1, generate
 115,  120,    1
*Elset, elset=_Surf-air2top_S4, internal, instance=Part-Air-1, generate
 392,  477,   17
*Elset, elset=_Surf-air2top_S1, internal, instance=Part-Air-1, generate
 936,  955,    1
*Surface, type=ELEMENT, name=Surf-air2top
_Surf-air2top_S2, S2
_Surf-air2top_S3, S3
_Surf-air2top_S4, S4
_Surf-air2top_S1, S1
*Elset, elset=_Surf-air2piezo_S1, internal, instance=Part-Air-1, generate
 956, 1016,    1
*Surface, type=ELEMENT, name=Surf-air2piezo
_Surf-air2piezo_S1, S1
*Elset, elset=_Surf-water2air_S3, internal, instance=Part-Water-1, generate
2633, 2658,    1
*Surface, type=ELEMENT, name=Surf-water2air
_Surf-water2air_S3, S3
** Constraint: casing2air
*Tie, name=casing2air, adjust=yes
Surf-air2casing, Surf-casing2air
** Constraint: casing2water
*Tie, name=casing2water, adjust=yes
Surf-water2base, Surf-casing2water
** Constraint: piezo2air
*Tie, name=piezo2air, adjust=yes
Surf-air2piezo, Surf-piezo2air
** Constraint: piezo2casing
*Tie, name=piezo2casing, adjust=yes
Surf-casing2piezo, Surf-piezo2casing
** Constraint: piezo2top
*Tie, name=piezo2top, adjust=yes
Surf-top2piezo, Surf-piezo2top
** Constraint: piezo2water
*Tie, name=piezo2water, adjust=yes
Surf-water2pzt, Surf-piezo2water
** Constraint: top2air
*Tie, name=top2air, adjust=yes
Surf-air2top, Surf-top2air
** Constraint: top2water
*Tie, name=top2water, adjust=yes
Surf-water2top, Surf-top2water
** Constraint: water2air
*Tie, name=water2air, adjust=yes
Surf-aie2water, Surf-water2air
*End Assembly
*Amplitude, name=Amp-cyclic, definition=PERIODIC
1, 6.28319, 0., 0.
0., 1.
**
** MATERIALS
**
*Material, name=Material-Air
*Conductivity
 0.0267,
*Density
 1.177,
*Specific Heat
1005.,
*Material, name=Material-Brass
*Conductivity
94.,
```



```
*Density
8310.,
*Specific Heat
400.,
*Material, name=Material-H2O
*Conductivity
 0.611,
*Density
996.,
*Specific Heat
4180.,
*Material, name=Material-PZT
*Conductivity
38.,
*Density
7700.,
*Specific Heat
800.,
**
** FIELDS
**
** Name: temp_Casing   Type: Temperature
*Initial Conditions, type=TEMPERATURE
Part-BrassCasing-1.Set-1, 303.
** Name: temp_air   Type: Temperature
*Initial Conditions, type=TEMPERATURE
Part-Air-1.Set-1, 303.
** Name: temp_piezo   Type: Temperature
*Initial Conditions, type=TEMPERATURE
Part-PiezoDisk-1.Set-1, 303.
** Name: temp_piezoTop   Type: Temperature
*Initial Conditions, type=TEMPERATURE
Part-TopPiezo-1.Set-1, 303.
** Name: temp_water   Type: Temperature
*Initial Conditions, type=TEMPERATURE
Part-Water-1.Set-1, 303.
** ----------------------------------------------------------------
**
** STEP: Step-1
**
*Step, name=Step-1, inc=100000
*Heat Transfer, end=PERIOD, deltmx=0.01
0.001, 8., 1e-09, 0.1,
**
** BOUNDARY CONDITIONS
**
** Name: BC-Casing Type: Temperature
*Boundary
Part-BrassCasing-1.Set-BC, 11, 11, 303.
**
** LOADS
**
** Name: Load-HeatFlux   Type: Body heat flux
*Dflux, amplitude=Amp-cyclic
Part-Air-1.Set-1, BF, 50000.
**
** OUTPUT REQUESTS
**
*Restart, write, frequency=1
**
** FIELD OUTPUT: F-Output-1
**
*Output, field, frequency=10
*Node Output
```

```
NT, RFL
*Element Output
HFL, TEMP
**
** HISTORY OUTPUT: H-Output-1
**
*Output, history, variable=PRESELECT, frequency=99999
*El Print, freq=999999
*Node Print, freq=999999
*End Step
```